Microwave effects in heterogeneous catalysis: Application to gas-solid reactions for hydrogen production

Proefschrift

ter verkrijging van de graad van doctor
aan de Technische Universiteit Delft,
op gezag van de Rector Magnificus prof. ir. K.C.A.M. Luyben,
voorzitter van het College voor Promoties,
in het openbaar te verdedigen op vrijdag, 17 mei 2013 om 10:00 uur

door

Tomasz DURKA

Master of Science in Chemical Engineering,
Warsaw University of Technology

geboren te Warsaw, Poland

Dit proefschrift is goedgekeurd door de promotor:
Prof. dr. ir. A. I. Stankiewicz

Copromotor:
Dr. G. D. Stefanidis

Samenstelling promotiecommissie:

Rector Magnificus	voorzitter
Prof. dr. ir. A.I.Stankiewicz	Technische Universiteit Delft, promotor
Dr. ir G.D. Stefanidis	Technische Universiteit Delft, copromotor
Prof. dr. J Santamaria	Universidad de Zaragoza
Prof. dr. ir. J. C. Schouten	Technische Univeriteit Eindhoven
Prof. dr. ir. F. Kapteijn	Technische Universiteit Delft
Dr. ir. T. van Gerven	Katholieke Universiteit Leuven
Prof. dr. H.Stitt	Johnson Matthey
Prof. dr. ir. T. J.H. Vlugt	Technische Universiteit Delft, reservelid

Cover designed by T.Durka

*To my beloved parents
and my wonderful wife Magdalena*

Table of Contents

Summary
Microwave effects in heterogeneous catalysis: Application to gas-solid reactions for hydrogen production

Due to the quest for more efficient production processes both from the energy and selectivity point of view, microwave irradiation has attracted significant scientific attention over the last three decades, as an alternative means of chemical activation. Over this period, striking process benefits, such as higher conversions and selectivities and/or a shorter reaction times, compared to the respective conventionally heated processes have been reported.

The aim of this work is to investigate the influence of microwave energy on heterogeneous gas-solid catalytic reactions. As example process, the steam reforming of methanol and the water-gas shift reaction were selected. In a first step, the interaction of microwaves with different catalysts was investigated in a non-reactive environment, followed by investigation of the microwave effects on the reactions themselves. Comparison of the microwave- and electrically heated processes was performed in terms of conversion, selectivity and energy efficiency of the reactor. Contrary to other works in the literature, a two-dimensional temperature map along the centre plane of the reactor was recorded with both heating modes.

The study of interaction of microwaves with the solid state catalysts revealed that the heating rate, the maximum temperature at constant power, and the heat distribution inside the catalyst bed strongly depend on the catalytic support morphology, the metal loading and the particle size of the catalyst. Moreover, the experiments proved that even

small catalytic samples (~2g) experience non-uniform heat distribution inside their volume when exposed to a well-defined, mono-mode type of microwave field. These temperature gradients, although sometimes being severe, are undetectable by the commonly employed in microwave chemistry infra-red temperature sensors. These types of sensors are often built-in in the microwave applicator and serve as benchmark for the power control unit, which adjusts the power delivered into the microwave cavity. Therefore, a fibre optic based direct temperature measurement was selected as more accurate method in further stages of the research.

The investigation of methanol steam reforming reaction was performed with employment of two catalysts - $PdZnO/Al_2O_3$ and $CuZnO/Al_2O_3$ – at an average reaction temperature ranging between $190^{o}C$ – $250^{o}C$ and $170^{o}C$ – $230^{o}C$, respectively. In order to account for possible temperature gradients occurring across the catalytic bed, multi-point temperature mapping was implemented. The experiments revealed that at corresponding thermal conditions, the feed conversion in the microwave-heated process is significantly higher than in the electrically-heated process, regardless of the employed catalyst. However, the product distribution remained unaffected.

Comparison of the reactor energy efficiency demonstrated that the MW-assisted process exhibits higher reactor energy efficiency than the corresponding electrically heated process for both catalysts and over the range of the studied reaction temperatures. This entails that a given conversion can be achieved with lower net heat input to the reactor under the microwave heating mode and thus indirectly confirms the selective microwave heating principle (microscale hot spot formation).

Pre-conditioning of the catalyst in the presence of the microwave field prior to the reaction did not affect the reaction performance. The catalyst surface investigation showed no difference in the morphology of the catalyst used either between the microwave and the conventionally heated process, or between the preconditioned and the non-preconditioned samples. Consequently, specific non-thermal microwave effects were excluded as justification for the enhancement of the reactor performance.

In order to confirm the thermal nature of the microwave effects observed in the methanol steam reforming reaction, a mildly exothermic process, a water-gas shift reaction, was investigated at the latest stage of the research. Contrary to steam

reforming, the water-gas shift reaction did not exhibit significant enhancement neither in terms of conversion nor in terms of reactor energy efficiency. This is because a significant part of the net heat input to the reactor comes from the heat of reaction; therefore, the heat input from microwave irradiation and the associated local overheating of active sites diminishes. Consequently, the microwave effect is not pronounced.

Based on the experimental experience obtained and the theoretical knowledge regarding the shortcomings of the available microwave types of equipment, an alternative reactor design, based on *travelling microwave fields*, is proposed for application to heterogeneous gas-solid catalytic reactions. The new concept may enable uniform spatial heating, improved electromagnetic energy utilization and electromagnetic field spatial localization (i.e. on the catalytic reactor walls).

Samenvatting
Microwave effects in heterogeneous catalysis: Application to gas-solid reactions for hydrogen production

In de zoektocht naar efficiëntere productieprocessen vanuit het perspectief van zowel energie als selectiviteit, heeft microgolfstraling de laatste dertig jaar aanmerkelijke wetenschappelijke aandacht gekregen als een alternatieve methode voor chemische activering. Gedurende deze periode zijn er opvallende procesvoordelen gerapporteerd, zoals een hogere conversie en verbeterde selectiviteit en/of kortere reactietijden vergeleken met conventioneel verhitte processen.

Het doel van dit proefschrift is om te onderzoeken wat de invloed is van microgolfenergie opgasfase reacties onder heterogene vaste-stof-katalyse. Als voorbeeldprocessen zijn stoomreforming van methanol en de watergasreactie gekozen. In een eerste stap is de interactie van microgolven met verschillende katalysatoren onderzocht onder niet-reactieve omstandigheden. Dit werd vervolgd door een onderzoek naar het effect van microgolven op de reacties zelf. De respectievelijke processen, enerzijds door microgolven verhit, anderzijds elektrisch verhit, zijn vergeleken op basis van conversie, selectiviteit en energetisch rendement van de reactor. In tegenstelling tot andere onderzoeken, die zijn beschreven in de literatuur, is er een tweedimensionale temperatuurverdeling in het middenvlak van de reactor gemeten voor beide verwarmingsmethoden.

Het onderzoek naar de interactie van microgolven met vaste katalysatoren, liet zien dat de verhittingssnelheid, de maximale temperatuur bij constant vermogen, en de warmteverdeling in het katalysatorbed alle sterk afhankelijk zijn van de morfologie van

de katalysatorondersteuning, het metaalgehalte en de katalytische deeltjesgrootte. Verder bewijzen de experimenten dat zelfs kleine katalysatormonsters (~2g) geen uniforme warmteverdeling in hun volume krijgen wanneer ze worden blootgesteld aan een goed gedefinieerd, enkelvoudig-modaal microgolfveld. Hoewel deze temperatuurgradiënten soms zeer groot zijn, zijn ze niet te detecteren met de, in de microgolfchemie veelgebruikte, infrarood temperatuursensoren. Dit type sensor vindt men vaak ingebouwd in microgolfapplicatoren en dient als referentie voor de vermogensregulatie waarmee het vermogen in de microgolfholte wordt geregeld. Als gevolg van deze tekortkomingen zijn glasvezelsensoren gekozen als nauwkeurigere meetmethode voor directe temperatuurmeting in de hierop volgende stappen van het onderzoek.

Het onderzoek naar de methanol-stoomreformingreactie is uitgevoerd met twee katalysatoren – PdZnO/Al$_2$O$_3$ en CuZnO/Al$_2$O$_3$ – bij een gemiddelde reactietemperatuur tussen, respectievelijk, 190°C – 250°C en 170°C – 230°C. Om mogelijke temperatuurgradiënten in kaart brengen, is de temperatuur op meerdere plaatsen gemeten. De experimenten tonen dat, onder overeenkomstige thermische omstandigheden, de conversie van de voeding in de met microgolven verhitte processen significant hoger is dan in de elektrisch verhitte processen, ongeacht de gebruikte katalysator. De verhouding tussen de reactieproducten bleef echter onveranderd. Een vergelijking van het energetische rendement van de reactor liet zien dat het microgolfgedreven proces een hoger reactorrendement heeft dan het overeenkomstige elektrisch verhitte proces, zowel voor beide katalysatoren als over het bereik van de bestudeerde reactietemperaturen. Dit houdt in dat een bepaalde conversie kan worden bereikt met een lagere netto warmtetoevoer naar de reactor onder microgolfverhitting en daarmee bevestigt dit indirect het selectieve microgolfverwarmingsprincipe (het ontstaan van hot spots op microschaal).

Voorbehandelen van de katalysator door blootstelling aan het microgolfveld vooraf aan de reactie beïnvloedt de prestatie van het proces niet. Onderzoek aan het oppervlak van de katalysator liet geen verschil in de katalysatormorfologie zien tussen de door microgolven verhitte processen en de conventioneel verhitte processen en ook niet tussen de voorbehandelde en niet-voorbehandelde monsters. Ten gevolge van deze

observaties zijn specifieke niet-thermische microgolfeffecten uitgesloten als verklaring voor de verbetering van de reactorprestaties.

Om te bevestigen dat de aard van de waargenomen microgolfeffecten in de methanol-stoomreformingreactie thermisch is, is in de laatste stap van het onderzoek een licht exothermisch proces, de watergasreactie, onderzocht. In tegenstelling tot stoomreforming, liet de watergasreactie geen duidelijke verbetering zien in de conversie, noch in het energetisch reactorrendement. De oorzaak is dat een groot gedeelte van de netto warmtetoevoer aan de reactor afkomstig is uit de reactiewarmte; dit verkleint de warmtetoevoer van de microgolfstraling en de hiermee samenvallende lokale oververhitting van actieve deeltjes. Ten gevolge hiervan is het microgolfeffect niet duidelijk zichtbaar.

Op basis van experimentele ervaring en theoretische kennis met betrekking tot de tekortkomingen van beschikbare microgolfapparatuur, wordt een voorstel gepresenteerd voor een alternatief reactorontwerp dat is gebaseerd op lopende microgolfvelden en dat zich richt op toepassingen met gasfase reacties onder heterogene vaste-stof-katalyse. Dit nieuwe concept zou verhitting ruimtelijk uniform kunnen verdelen, een verbeterde aanwending van elektromagnetische energie mogelijk kunnen maken, en het elektromagnetische veld ruimtelijk gericht kunnen toepassen (i.e. op katalytische reactorwanden).

1

Introduction

1.1 The battle for the future energy source

The world energy consumption increases continuously year by year mainly due to increasing world population and progressive industrialization of developing countries. More than 80% of the consumed energy comes from fossil fuels and according to the U.S. Department of Energy the share of this energy source will stay predominant with a drop to ~63% by 2035[1]. Although the coal peak is predicted to take place around the year 2075, which seems to be far future, the oil peak will become true earlier. Depletion of the fossil fuel resources increases the energy cost in all sectors; domestic use, industrial and transportation.

The cost of energy in general and electricity in particular are the main contributors to the end price of many products. Further, the rapid increase in the energy cost together with the rising concern about the environmental impact of greenhouse gas emissions have intensified the interest in alternative sources of energy. Wind, hydro, solar and nuclear energy are potential candidates to significantly contribute to global energy production. In the coming years, however, their share in energy production is estimated to be growing by 3% annually on world scale in the next 20 years. Moreover, while conversion of the aforementioned energy sources to electricity for household and industrial applications, as substitute for coal generated electricity, is relatively simple, their employment in transportation is rather difficult.

The dominance of the oil-based fuels in transportation is mainly due to simple handling and storing, high volumetric energy density and available distribution and refueling infrastructure. Therefore, the future energy source for this specific sector should provide these and/or other advantages to overcome the investment cost.

The potential non-crude oil fuels being considered at this moment for the transportation sector are mainly biogas/bioalcohols, hydrogen and electricity. None of these technologies offers the advantages of the oil-based fuels and moreover each of them has serious limitations to become a widely used, new generation of transportation fuel.

The selection of the alternative fuel strongly depends on the local conditions, such as availability of the harvesting areas, geographical conditions or climate as well as on

the type of transportation, e.g. road, maritime or aerial. Finally, the choice of future transportation energy source will largely depend on the sustainability, energy efficiency, cost effectiveness and storing capabilities.

In this thesis, the focus is on production of hydrogen from (bio-)alcohols for the automotive application and decentralized systems.

1.2 Hydrogen as an energy carrier

Hydrogen is often mentioned as the alternative fuel of the future. The high efficiency of chemical energy conversion (45-65%) when fuel cells are used [2, 3], zero emissions of CO_2 and NO_X, the wide range of primary energy sources and the diversity of production methods are the main arguments promoting hydrogen economy as a potential important player in the future energy scene.

However, hydrogen storage is a problem, especially when transportation and decentralized systems are considered. Despite hydrogen having ~3 times higher energy content by weight than that of gasoline, 3100 litres of hydrogen under atmospheric pressure have the same energy equivalent as 1 litre of gasoline. Given that 4 kg-8 kg of hydrogen are needed to drive 600 km with a passenger car (depending on whether hydrogen is consumed in a fuel cell or in a combustion engine), very large volumes are necessary for hydrogen storage [3, 4]. Despite the very intensive R&D activities in the field of on-board hydrogen storage, the available technologies (compressed gas, liquid hydrogen, materials-based storage) still requires ~70% higher volume compared to gasoline to store the same amount of energy[5].

Finally, hydrogen is not an energy source, but an energy carrier. In nature, hydrogen is always bounded to other elements, such as carbon and oxygen, and therefore it must be produced from one of the hydrogen-rich sources like solid and liquid hydrocarbons, biomass or water. The present hydrogen production and downstream purification processes are considerably energy demanding.

1.3 Hydrogen production technologies

Hydrogen production technologies can be divided into three main categories:
- Electrolytic processes

- Photolytic processes
- Thermal processes

A summary of the major hydrogen production technologies along with their feedstock, state of development and efficiencies is presented in Table 1.1. The exact definition of efficiency is technology dependant.

Primary method	Process	Feedstock	Maturity	Efficiency
Electrolytic	Electrolysis	Water, Biomass	Commercial to long term; depends on type of electrolyzer	50-70%[a]
Photolytic	Photoelectorchemical	Water	Long term	12.4%[b]
	Photobiological	Algae, Biomass	Long term	0.1%[c]
Thermal	Reforming	Hydrocarbons, Bio-alcohols	Commercial	70-85%[d]
	Catalytic partial oxidation	Hydrocarbons, Bio-alcohols	Commercial	60-75%[d]
	Gasification	Coal, Biomass	Commercial	35-50%[d]
	Pyrolysis	Biomass	Near term	25-45%[d]
	Water Splitting	Water	Long term	35~50%[e]

Table 1.1 Major hydrogen production processes (adapted from [6, 7])

[a] Lower heating value of hydrogen produced divided by the electrical energy to the electrolysis cell.
[b] Solar to hydrogen via water splitting and does not include hydrogen purification
[c] Solar to hydrogen via organic materials and does not include hydrogen purification.
[d] Thermal efficiency; higher heating value of produced hydrogen divided by the higher heating value of fuel.
[e] Utilized heat to higher heating value of produced hydrogen

1.3.1 Electrolytic Processes

The electrolytic process takes place in an electrolyser where water molecules are split into oxygen and hydrogen, as result of electric current flowing through electrodes immersed in the water. Hydrogen production via electrolysis may result in no greenhouse gas emissions. However, the amount of electricity needed to split water molecules is approximately double the amount of electricity obtained from the inverted

process, i.e., generation of electricity in a fuel cell [8]. Therefore, this method can have potential application only if the energy necessary for the process is cheap and clean e.g. hydropower or nuclear.

1.3.2 Photolytic Processes

Two main types of photolytic processes can be distinguished; photobiological and photoelectrochemical processes. Photobiological processes involve production of hydrogen from biomass fermentation or as a metabolic product of living organisms, e.g. algae and bacteria, where light is the main source of energy for the process. Photoelectrochemical processes require the light source and a special semiconductor photoelectrode containing photovoltaics and catalyst to enable water split. Although this method is still at experimental stage, it is considered as one of the cleanest methods of production of ultra-pure hydrogen.

1.3.3 Thermal Processes

In thermal processes, hydrogen sources such as natural gas, coal, biomass or water, are subjected to thermal treatment to release hydrogen, which is part of their molecular structure. Thermal processes include:

- Steam Reforming of natural gas and renewable liquid fuels
- Catalytic partial oxidation of natural gas and renewable liquid fuels
- Gasification of coal and biomass
- Pyrolysis of biomass
- High-temperature water splitting

Among all thermal processes, the most popular and commercially applied method to hydrogen production is the conversion of natural gas, containing ~95% methane (CH_4), into syngas (H_2 and CO) in a steam reforming process (SR). Currently, steam reforming of natural gas accounts for ~50% of the global production of H_2, which is then used as fuel or raw material in the chemical and petroleum industry (e.g. oil hydrogenation or ammonia synthesis) [9, 10].

SR of hydrocarbons is generally described formula 1.1. The process is usually carried out under pressure and is strongly endothermic. The reaction is performed using

solid catalyst with composition depending on the hydrocarbon feedstock. For steam reforming of natural gas, Ni-based catalysts are typically used. The SR process occurs in parallel with the water-gas shift reaction (WGSR), which converts part of the CO produced into CO_2 and additional H_2 (Eq.1.2). WGSR is exothermic and inextricably connected to SR. Furthermore, one or more WGS reactors are usually placed downstream of the SR reactor to maximize hydrogen production. In comparison to partial oxidation (POX), SR runs at lower temperature, does not require O_2/N_2 separation (from air) and results in higher H_2/CO ratio (3 vs. 2 in case of methane feed). On the other hand, SR requires steam generation. The steam reforming and water-gas shift reactions have been investigated in detail in this thesis and they are discussed explicitly in Chapters 4 and 5, respectively.

$$C_nH_{2n+2} + nH_2O \leftrightarrow nCO + (2n+1)H_2$$
(1.1)

$$CO + H_2O \leftrightarrow CO_2 + H_2$$
(1.2)
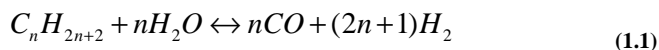
1.4 Process intensification in chemical engineering

To meet the future energy consumption needs, exploration of alternative, sustainable energy sources is a key task for researchers from many scientific disciplines (chemistry, biotechnology, materials and chemical engineering), who try to develop new technologies for energy and chemicals production from the renewable sources. However, this approach is only partially rational since many manufacturing processes exhibit extremely low energy efficiency. Furthermore, fabrication of highly specialized and sophisticated equipment raises its cost, due to its complexity, generates enormous amounts of wastes and often requires application of hardly degradable materials. One could think of going back to the Stone Age as the best option for energy and waste reduction. Is this really the only remaining option? What if we could drastically improve manufacturing processes to keep them economically feasible and profitable while increasing the utilization efficiency of the renewable feedstock? The question is how to achieve this goal.

Process Intensification (PI) is a relatively young discipline. Its history goes back to 1970s when the term Process Intensification appeared for the first time. Nowadays, PI has become one of the significant trends in modern chemical engineering and constantly

attracts increasing attention from both the industrial and academic research communities [11].

In fundamental sense, Process Intensification is based on four generic principles and is realized via specific approaches in four domains: spatial, thermodynamic, functional and temporal [12] (see also Fig.1.1). In order to facilitate better understanding of the advantages offered by the PI approaches and to give a flavour of the achieved improvements, compared to conventional technologies, a few examples of applications of some PI technologies are listed in Table 1.2.

- **maximizing the effectiveness of infra- and intermolecular events**
- **giving each molecule the same processing experience**
- **optimizing the driving forces and maximizing the specific surface area to which these forces apply**
- **maximizing synergetic effects from partial processes**

Process Intensification

- **STRUCTURE** (spatial domain)
- **ENERGY** (thermodynamic domain)
- **SYNERGY** (functional domain)
- **TIME** (temporal domain)

Figure 1.1 Fundamental of process intensification (adopted from [12]).

1.5 Microwave energy as a PI tool

One of the domains of PI is the thermodynamic domain, where the main focus lies in process activation using alternative forms of energy compared to conductive heating. In general, precise dose of energy should be delivered to the required location, where a reaction and/or a separation process takes place, in a form ensuring the highest efficiency. In the ideal case, energy is to be delivered solely to reactants at the precise amount needed to form the desired product. In practice, however, some reagent molecules obtain insufficient energy to pass the activation energy barrier and some absorb excessive amount of energy and may form undesired by-products. This kind of

Approach	Process	Conventional technology	PI technology	Benefits
STRUCTURE	Azidation reaction[13]	Stirred tank reactor	Microreactor	• Productivity increase from 10kg/m^{3}h to 10 t/m^{3}h • 20% higher selectivity • Change in operation mode from batch to continuous
	Ritter reaction[13]			• Volume reduction from 10m^3 to 3dm^3 maintaining high throughput (1.7t/h)
	Oxidation of Ethanol to Acetic Acid [14]			• Shortening residence time from 3h to 3s. • Increased conversion (30-95% to 99%) • Reduction of reaction volume by factor 1000
ENERGY	Transestrification reaction[15, 16]	Oil bath	Microwave reactors	• Shorter reaction time (by factor 10 to 100) • Higher energy efficiency (factor 3 to 4) • Improved process control
SYNERGY	Methyl acetate synthesis[17, 18]	A system consisting of extractor and 10 extraction and distillation columns	Multifunctional reactor column with integrated reactive and extractive distillation steps	• Reduction of plant size from 28 to 3 unit operations • Reductions of energy consumption by a factor 5
TIME	Saponification reaction [19]	Stirred tank reactor	Continuous Oscillatory Baffle Flow Reactor	• Uniform, radial and axial velocities • Reduction in reaction time factor 2-10 • 100-fold reduction in reactor size

Table 1.2 Some of spectacular process improvements through application of PI technologies.

problem is very common in chemistry and results in low product yield and/or selectivity. To overcome these limitations, energy input much higher than the required minimum is provided. As a result, non-uniform heating inside the reactor takes place; a characteristic feature of thermal conductive heating. Thermal gradients present inside the reactor can be significantly reduced by miniaturization of the reactor itself (PI spatial domain) or by application of an alternative source of energy which allows for energy delivery in a controllable and volumetric manner.

One of the alternative heating methods is the application of microwave energy. Microwaves are a form of electromagnetic radiation situated between the radio and the infrared frequencies, i.e. between 300 MHz and 300 GHz, which corresponds to wavelengths from 1m to 1mm [20]. Due to legislation, the commercially available magnetrons for chemical processing operate at one of the following frequencies: 915 MHz, 2.45 GHz and 5.85 GHz.

1.5.1 Interaction of microwaves with materials[a]

When matter is exposed to microwave radiation (Fig.1.2), microwaves can be reflected from its surface (highly conductive materials e.g. metals, graphite), can penetrate material (insulators e.g. ceramics, quartz glass) or can be absorbed causing heating (dielectric lossy materials e.g. silicon carbide) [21].
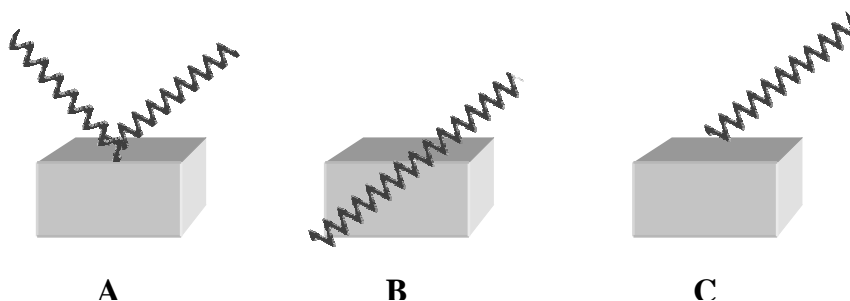

A   **B**   **C**

Figure 1.2 Microwaves interactions with different types of materials: (A) conductive material (B), insulating material, (C) absorbing material.

---

[a] This subchapter is published in Chemical Engineering Technology 2009, 32, No.9, 1301-1312

The advantages of microwave heating are: fast and more effective heat absorption, reduction of thermal gradients, selective heating and better thermal control of the process [22, 23].

In order to apply microwave energy to a chemical process at least one component of the system must be a good microwave absorber. Fortunately, many organic compounds, metal oxides and popular solvents are good or at least moderate absorbers and perfectly fulfil this requirement.

The parameter which describes the microwave propagation and the ability of materials to absorb microwave radiation are complex permittivity, ε^*[-], and complex permeability, μ^* [-].

$$\varepsilon^* = \varepsilon' - j\varepsilon'' = \varepsilon_0 \left(\varepsilon_r' - j\varepsilon_{eff}'' \right)$$

(1.1)

$$\mu^* = \mu' - j\mu''$$

(1.2)

The real part (ε' [-]) of the relative permittivity (i.e. the dielectric constant) characterizes the ability to propagate microwaves into the material whereas the imaginary part (ε'' [-]) is the loss factor that reflects the ability of material to dissipate the energy. The real part of complex permeability (μ' [-]) represents the amount of magnetic energy stored within the material while the imaginary part (μ'' [-]) represents the amount of magnetic energy which can be converted into thermal energy. Most of the materials encountered in heterogeneous catalysis are non-magnetic materials and the magnetic losses can therefore be neglected. However in metal oxides such as iron, nickel and cobalt magnetic losses are high. For more convenient characterization of materials in microwave conditions other terms have been introduced: loss tangent (tan δ), which is the ratio of ε'' and ε' for non-magnetic materials (Eq. 1.3), and magnetic loss tangent (tanδ_μ), which is the ratio of μ'' and μ'' for magnetic lossy materials – (Eq. 1.4).

$$\tan \delta = \frac{\varepsilon''}{\varepsilon'}$$

(1.3)

$$\tan \delta_\mu = \frac{\mu''}{\mu'}$$

(1.4)

From Eq.1.3 it can be seen that for the most effective heating the ε'' should be as high as possible while simultaneously keeping ε' in moderate range (sufficient penetration inside a material). This specific combination of ε' and ε'' gives high tanδ and ensures optimum microwave coupling [21]. The same holds for the magnetic analogues. As the latter are often not relevant, the magnetic component of microwave heating will not be discussed further in this review. The values of ε', ε'' and tan δ for some common materials are presented in Table 1.3.

Material	Dielectric Constant ε'	Dielectric Loss ε''	Loss tangent tan δ
Vacuum	1.00	0	0
Air	1.0006	0	0
Water	80.4	9.89	0.123 (2.45 GHz)
Methanol	32.6	21.48	0.659 (2.45 GHz)
Ethanol	24.3	22.86	0.941 (2.45 GHz)
Glass (pyrex)	4.82	0.026	0.0054 (3 GHz)
Styrofoam	1.03	0.0001	0.0001 (3 GHz)
PTFE	2.08	0.0008	0.0004 (10 GHz)
Titanium dioxide	50	0.25	0.005
Zirkonia	20	2	0.1
Zinc oxide	3	3	1
Magnesium oxide	9	0.0045	0.0005
Aluminum oxide	9	0.0063	0.0007

Table 1.3 Dielectric constant (ε'), dielectric loss (ε'') and loss tangent (tan δ) of common materials at 25°C (adapted from [24-26])

The frequency dependence of ε' and ε'' is described by the Debye equations [20]:

$$\varepsilon^{'} = \varepsilon^{'}_{\infty} + \frac{\left(\varepsilon^{'}_{0} - \varepsilon^{'}_{\infty}\right)}{\left(1 + \omega^{2}\tau^{2}\right)}$$

(1.5)

$$\varepsilon^{''} = \frac{\left(\varepsilon^{'}_{0} - \varepsilon^{'}_{\infty}\right)\omega\tau}{\left(1 + \omega^{2}\tau^{2}\right)}$$

(1.6)

Where $\acute{\varepsilon}_{0}$ is the static dielectric constant [-], $\acute{\varepsilon}_{\infty}$ is the high frequency constant [-], ω the angular frequency (ω=2πf [s^{-1}]), and τ the relaxation time [s] characterizing the rate

of build up and decay of polarization. In liquids dipoles are randomly oriented and orientation is changing continuously due to the thermal motions, therefore the relaxation time is defined by the following expression:

$$\tau = \frac{4\pi r^3 \mu}{kT}$$

<div align="right">(1.7)</div>

where r is a radius of the dipole [m], μ the dynamic viscosity [kg·m^{-1}·s^{-1}], k the Boltzman's constant [kg·m^2·s^{-2}·K^{-1}] and T the temperature [K] [20].

For an ideal solid in which molecules interact with each other, a dipole has a number of equilibrium positions. For dipole positions separated by a potential barrier U$_a$ [kg·m^2·s^{-2}], the following relationship between τ and dielectric constant may be derived from Boltzman statistics [20]:

$$\tau = \frac{e^{U_a/kT}(\varepsilon_0' + 2)}{\mu\left(\varepsilon_\infty' + 2\right)}$$

<div align="right">(1.8)</div>

From equations 1.5 - 1.8 it is seen that the efficiency of microwave heating not only depends on the dielectric properties of the material but also on the frequency of electromagnetic field and the temperature of the material. It also depends on dimensions of irradiated material. The microwave irradiation can only penetrate material up to a certain depth, called penetration depth – D_p [m] – which is usually described as the depth where the microwave power drops to about 37% of the initial value. The penetration depth is proportional to the wavelength of the radiation and depends on the dielectric properties of material. For materials where $\varepsilon''/\varepsilon'<1$ (lossy dielectrics) D_p can be described as follows:

$$D_p = \frac{\lambda}{2\pi} \frac{\sqrt{\varepsilon'}}{\varepsilon''}$$

<div align="right">(1.9)</div>

Based on the discussion above, it clearly visible that in microwave heating systems the dielectric properties of a material control the power, which can be absorbed by the given material. The average power (P) dissipated in a volume (V) is related to electric field strength (E), magnetic field strength (H) and the dielectric properties of material by the equation:

$$P = \omega\varepsilon_0\varepsilon'' E_{rms}^2 V + \omega\mu_0\mu'' H_{rms}^2 V$$

<div align="right">(1.10)</div>

where E_{rms} is the root mean square of the electric field [V/m], H_{rms} is the root mean square of the magnetic field [A/m], ω the angular frequency ($\omega=2\pi f$ [s^{-1}]) and ε_0, μ_0 are permittivity and permeability of the free space, respectively. In the case of dielectric materials, there are no magnetic losses and the second term on the right-hand side of Eq. 1.10 is negligible [27].

It is known from experiments that bulk metals are opaque to microwave and are good reflectors, due to the so-called skin-effect. They can undergo surface heating only, due to the limited penetration of the microwave radiation [28]. However, powdered samples are very good absorbers of microwaves and can be heated efficiently. The heating mechanism of metallic powders has not been fully established yet but one of the theories indicates that electrical conductivity of metal particles decreases when the particle size decreases below 5 μm (Eq. 1.11) [29].

$$\sigma_e = \left(\frac{D_p}{5 \times 10^{-6}} \right)^3 \sigma_0$$

(1.11)

Here, σ_e is the effective electrical conductivity of metal particle, D_p is the diameter of particles and σ_0 is the bulk conductivity of metal.

The field inside the supported metal particle is described as function of complex permittivity of the support, ε_1^* and the metallic particle, ε_2^*.

$$E = \frac{3\varepsilon_1^*}{2\varepsilon_1^* + \varepsilon_2^*} E_0$$

(1.12)

The volumetric heat generation, $\dot{q}_p$, is described by the following equation.

$$\dot{q}_p = \sigma_e \left| E \right|^2$$

(1.13)

1.5.2 Microwave effects in catalysis [a]

When discussing influence of electromagnetic field on chemical reaction it is impossible to be indifferent to microwave effects. To interpret the observations of

---

[a] This subchapter is published in Chemical Engineering Technology 2009, 32, No.9, 1301-1312

higher conversion and/or enhanced selectivity of microwave-assisted chemical reactions two hypotheses were proposed.

The first one assumes the existence of a purely thermal effect only, i.e. a different temperature regime. The second theory assumes that besides thermal effects also non-thermal effects, like molecular interaction of substrates with microwave field or shifting reaction equilibrium can exist and cause the enhancement of the reaction rate. The existence of non-thermal effects was often claimed especially in early studies on microwave-assisted catalysis when the results could not be explained by the observed temperature differences. However, together with increasing enthusiasm for dielectrically heated reactions also improved temperature measuring methods suitable for microwave conditions were developed and the non-thermal effects are nowadays rarely postulated.

The reported thermal effects of microwave irradiation are due to three phenomena:

- hot-spot formation
- selective heating
- and superheating

In gas/solid heterogeneous catalytic systems hot-spot formation and selective heating are primarily considered to be mechanisms responsible for the enhanced rate of reaction while selective heating and superheating are mainly postulated in homogeneous systems. Hot-spots are places inside the catalytic bed where temperature is considerably higher than the average temperature and hence reaction occurs at a much higher rate [30-33]. Very often the existence of this phenomenon is explained by the non-homogenous distribution of the electromagnetic field inside the catalytic bed. Sizes of hot-spots are in the range of 90-1000 μm and temperatures can be 100-200 K higher than the bulk temperature of the catalytic bed [34].

An evidence on hot spot formation was presented by Zhang *et al.* [33] in his study on the catalytic reduction of sulphur dioxide with methane over MoS_2/Al_2O_3 catalysts. The morphological study of the catalyst showed that observed phase transition of γ-alumina to α-alumina which normally occurs at temperatures above 1273 K took place when the reactor bulk temperature did not exceed 1000K. In the other study Zhang, Hayward and Mingos [34] investigated the decomposition of hydrogen sulphide. Also in this study the presence of hot-spots was postulated as a possible explanation of the

observed higher conversion under microwave field than when conventional heating was applied. The conclusion was consistent with the observations made in the experiments on catalytic reforming of methane with carbon dioxide over platinum catalyst [35]. However, in a later theoretical study on temperature difference between MoS_2 and Al_2O_3 support the existence of significant temperature gradient was excluded [30]. Chang and Wang [36, 37] who studied reduction of NO with methane observed that application of microwave energy allows reaching the given conversion at much lower temperature than in conventionally heated reaction; what can be seen as potential occurrence of the hot-spot inside the catalytic bed. The existence of the hot-spots was postulated also by Bi and coworkers [38] as a possible explanation of observed higher conversion of methane and higher selectivity to hydrogen when microwave power was applied. It was also observed that at the same conversion the temperature of the catalytic bed under microwave conditions was around 200 K lower than for the conventional heating. However, the temperature of these hot-spots was not determined. Bond *et al.* [31] measured temperature inside the reactor with two different techniques to avoid potential uncertainty, however they admitted that non-uniform temperature distribution inside the catalytic bed could not be excluded and hot-spots were probably formed.

Obviously, the microscale nature of this phenomenon induces technical problems with measuring the temperature of hot-spots by the available techniques and hence experimental proof of their existence is lacking.

Selective heating can occur in different ways depending on whether homogeneous or heterogeneous systems are subjected to microwave irradiation. In a homogeneous system the effect consists simply in different microwave power absorption due to the differences in the dielectric properties of the substances taking part in a reaction. In gas/solid systems selective heating appears in two forms that may occur simultaneously. The first form is the selective heating of a catalyst particle while the gas phase remains at lower temperature. This form of selective heating was proposed by Roussy *et al.* [39] as the probable reason of the observed enhanced selectivity towards higher hydrocarbons in a microwave field. The second form consists in the created temperature difference between the nanoparticles of the catalyst and the support material. It is known that metal particles (present in the support) can be heated up by microwave

irradiation very rapidly to high temperatures. The required metal particle size has to be smaller or equal to the penetration depth, which for most metals is in the range 1-10μm at 2.45 GHz [40]. This phenomenon is considered by some researchers to be responsible for the observed higher reaction rate and higher selectivity of products formed [22, 41-45]. However, this hypothesis is also contested. Perry *et al.* [46, 47] presented results from their experimental and theoretical work, which deny the existence of a temperature difference between the active sites of catalyst and its support.

1.6 Scope of the thesis

The scope of the thesis was to explore the application of microwaves as alternative energy source to intensify gas-solid catalytic processes with application to hydrogen production. To this end, microwave-activated methanol steam reforming (endothermic reaction) and water-gas shift (exothermic reaction) have been investigated. Although the application of microwave heating to gas-solid catalytic reactions has been subject of research for the last 10-15 years, the aforementioned reactions have attracted very little attention. Further, little information is available in the relevant literature on the (non-) thermal interaction of microwaves with solid catalyst particles and on the actual temperature conditions in the microwave-irradiated catalytic bed.

In this context, the (threefold) aim was to *a) investigate the thermal nature of microwave-solid particles interactions (Chapter 2,4 and 5), b) to verify advantages and limitations of microwave driven reactors (Chapter 2,4 and 5)* and *c) to evaluate the selected processes in terms of fuel conversion, product distribution and energy efficiency (Chapter4 and 5)*.

The specific research questions addressed in the thesis are

- Can microwaves selectively heat catalyst particles and how pronounced is the effect? What is the role of catalyst type, particle size and support in this process?

- How do microwaves affect temperature distribution inside packed bed reactors?

- How should temperature distribution inside microwave-irradiated packed bed reactors be monitored? How do available temperature measurement techniques compare?

- How does microwave activation affect the processes of methanol steam reforming and water gas shift in terms of fuel conversion, product distribution and energy efficiency?

1.7 Outline of the thesis

The thesis consists of five main chapters. In Chapter 2, the problem of correct temperature measurement in the microwave field is described. This includes selection of the most suitable temperature measurement technique and discussion on its sensitivity to changing catalyst weight and volume. This chapter also addresses temperature distribution inside a catalytic bed exposed to microwave irradiation under steady state conditions. Chapter 3 contains a literature review on microwave-activated gas-solid catalysis. Possible mechanisms justifying microwave-enhanced reaction performance are also reviewed in this chapter. Experimental results from a comparative study on microwave- and electrically-activated methanol steam reforming and water-gas shift reaction are presented in Chapter 4 and Chapter 5, respectively. Chapter 6 summarises the limitations of the available microwave equipment in terms of predictability of process conditions and scale-up and discusses potential technical solutions to address these challenges. In the last chapter, the general conclusions are collected and recommendations for follow-up research are presented.

1.8   Nomenclature

ε_r - dielectric constant [-],

ε^* - complex electric permittivity [-],

ε' - the real part of the relative permittivity ($\varepsilon^* = \varepsilon' - j\varepsilon''$) [-],

ε'' - loss factor (the imaginary part of the relative permittivity $\varepsilon^* = \varepsilon' - j\varepsilon''$) [-],

μ^* - complex magnetic permeability [-],

μ' - the real part of the relative permeability [-],

μ'' - the imaginary part of the relative permeability [-],

$\tan\delta$ – dielectric loss tangent [-],

$\tan\delta_\mu$ – magnetic loss tangent [-],

ε'_0 - the static dielectric constant [-],

ε'_∞ - the high frequency constant [-],

ω - the angular frequency ($\omega = 2\pi f$) [rad·s^{-1}],

λ - wavelength [m],

f – frequency [s^{-1}],

τ -the relaxation time for dipoles [s],

U_a – barrier potential of two alternated dipole positions in a solid material [kg·m^2·s^{-2}],

r - radius of the dipole [m],

μ - dynamic viscosity [kg·m^{-1}·s^{-1}],

k - the Boltzman's constant - 1.380×10^{-23} [kg·m^2·s^{-2}·K^{-1}],

T - temperature [K],

D_p - penetration depth [m],

P - power dissipated in a material [kg·m^2·s^{-3}],

μ_0 - permeability of free space - $4\pi \times 10^{-7}$ [kg·m·s^{-2}·A^{-2}],

ε_0 - permittivity of free space - 8.854×10^{-12} [A^2·s^4· kg^{-1}·m^{-3}],

E_{rms} - the root mean square of the electric field [kg·m·A^{-1}·s^{-3}],

H_{rms} - the root mean square of the magnetic field [A/m],

σ_0 - conductivity of a bulk metal [m^{-3}·kg^{-1}·s^3·A^2],

σ_e - conductivity of metal particles [m^{-3}·kg^{-1}·s^3·A^2],

E_0 - exterior electric field [kg·m·A^{-1}·s^{-3}]

Bibliography

1. *International Energy Outlook 2010.* [cited 2011 April 10th]; Available from: www.eia.gov/oiaf/ieo/index.html.
2. Peighambardoust, S.J., et al., *Review of the proton exchange membranes for fuel cell applications.* International Journal of Hydrogen Energy, 2010. **35**(17): p. 9349-9384.
3. Schlapbach, L. and A. Zuttel, *Hydrogen-storage materials for mobile applications.* Nature, 2001. **414**(6861): p. 353-358.
4. Schimmel, H.G., *Towards a Hydrogen-Driven Society? Calculations and Neutron Scattering on Potential Hydrogen Storage Materials*, in *Radiation, Radionuclides and Reactors, faculty of Applied Sciences*. 2005, Delft University of Technology: Delft. p. 144.
5. Zuttel, A., *FUELS - HYDROGEN STORAGE | Hydrides*, in *Encyclopedia of Electrochemical Power Sources*, G. Jurgen, Editor. 2009, Elsevier: Amsterdam. p. 440-458.
6. *Hydrogen production overview.* [cited 2011 April 4th]; Available from: http://www.fchea.org/core/import/PDFs/factsheets/factSheet_production.pdf.
7. Holladay, J.D., et al., *An overview of hydrogen production technologies.* Catal. Today, 2009. **139**(4): p. 244-260.
8. Kreith, F. and R. West, *Fallacies of a Hydrogen Economy: A Critical Analysis of Hydrogen Production and Utilization.* Journal of Energy Resources Technology, 2004. **126**(4): p. 249-257.
9. Haryanto, A., et al., *Current Status of Hydrogen Production Techniques by Steam Reforming of Ethanol: A Review.* Energy & Fuels, 2005. **19**(5): p. 2098-2106.
10. Chen, W.-H. and B.-J. Lin, *Effect of microwave double absorption on hydrogen generation from methanol steam reforming.* International Journal of Hydrogen Energy, 2010. **35**(5): p. 1987-1997.
11. Stankiewicz, A. and A.H. Drinkenburg, *Process intensification: History, philosophy, principles.*, in *Re-engineering the chemical processing plant*, A. Stankiewicz and J.A. Moulijn, Editors. 2004, NewYork Dekker. p. 1-32.
12. Van Gerven, T. and A. Stankiewicz, *Structure, Energy, Synergy, Time—The Fundamentals of Process Intensification.* Industrial & Engineering Chemistry Research, 2009. **48**(5): p. 2465-2474.
13. Poechlauer, P., *The Future for Cost-Effective, Environmentally Friendly Large-Scale API Production*. 2009.
14. Pennemann, H., et al., *Benchmarking of Microreactor Applications.* Organic Process Research & Development, 2004. **8**(3): p. 422-439.
15. Azcan, N. and A. Danisman, *Alkali catalyzed transesterification of cottonseed oil by microwave irradiation.* Fuel, 2007. **86**(17â€"18): p. 2639-2644.
16. Barnard, T.M., et al., *Continuous-Flow Preparation of Biodiesel Using Microwave Heating.* Energy & Fuels, 2007. **21**(3): p. 1777-1781.
17. Harmsen, G.J., *Reactive distillation: The front-runner of industrial process intensification: A full review of commercial applications, research, scale-up, design and operation.* Chemical Engineering and Processing: Process Intensification, 2007. **46**(9): p. 774-780.

18. Sharma, M.M. and S.M. Mahajani, *Industrial Applications of Reactive Distillation*, in *Reactive Distillation*. 2002, Wiley-VCH Verlag GmbH & Co. KGaA. p. 1-29.

19. Harvey, A.P., et al., *Operation and Optimization of an Oscillatory Flow Continuous Reactor.* Industrial & Engineering Chemistry Research, 2001. **40**(23): p. 5371-5377.

20. Mingos, D.M.P. and A.G. Whittaker, *Microwave dielectric heating effects in chemical synthesis*, in *Chemistry under Extreme or Non-Classical Conditions* R.V. Eldik and C. D.Hubbard, Editors. 1997, John Wiley and Sons: New York. p. 479-514.

21. Bogdal, D. and A. Prociak, *Microwave-Enhanced Polymer Chemistry and Technology*. 2007: Blackwll Publishing Profesional.

22. Chemat-Djenni, Z., et al., *Atmospheric Pressure Microwave Assisted Heterogeneous Catalytic Reactions.* Molecules, 2007. **12**(7): p. 1399-1409.

23. Clark, D.E. and W.H. Sutton, *Microwave Processing of Materials.* Annual Review of Materials Science, 1996. **26**(1): p. 299-301.

24. *Dielectric materials chart.* [cited 2011 June 7th]; Available from: http://www.eccosorb.com/file/1138/dielectric-chart.pdf.

25. Hayes, B.L., *Microwave Synthesis: Chemistry at the Speed of Light*. 2002, Matthews, NC: CEM Publishing.

26. Pozar, D.M., *Microwave Engineering*. 2nd Edition ed. 1998: John Wiley & Sons Canada, Ltd.

27. Dincov, D.D., et al., *A new computational approach to microwave heating of two-phase porous materials.* International Journal of Numerical Methods for Heat & Fluid Flow, 2004. **14**(6): p. 783-802.

28. Buchelnikov, V.D., et al., *Modeling of microwave heating of metallic powders.* Physica B: Condensed Matter, 2008. **403**(21-22): p. 4053-4058.

29. Nimtz, G., et al., *Size-induced metal-insulator transition in metals and semiconductors.* Journal of Crystal Growth, 1990. **86**(1-4): p. 66-71.

30. Zhang, X., et al., *Effects of Microwave Dielectric Heating on Heterogeneous Catalysis.* Catalysis Letters, 2003. **88**(1): p. 33-38.

31. Bond, G., et al., *Recent applications of microwave heating in catalysis.* Catalysis Today, 1993. **17**(3): p. 427-437.

32. Chen, C., et al., *Microwave effects on the oxidative coupling of methane over proton conductive catalysts.* Journal of the Chemical Society, Faraday Transactions, 1995. **91**(7): p. 1179-1180.

33. Zhang, X., et al., *Microwave assisted catalytic reduction of sulfur dioxide with methane over MoS2 catalysts.* Applied Catalysis B: Environmental, 2001. **33**(2): p. 137-148.

34. Zhang, X., et al., *Apparent equilibrium shifts and hot-spot formation for catalytic reactions induced by microwave dielectric heating.* Chemical Communications, 1999(11): p. 975-976.

35. Zhang, X., et al., *Carbon Dioxide Reforming of Methane with Pt Catalysts Using Microwave Dielectric Heating.* Catalysis Letters, 2003. **88**(3): p. 129-139.

36. Chang, Y.-f., et al., *Microwave-assisted NO reduction by methane over Co-ZSM-5 zeolites.* Catalysis Letters, 1999. **57**(4): p. 187-191.

37. Wang, X., et al., *Microwave effects on the selective reduction of NO by CH4 over an In–Fe2O3/HZSM-5 catalyst.* Chemical Communications, 2000(4): p. 279 - 280.

38. Bi, X.-j., et al., *Microwave effect on partial oxidation of methane to syngas.* Reaction Kinetics and Catalysis Letters, 1999. **66**(2): p. 381-386.
39. Roussy, G., et al., *Controlled oxidation of methane doped catalysts irradiated by microwaves.* Catalysis Today, 1994. **21**: p. 349-355.
40. Gupta, M. and E. Wong Wai Leong, *Microwaves and Metals.* 2007: Wiley.
41. Chemat, F., et al., *The Role of Selective Heating in the Microwave Activation of heterogeneous Catalysis Reactions Using a Continuous Microwave Reactor.* Journal of Microwave Power and Electromagnetic Energy 1998. **33**(2): p. 88-94.
42. Stuerga, D. and P. Gaillard, *Microwave heating as a new way to induce localized enhancements of reaction rate. Non-isothermal and heterogeneous kinetics.* Tetrahedron, 1996. **52**(15): p. 5505-5510.
43. Roussy, G., et al., *Permanent change of catalytic properties induced by microwave activation on 0.3% Pt/Al2O3 (EuroPt-3) and on 0.3% Pt-0.3% Re/Al2O3 (EuroPt-4).* Applied Catalysis A: General, 1997. **156**(2): p. 167-180.
44. Seyfried, L., et al., *Microwave Electromagnetic-Field Effects on Reforming Catalysts .: 1. Higher Selectivity in 2-Methylpentane Isomerization on Alumina-Supported Pt Catalysts.* Journal of Catalysis, 1994. **148**(1): p. 281-287.
45. Thiebaut, J.M., et al., *Durable changes of the catalytic properties of alumina-supported platinum induced by microwave irradiation.* Catalysis Letters, 1993. **21**(1): p. 133-138.
46. Perry, W.L., et al., *Kinetics of the Microwave-Heated CO Oxidation Reaction over Alumina-Supported Pd and Pt Catalysts.* Journal of Catalysis, 1997(171): p. 431–438.
47. Perry, W.L., et al., *On the possibility of a significant temperature gradient in supported metal catalysts subjected to microwave heating.* Catalysis Letters, 1997. **47**(1): p. 1-4.

2

Temperature measurements of solid materials in microwave applications[§§]

The accuracy and reproducibility of temperature measurements in solid materials under microwave heating is investigated in this work using two of the most celebrated temperature measurement techniques, namely fiber optic probes (FO) and infra red (IR) sensors. We investigate a number of effects ranging from purely technical issues, such as the use of a glass probe guide, over process operation parameters, such as the kind and the volume of the heated sample, to measurement related issues, such as the exact allocation of the probe in the sample. In this frame, the FO and IR methods are benchmarked. It was found that when using bare FO probes not only is their lifetime reduced but also the reproducibility of the results is compromised. Using a glass probe guide greatly assists in precise allocation of the probe in the sample resulting in more reproducible temperature measurements. The FO reproducibility, though, decreases with increasing temperature. Besides, contrary to conventional heating, the sample temperature decreases with decreasing sample mass (and volume) at constant irradiation power level confirming the volumetric nature of microwave heating. Furthermore, a strongly non-uniform temperature field is developed in the reactor despite the use of a monomode cavity and small amounts of samples. These temperature variations depending on the volume and position can only by detected by FO.

2.1 Temperature measurement techniques applied in microwave chemistry

Correct temperature measurement of the radiated materials is indeed the most important problem in both monomode and multimode microwave systems. The most popular temperature measurement techniques used during conventional heating, such as infra-red pyrometers, optical fiber thermometry or thermocouple, can be used during microwave processing with appropriate modification. Their most important features are summarized in Table 2.1. It is noted that temperature measurements under microwave conditions require special attention since the temperature measurement device should not disturb the microwave field, be affected by the field, or significantly disturb the thermal distribution within the sample [1].

Using conventional thermocouples is strongly discouraged due to interferences between the electromagnetic field and the metallic probe, which can potentially lead to sparking. Moreover, Pert at el. [1] placed a thermocouple into an empty microwave cavity with 150 W applied power at 2.45 GHz and found that the thermocouple indication was $100^{o}C$ while the ambient temperature was only $26^{o}C$. This supports the fact that the thermocouple itself can be heated directly by the microwave field. The sparking problem can be partially mitigated via shielding and grounding; the risk can not be completely avoided, though [2]. Some authors proposed to measure temperature with conventional thermocouple immediately after switching off the magnetron, but later experiments showed that this method considerably underestimated the temperature measured under microwave radiation [3, 4].

The most popular and widely used method for control of the reaction temperature in microwave applications is infrared thermometry (IR). Two IR measurement techniques are commonly used namely, IR sensors built-in microwave ovens and external IR cameras. Both techniques induce different problems depending on the particular application. It has been suggested by Stuerga and Gillard [5] that for heterogeneous solvent-free processes the IR measurement is more reliable than other techniques as it is non-invasive and independent of the thermal properties of the probe, i.e. its thermal capacity and thermal resistance. On the other hand it has been reported that using a

conventional IR sensor is not appropriate if a very accurate comparative study has to be performed [6, 7].

	Radiation pyrometer	Fiber optic thermometer	Thermocouple
Measurement range [°C]	-40 to 2000	-200-2000	-270-2300
Accuracy	$\pm$ 2 °C	0.5 °C	$\pm$ 0.5 - $\pm$ 2 °C
Response speed	Very fast	Fast/Very fast	Very fast
Interference with MW field	No	No [1]	Yes [2]
Cost	High	Mid to High	Very Low
Drawbacks	- Dependent on the reactor material - Sensitive to the emissivity magnitude - Suitable only for surface temperature measurements	Probe delicate and sensitive to contamination/degradation	- Interferes with the microwave field - Self-heated in a microwave field

Table 2.1. Comparison of the most popular temperature measurement techniques for microwave applications*

* References [1, 8]
[1]As long as the probe does not contain metal coating
[2]In specific cases can be significantly minimized

The IR technique, by nature, allows to measure temperature only on the surface of the reaction vessel or on the top surface of the reaction mixture. This makes the IR measurement accurate only for very thin sample layers, where the surface temperature is close to the bulk temperature. Another issue with IR sensors is the need for frequent recalibration due to their sensitivity to the ambient conditions and due to the dependency of the measured temperature on the material properties of the reaction vessel. Aside from IR sensors, Bogdal and Lukasiewicz [3, 9] measured the temperature of a well-absorbing solid material immersed in a low-absorbing solvent using a thermovision camera. Although the solid surface had a higher temperature than the boiling point of the surrounding solvent, no boiling of the solvent was observed even

near the surface. Moreover, due to the invert temperature gradient, the temperature recorded near the wall was lower than in the bulk of the solvent, although the contrary would be expected due to the hotter solid surface. This example shows how critical is to assure accurate temperature measurements in order to avoid not only quantitatively but also qualitatively misleading conclusions and trends in the underlying physics of the process under investigation.

Another temperature measurement method, widely used in microwave-assisted chemistry, is the fiber-optics thermometry (FO). This method presents many advantages compared to IR: 1) The FO measurement is independent of the reaction vessel material, 2) There is no need for recalibration before each experiment and 3) There is possibility to measure temperature inside the reaction vessel at various positions. It appears, therefore, that the FO technique offers a significant improvement. However, using FO requires that particular attention is paid to sensor positioning in order to avoid damaging of the probe and to ensure reproducible results. Although it is generally accepted that the application of FO for temperature measurement under microwave irradiation is one of the best techniques [7, 10, 11], Bogdal et al. [10] have shown that in viscous homogeneous reaction media or heterogeneous solid samples the temperature obtained via FO is only "local" temperature – different than the average bulk temperature.

Finally, it should be remarked that even in homogeneous liquid systems, the available technologies do not provide the appropriate tools to measure temperature in the micrometer scale; the presence of meso/microscopic hot spots is often regarded as the thermal effect that brings about the significant acceleration in reaction rates observed under microwave heating. Both IR and FO measure temperature at the macroscale and therefore the so-called meso/microscopic hot spots remain out of the measurement range. This chapter discusses temperature measurements in microwave applications, where solid particles are involved (e.g. in gas-solid/liquid-solid heterogeneous catalytic systems). Uniform heating of solid materials under microwave conditions is of paramount importance but difficult to achieve. In cases of reactors with fixed solid (catalytic) particles, high temperature gradients (in 3D) inside the reactor bed may develop, as opposed to liquid phase reactors, where stirring conditions can mitigate spatial temperature gradients. Therefore, multipoint temperature monitoring is crucial.

Nonetheless, measuring temperature in solid materials irradiated by electromagnetic waves is not a trivial task as a number of commonly applicable techniques are often impractical due restrictions arising from the design of the microwave applicator (limited access to the sample), the immunity of the sensor and possible loss of contact between the probe and the solids. Finally, the stochastic geometry inside the bed, due to random packing, results in reactor-microwave field interactions, which are very difficult, if not impossible, to predict and has implications in the controllability and reproducibility of the temperature field. The reproducibility and accuracy of the two most widely used techniques, FO and IR, was verified experimentally.

2.2 Materials and methods

Experiments were performed in a monomode microwave oven (Discovery – CEM Company) in 10 ml Pyrex glass vials (emissivity of 0.92 [12]) under ambient pressure and a constant microwave power of 10 W for 40 min. The cooling mode was switched off during the tests. Although Pyrex is not completely transparent for electromagnetic waves, heating experiments of an empty vial showed that for the microwave power applied in this study, no significant temperature rise was observed. The temperature was measured both via the built-in IR sensor of the device and via an external FO sensor (FISO Technologies – FOT-L-BA) simultaneously. The fiber optic sensor used in this study is a single-point sensor operating based on the Fabry-Pérot white-light interferometry technique. The sensor consists of two parallel perfectly flat semi-reflecting mirrors positioned at a certain distance from each other (few nanometers). The light passing through the first mirror is reflected back and forward between the mirrors. At each reflection a fraction of light is lost; therefore, each beam leaving the interferometer is less intensive. All reflected beams travel through the optical fiber to a signal conditioner, where the light is separated by a 2x2 coupler. The light sent to the light source is lost, whereas the rest of the light is directed and spread over a Fizeau wedge to reconstruct the interference pattern, which is detected and recorded by a charge coupled device (CCD). By finding the maximum intensity of the interference pattern related to changes of the optical path differences (generated by a temperature change) the temperature value can be calculated [13]. The temperature measured by the

FO probe was recorded with a multichannel fiber-optic signal conditioner (UMI 4), whereas the temperature measured by the IR sensor was read out from the display of the microwave oven. The IR sensor used in this study is a typical two-piece infrared temperature measurement system with separate electronics. Since the sensor is an integral part of the microwave applicator, it was considered as optimally configured by the manufacturer. The sensor operates over the spectrum 8-14 μm. Depending on the surface of the reactor used, manual correction of the emissivity and transmission over the range 0.1 to 1.1 may be necessary. These parameters have not been adjusted in our work, though, since the experiments were performed with testing vials delivered by the manufacturer of the microwave applicator and thus, they were considered optimized. The sensor allows temperature measurements between $-40^{\circ}C$ and $600^{\circ}C$ with accuracy of 1% over the entire range. The optical resolution of the used sensor is 10:1 and the spot size at 0 mm distance is 5 mm. Both sensors used in this study have been bought calibrated by the manufacturer.

Two undried catalytic supports, CeO_2-ZrO_2 and Al_2O_3, commonly used for steam reforming of oxygenated fuels (the reaction under investigation in our project) were employed for these tests. In each test, 2 g of the support was used unless otherwise stated. The CeO_2–ZrO_2 support was prepared by precipitation with an ammonia solution (32 wt%) from 0.2 mol solutions of cerium and zirconium nitrates (Aldrich, purity 99%). After filtration and subsequent washing with de-ionized water and drying at 120°C for 8 h, the hydroxide precursors were calcinated at 680°C for 12 h [14]. The prepared support was then crushed using a mortar and pestle and sieved to the desired fraction. The fraction between 70-125 μm was used for all tests. The Al_2O_3 support was commercially available (Alfa Aesar, purity 99.5%). As mentioned above, the experimental results presented in this work were obtained with support that was not dried before use. Some limited experiments with dried alumina samples (at $200^{\circ}C$ for several days) were also performed and resulted in lower steady-state temperatures (up to $35^{\circ}C$). Since the main aim in this work is to explore spatial temperature non-uniformities and benchmark FO and IR measurements, the results with dried alumina

are not presented here. It is finally noted, that all tests were repeated at least three times to improve the accuracy of the measured data.

2.3 Experimental

Five series of experiments, described below, were performed to elucidate different effects on temperature measurements under microwave heating. The most important findings are summarized in Table 2.2.

2.3.1 Effect of the probe guide.

The first experiment was performed with a CeO_2 – ZrO_2 sample. The sample was weighed and then inserted in the glass testing vial. The vial was closed with a Teflon cap. The FO was introduced in the sample (through a small opening in the cap) and positioned at the center by visual inspection. After each test, the vial was removed from the microwave cavity and put in a sample holder to cool down to ambient temperature. The cooled sample was then removed from the vial, weighed and placed back in the vial for the next test. As the FO sensor is more sensitive and accurate ($0.1^{o}C$), the temperature measured by the FO probe was noted every 10 seconds during the first 10 minutes of the experiment and then every 1 minute until the end of the test. Due to the measuring accuracy of the IR sensor being coarser (only $1^{o}C$), the temperature readout from the microwave unit was noted with random frequency, but at least once every 3 minutes.

Figure 2.1 shows that the temperature measured by the IR sensor is clearly lower than that measured by FO. Moreover, two tests with FO gave temperature results that differ up to $9^{o}C$. It is not surprising that the IR sensor ensures better reproducibility than FO, as it is permanently attached to the microwave unit and is able of measuring temperature at a precisely defined spot (i.e. at the exterior of the glass vial bottom). On the other hand, the position of the FO probe in two different experiments cannot be exactly the same as the sensor is flexible and tends to bend.

Exp. #	Sample	Effect	Major observation	Max. Temp. recorded by IR [°C]	Max. Temp. recorded by FO [°C]
1	2 g CeO$_2$-ZrO$_2$	Without probe guide	No reproducible measurements	70	70-80
2	2 g CeO$_2$-ZrO$_2$	With probe guide	Reproducible measurements	65	70
3	2 g Al$_2$O$_3$	Kind of heated sample	The FO reproducibility deteriorates with increasing temperature	90	140
4	0.5 g Al$_2$O$_3$	Sample volume	• The FO recorded temperature depends on the sample volume • IR significantly under predicts the reactor temperature • IR is relatively insensitive to variations in the amount of solids	95	110
5	2 g CeO$_2$-ZrO$_2$	Temperature uniformity in the axial direction	• Temperature non-uniformity in the axial direction • The IR sensor consistently underestimates the actual temperature in various positions inside the reactor	62[*]	63-69
6	2 g Al$_2$O$_3$	Temperature uniformity in the axial direction		90	128-138[*]
7	2 g Al$_2$O$_3$	Temperature uniformity in the radial direction	• Temperature non-uniformity in the radial direction. Maximum temperature at the center • Same conclusion for the IR method as in experiment #6	100	110/140[**]

Table 2.2. Summary of experimental tests

[*]Depends of the probe position
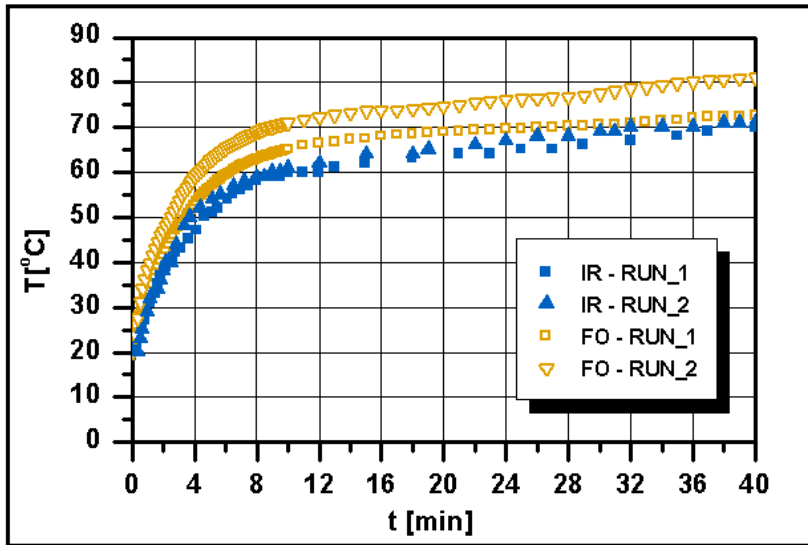[**]Depends of the sensor position

Figure 2.1. Comparison of temperature profiles obtained with IR and FO for a 2 g CeO$_2$-ZrO$_2$ sample. The FO recorded temperature is measured on the vertical centerline at 6 mm above the bottom of the glass vial. Only the bare probe without glass protection was inserted in the sample.
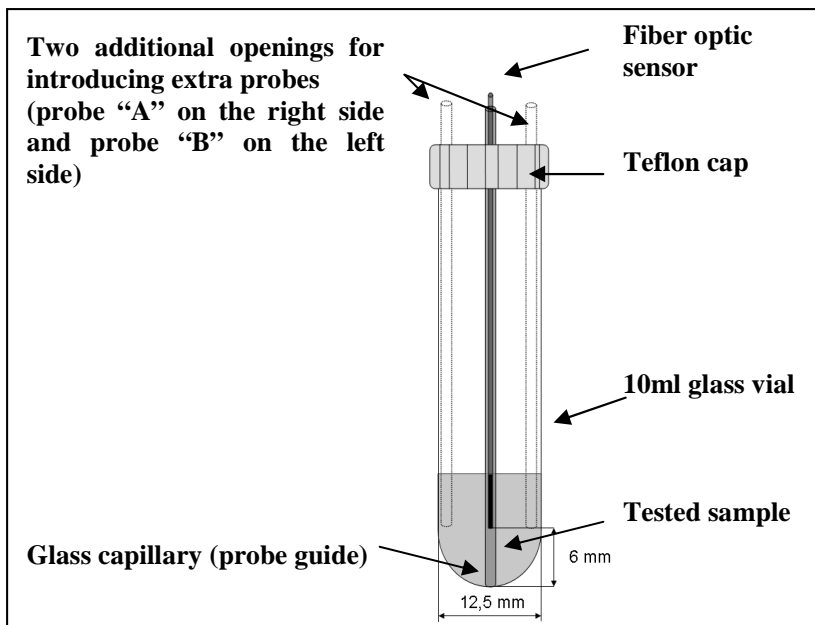

Figure 2.2. Schematic view of the 10 ml glass vial containing 2 g of solid sample with inserted fibre optic sensor

Moreover, insertion of the delicate probe in a bed of solid particles results in partial degradation of its material.

To achieve more reproducible results and protect the probe against breaking the rest of experiments were performed with the FO probe introduced into the sample through a 2 mm O.D. capillary made from borosilicate glass (Figure 2.2).

This "probe guide" was placed inside the vial in such a way that the position of the FO probe could change in the axial direction if needed. Although it was possible to move the sensor inside the glass capillary, the FO probe fitted the capillary tightly enough to prevent position change during the measurements. To ensure the correct position, marks were put both on the probe and on the glass capillary. At the desired probe location, the two marks overlap with each other. All subsequent experiments have been performed with the probe (in the glass capillary) situated 6 mm above the bottom of the vial unless otherwise stated. This specific location of the tip of the FO probe was chosen such that side effects of the vial walls are minimized and the central position of the probe inside the sample is ensured. It should be noted here that the spatial temperature measurements in this work refer to the distance of the tip of the probe from the bottom of the vial. It is stressed, however, that the set of mirrors of the sensor interferometer is located ~2 mm above the tip of the probe. Figure 2.3 shows that when a glass probe guide was applied (open symbols) the reproducibility of temperature measurements by FO was significantly improved in comparison to results obtained without the probe guide (open symbols, Figure 2.1). It can be seen that the temperature profiles with FO in all three runs of Fig.2.3 virtually overlap (0.5°C margin of error). Finally, it was observed that application of a probe protection greatly increases the lifetime of the FO probe.

2.3.2 Effect of the heated sample

The CeO_2-ZrO_2 is not a good microwave energy absorber. Therefore, it was decided to also perform another set of experiments with a different material. The aim of changing the test material was to investigate whether its ability to absorb microwave energy has any influence on the reproducibility of the temperature measurements. From a wide pallet of different catalytic supports for ethanol steam reforming Al_2O_3 was

chosen. Although Al_2O_3 is described in the literature as a low microwave energy absorber, it has been concluded experimentally that it is a much better absorber than CeO_2-ZrO_2.

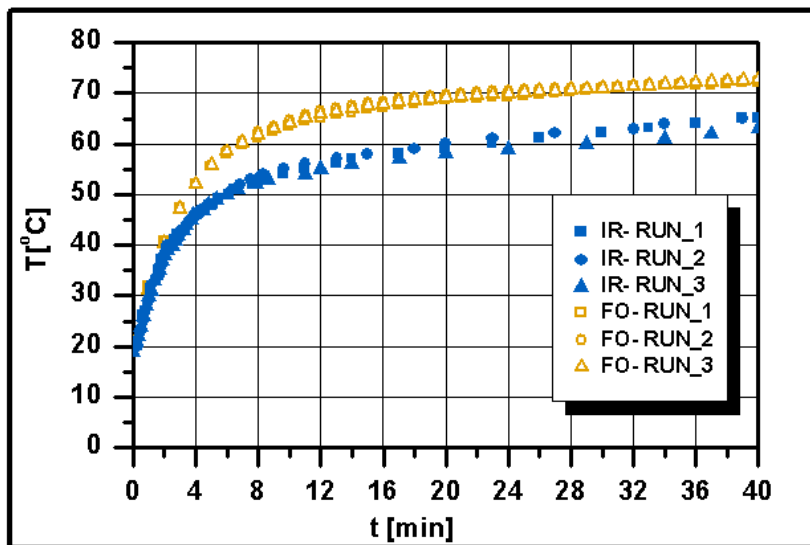**Figure 2.3. Comparison of temperature profiles obtained with IR and FO for a 2 g CeO_2-ZrO_2 sample. The FO recorded temperature is measured on the vertical centerline at 6 mm above the bottom of the glass vial. Now the FO probe is placed in a glass probe.**

Figure 2.4 shows that the measurement reproducibility for three samples tested in sequence was 5^oC for both the FO and IR sensor at steady state. This error is almost the same as that obtained with IR at the low temperature experiments when testing CeO_2-ZrO_2 but ~1 order of magnitude higher than that obtained with FO in case of CeO_2-ZrO_2 (5^oC vs. 0.5^oC). Therefore, it is concluded that the reproducibility with the FO method deteriorates with increasing temperature (better microwave absorbers). Besides, figure 2.4 shows that the temperature recorded with the IR method is ~45-50^oC lower than that with the more reliable FO method at steady state. This should be contrasted to ~10^oC difference in Figure 2.3 displaying experiments with CeO_2-ZrO_2 at a lower temperature level and manifests an increasing discrepancy between the two methods as the temperature level increases. It is remarked here that the Discover system is tailor made for organic synthesis with solvents under magnetic stirring conditions. Therefore, it can be expected that since the solid particles in our work are not stirred, discrepancies between the temperature readings of the FO and the IR sensor will occur. However, in a

fixed bed reactor, as the one we study, the catalytic support is inherently static and thus the same issue will actually be present in other types of commercial monomode and multimode microwave cavities as well. To this end, it is one of the targets of this work to identify the problem and quantify the discrepancies between the actual internal temperature measurements with the optical fibers and the output of the infrared thermometer.
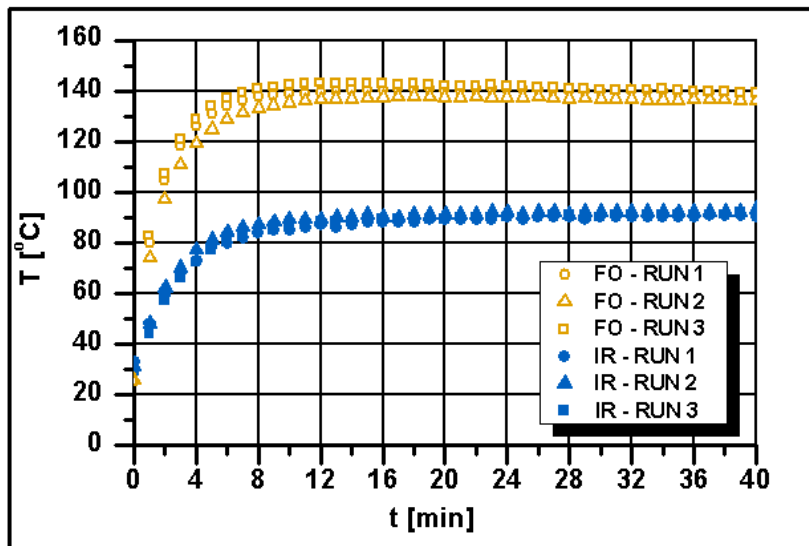

Figure 2.4. Comparison of temperature profiles obtained with IR and FO for a 2 g Al$_2$O$_3$ sample. The FO recorded temperature is measured on the vertical centerline at 6 mm above the bottom of the glass vial.

2.3.3 Effect of the sample volume

Due to Al$_2$O$_3$ having a lower volumetric density than CeO$_2$-ZrO$_2$ a larger volume of Al$_2$O$_3$ is irradiated when using equal mass samples, as was the case in the previous section. This difference may affect the sample temperature since microwave energy provides volumetric heating [15, 16]. Therefore, another set of experiments was performed using IR and FO with a smaller amount of Al$_2$O$_3$ sample (0.5 g) in order to keep the volume equal to that of 2 g of CeO$_2$-ZrO$_2$. Figure 2.5 presents the sample temperature measured by IR and FO as a function of time for the two supports. Several interesting conclusions are obtained: 1) The temperature measured by the FO probe is significantly lower (by ~30°C) in the 0.5 g sample than in the 2 g one thus confirming

the volumetric character of microwave heating. Furthermore the CEM Discover has an electric field maximum at the highest part of the vial, which may result in a more effective interaction between the electromagnetic field and the sample as the sample volume increases. It should be underscored here that in conventional heating the reverse effect is expected; application of equal amount of power to a smaller sample would *increase* its temperature as the total heat capacity decreases. 2) Same as in section 3.2, the IR sensor predicts significantly lower temperatures (~30°C) compared to the FO method and 3) The IR is relatively insensitive to variations in the amount of solids; the temperature registered by IR in case of the 0.5 g sample is only 5-7°C lower than that of the 2 g sample (Figure 2.5). Physically counterintuitive notwithstanding, it is actually not surprising if one bears in mind that the IR sensor actually measures temperature at the exterior of the vial glass bottom rather than in the sample itself.
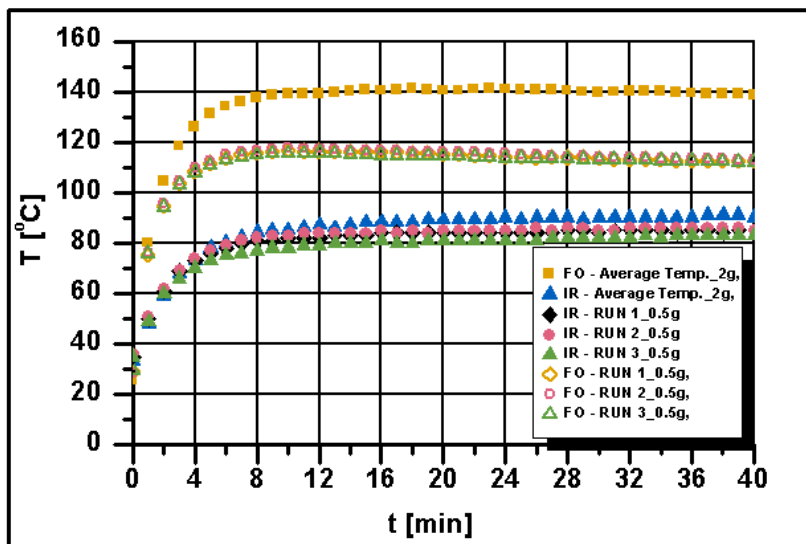

Figure 2.5. Comparison of temperature profiles obtained with IR and FO for 0.5 g and 2 g Al$_2$O$_3$ samples. The FO recorded temperature is measured on the vertical centerline at 6 mm above the bottom of the glass vial.

2.3.4 Effect of the vertical (axial) position

To evaluate temperature uniformity a set of experiments was performed in which the position of the FO probe varies along the vertical centerline. At the beginning of each run the FO sensor is located 10 mm above the bottom of the vial. After 30 min of

irradiation, when the sample temperature reaches steady state, the position of the probe is lowered by 2 mm (i.e. a position located 8 mm above the glass bottom). As the response time of the FO is relatively short, the new temperature was measured within a few seconds and, subsequently, a new steady state temperature was reached. After one minute, the position of the sensor was changed again to the next position situated 2 mm below the previous one. This procedure was repeated until the sensor was situated exactly at the bottom of the vial. At the end of the experiment, after the sensor had been located on the bottom of the vial for 1 min, the position was changed back to the first position of 10 mm.

Figure 2.6 shows the results of this experimental procedure in terms of temperature vs. time in the event of CeO_2-ZrO_2 support using an FO probe and an IR sensor. The inset in Fig. 6 is a zoom-out of the upper left window of the graph and is meant to present clearly the temperature variation as the position of the FO probe changes. An ascending temperature trend is observed as the FO probe moves deeper in the sample and a maximum ΔT of 6°C is found along the vertical axis; this ΔT is not negligible considering that it characterizes a very short sample length of 1 cm and is ~10% of the absolute temperature recorded (~60°C). It is also surprising that at the 0 mm position (the sensor touches the glass wall from the inside) the temperature measured by the FO probe, on the inside wall of the vial, is quite higher than the temperature measured on the outside, by the IR sensor (>6°C difference). Albeit the temperature measured on the inside should be higher than outside due to the invert temperature gradient in microwave heating, such a large difference was not expected after 35 min of radiation when the temperature profile had already reached steady state.

Figure 2.7 is the counterpart of Fig. 2.6 in the case of Al_2O_3. Unlike CeO_2-ZrO_2, a descending temperature trend is now observed as the probe moves deeper in the sample. The maximum temperature difference along the height of the sample is now ~10°C. Despite the decrease, the temperature measured by the FO probe on the internal glass wall of the vial bottom is ~35°C higher than the temperature measured at the same time by the IR sensor on the outside of the vial. The take-home message from this experimental parametric study with respect to the axial FO probe position is twofold: 1) the temperature field obtained when irradiating even small amounts of solid particles in

monomode cavities is *non-uniform*. Multiple-coordinate measurement is needful to map out the reactor temperature. 2) The IR sensor consistently underestimates the actual temperature in various positions inside the reactor. The modeler and the experimentalist should be rather circumspect in accepting the IR output as a representative reactor temperature.
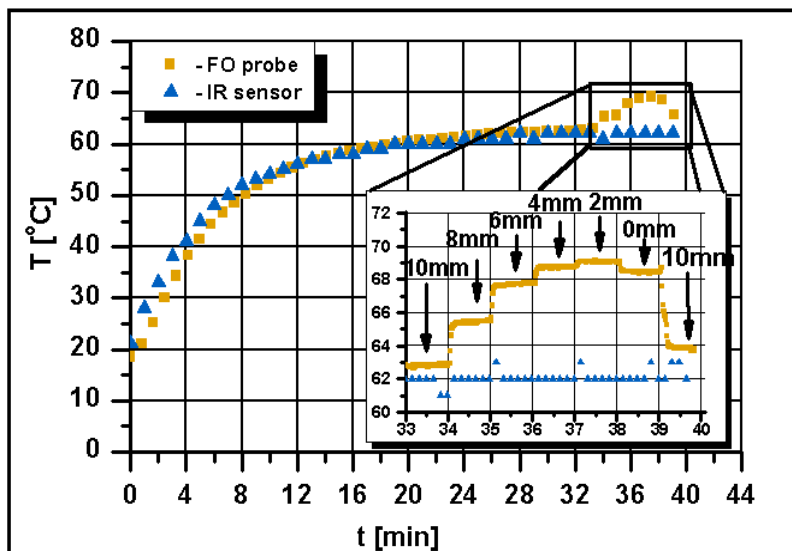

Figure 2.6. Comparison of temperature profiles obtained with IR and FO for a 2 g CeO$_2$-ZrO$_2$ sample. The FO recorded temperature is measured on the vertical centerline of glass vial at 10 mm above the bottom of the glass vial. The inset shows the temperature distribution along the vertical centerline at steady state.

2.3.5 Effect of the horizontal (radial) position

In this section, we investigate temperature variation in the horizontal plane (radial direction). Temperature was measured with three FO probes inside the sample of 2.5 g crushed Al$_2$O$_3$ pellets. Three fiber optic probes were introduced into the tested sample, via glass capillaries, in three positions being on the left side near the vial wall, in the middle (as in the previous experiments), and on the right side near the vial wall (Figure 2.2). All probes measure temperature simultaneously on the same horizontal plane at 6 mm above the bottom of the vial. The temperature measured by IR, on the outside wall of the bottom of the vial, has been recorded as well.

Figure 2.8 presents the horizontal temperature distribution, as recorded by FO, as well as the IR indication vs. time. The probe on the right side is designated as "FO-

Right" the probe in the middle as "FO-Center" and the probe on the left side as "FO-Left". The highest temperature is reached at the center of the sample (Figure 2.8). This is not surprising given that the cavity is designed such that the maximum electric field strength occurs at the center. The two side probes show almost the same temperature at steady-state (nearly symmetrical profile), which is ~40°C lower than that in the middle. Moreover, the IR indications (solid square symbols) are always quite lower than the FO indications. All in all, the findings here confirm the conclusions of the previous section, which are the presence of temperature non-uniformity not only in the axial but also in the radial direction as well as the inability of the IR method to yield reliable reactor temperature indications.
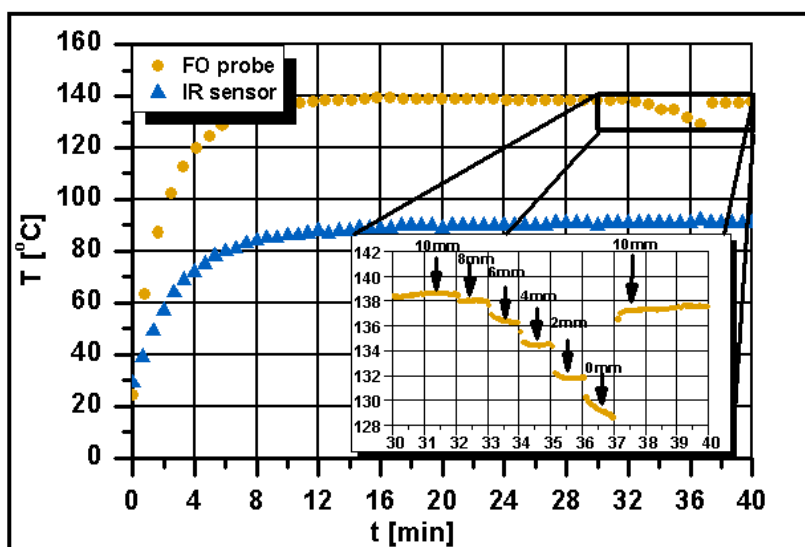

Figure 2.7. Comparison of temperature profiles obtained with IR and FO for a 2 g Al$_2$O$_3$ sample. The FO recorded temperature is measured on the vertical centerline of the glass vial at 10 mm above the bottom of the glass vial. The inset shows the temperature distribution along the vertical centerline at steady state.
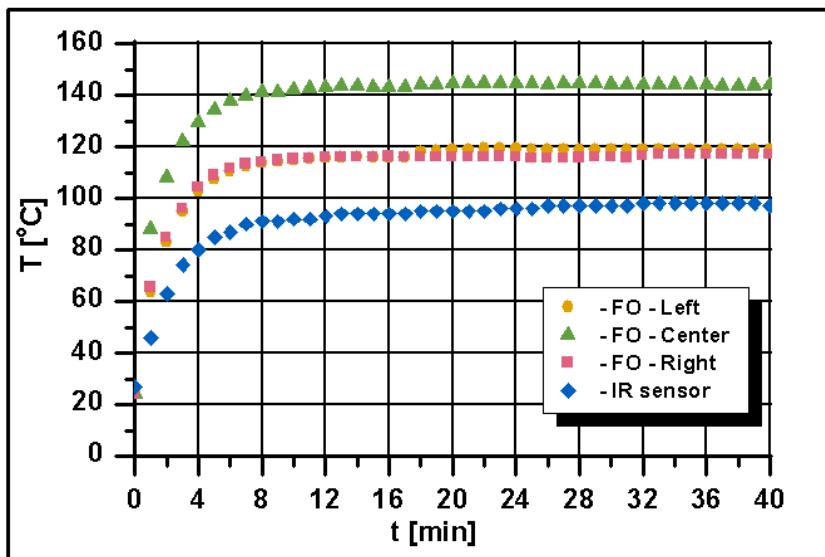
Figure 2.8. Horizontal temperature distribution profiles obtained with FO inside a 2.5 g Al$_2$O$_3$ sample at 6 mm above the bottom of the glass vial. The black square dots denote the IR temperature indication.

2.3.6 Effect of metal concentration on catalyst heating

To investigate the ability of catalyst to be heated by microwave radiation, a number of experiments was performed with different catalyst composition. Four types of catalyst have been investigated - Rh/CeO$_2$-ZrO$_2$, Rh/Al$_2$O$_3$, Ni/CeO$_2$-ZrO$_2$ and Ni/Al$_2$O$_3$ in the context of this research.

In most cases, higher temperature was observed for the catalyst with higher metal concentration. For instance, the Rh/CeO$_2$-ZrO$_2$ catalyst containing 4.2% Rh was able to reach very high temperatures (up to 260°C) in a relatively short time (~4 min), whereas for the same time period, a sample containing 2% Rh reached up to 115°C only. Furthermore, the temperature attained by the pure catalytic support was almost three times lower (~60°C) (Figure 2.9). The effect is more pronounced with the CeO$_2$-ZrO$_2$ support than with the Al$_2$O$_3$ support, where the maximum temperature reached was up to ~160°C at steady state conditions for 5% Rh loading (Figure 2.10).
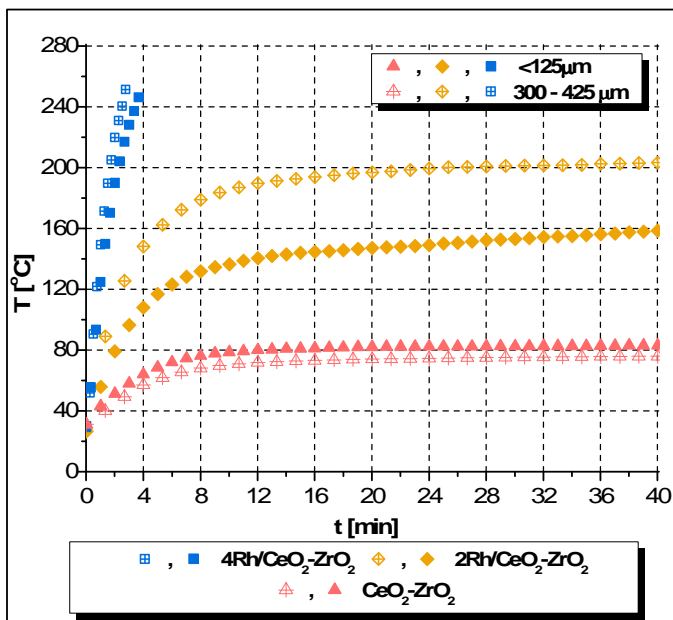
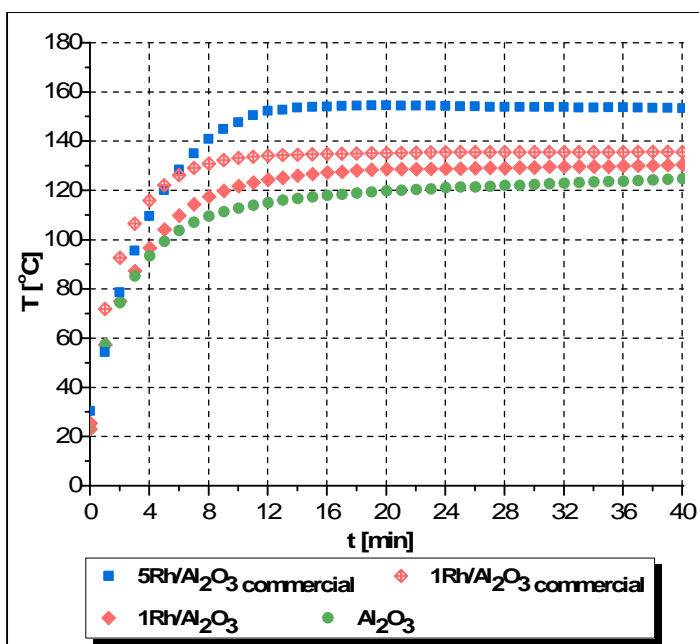**Figure 2.9. Effect of metal concentration and particle size on temperature during microwave irradiation of Rh/CeO$_2$-ZrO$_2$ catalysts**

Figure 2.10. Effect of metal concentration and particle size on temperature during microwave irradiation of Rh/Al$_2$O$_3$ catalysts
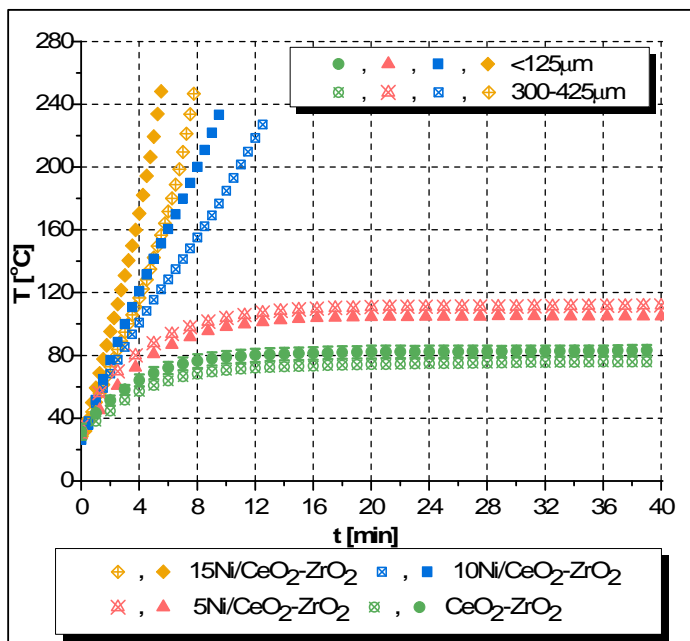
Figure 2.11. Effect of metal concentration and particle size on temperature during microwave irradiation of Ni/CeO$_2$-ZrO$_2$ catalysts

Further, nickel-based catalysts demonstrate similar behaviour. For instance, Ni/CeO$_2$-ZrO$_2$ with 15% and 10% Ni loading reach very high temperatures (~240 ^{o}C) after a short irradiation time, whereas low Ni loading (5%) results in significantly lower temperatures (<120°C) (Figure 2.11).

When the Ni/Al$_2$O$_3$ catalyst was examined, it was discovered that it behaves different than the other examined catalysts (Figure 2.12). More specifically, when the temperature profiles for the Ni-catalyst are compared among each other, the trend is the same as for Ni/CeO$_2$-ZrO$_2$ and both Rh catalysts, that is, increasing metal concentration results in higher temperature. However, in comparison to the alumina support only (Figure 2.12), the temperatures attained with the Ni/Al$_2$O$_3$ catalysts are significantly lower. Moreover, although the maximum concentration of Ni on Al$_2$O$_3$ support is as high as for the CeO$_2$-ZrO$_2$ based catalyst and three times higher (up to 15%) than the Rh catalysts, the temperature obtained for Ni/Al$_2$O$_3$ is much lower (65°C for 15%Ni) (Figure 2.12). In addition, not only are the reached temperatures much lower compared to the Rh-catalyst, but the influence of metal concentration on the attained temperature

is also much weaker. The results for Al_2O_3 and Ni-impregnated Al_2O_3 seem to be contradicting.

2.3.7 Effect of catalyst particles size on catalyst heating

Another parameter that has been investigated is the influence of catalyst particle size on temperature. To investigate this effect each catalyst has been prepared in two different particles sizes – below 125µm and between 300-425µm. Experiments have demonstrated that whether bigger particles are heated more efficiently than smaller ones, or vice versa, is strongly dependent on the type of catalyst and on the metal concentration in the catalytic support. In the case of the CeO_2-ZrO_2 catalyst, significant temperature differences between each granulation range are noted (Figure 2.9 and Figure 2.11). On the contrary, the effect is negligibly small with the Al_2O_3 catalyst (Figure 2.12).
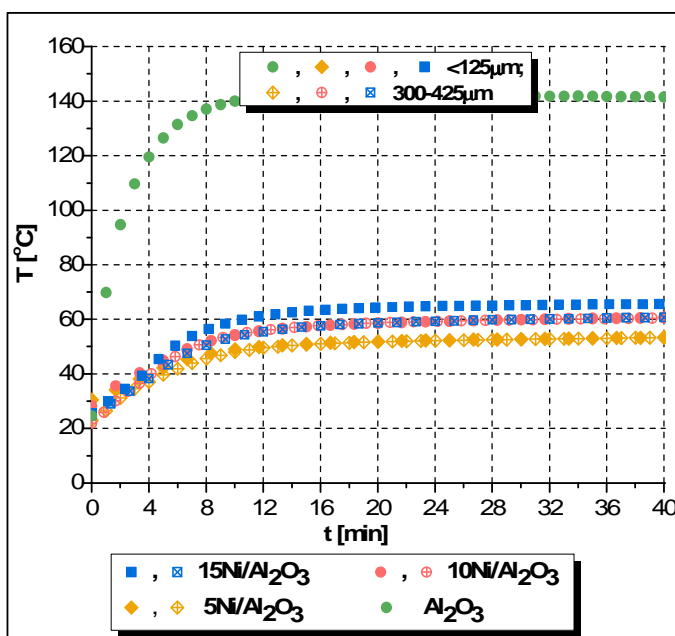

Figure 2.12. Effect of metal concentration and particle size on temperature during microwave irradiation of Ni/Al$_2$O$_3$ catalysts

With respect to the type of the doped metal, it can be seen that in the case of Ni catalyst, smaller particles are heated more rapidly, whereas in the case of Rh catalyst,

the trend is opposite. It must be noticed that, regardless of the observed trend, the temperature differences between smaller and bigger particles of the same catalyst are more pronounced for catalysts with higher metal concentration and are hardly visible for low or no metal loading.

2.3.8 Conclusions

Two of the most celebrated temperature measurement techniques (i.e. fiber optic probes (FO) and infra red (IR) sensors) have been benchmarked in the context of microwave heating of solid particles (CeO_2-ZrO_2 and Al_2O_3 particles) with a number of important applications in heterogeneous catalysis. It was found that when using bare FO probes their lifetime is reduced and the reproducibility of the results compromised. Using a glass probe guide greatly assists in precise positioning of the probe and thus in obtaining reproducible temperature measurements. The FO reproducibility, though, decreases with increasing temperature level. Besides, contrary to conventional heating, the sample temperature decreases with decreasing sample mass (and volume) at constant irradiation power level confirming the volumetric nature of microwave heating. This temperature change can be detected by an FO probe immersed in the sample; on the other hand, IR remains nearly insensitive to it, at it actually measures temperature at the exterior of the vial glass wall. Furthermore, significant temperature non-uniformities were found by using FO in both the axial and radial direction despite the use of a monomode cavity and the small amount of samples tested. This indicates that temperature measurements at multiple coordinates are requisite to obtain the temperature map in the reactor. Once again, IR was unable to capture these spatial variations and consistently underestimated the real temperature in various positions in the reactor.

With respect to the effect of metal loading, higher temperatures are observed for the catalyst with higher metal concentration. However, not every catalyst is as easily heated under microwave conditions. An example is the Ni/Al_2O_3 catalyst. In this case, not only are the reached temperatures are much lower than for Rh-catalyst, but the influence of metal concentration on the attained temperature is also much weaker.

Experiments have demonstrated that the catalyst particle size plays a significant role in the microwave heating process. The observed effect depends on the type of catalyst and metal loading. The CeO_2-ZrO_2 catalyst demonstrates a stronger effect than the Al_2O_3-based catalyst, which becomes more pronounced for high metal concentrations. The effect seems to be governed by the type of metal; however, the available data are not sufficient to draw conclusions. At present, no consistent explanation can be given for the effect of grain size on temperature.

Bibliography

1. Pert, E., et al., *Temperature Measurements during Microwave Processing: The Significance of Thermocouple Effects.* Journal of the American Ceramic Society, 2001. **84**(9): p. 1981-1986.
2. Will H., et al., *Multimode Microwave Reactor for Heterogeneous Gas-Phase Catalysis.* Chemical Engineering & Technology, 2003. **26**(11): p. 1146-1149.
3. Bogdal, D., et al., *Microwave-assisted oxidation of alcohols using Magtrieve(TM).* Tetrahedron, 2003. **59**(5): p. 649-653.
4. Will, H., et al., *Heterogeneous Gas-Phase Catalysis Under Microwave Irradiation—a New Multi-Mode Microwave Applicator.* Topics in Catalysis, 2004. **29**(3): p. 175-182.
5. Stuerga, D. and P. Gaillard, *Microwave heating as a new way to induce localized enhancements of reaction rate. Non-Isothermal and heterogeneous kinetics.* Tetrahedron, 1996. **52**: p. 5505-5510.
6. Herrero, M.A., et al., *Nonthermal Microwave Effects Revisited: On the Importance of Internal Temperature Monitoring and Agitation in Microwave Chemistry.* J. Org. Chem., 2008. **73**(1): p. 36-47.
7. Nüchter M., et al., *Contribution to the Qualification of Technical Microwave Systems and to the Validation of Microwave-Assisted Reactions and Processes.* Chemical Engineering & Technology, 2005. **28**(8): p. 871-881.
8. Childs, P.R.N., et al., *Review of temperature measurement.* Review of Scientific Instruments, 2000. **71**(8): p. 2959-2978.
9. Lukasiewicz M., et al., *Microwave-Assisted Oxidation of Side Chain Arenes by Magtrieve.* Advanced Synthesis & Catalysis, 2003. **345**(12): p. 1269-1272.
10. Bogdal, D., et al., *Microwave induced thermal gradients in solventless reaction systems.* Tetrahedron, 2006. **62**(40): p. 9440-9445.
11. Moseley, J.D., et al., *The importance of agitation and fill volume in small scale scientific microwave reactors.* Tetrahedron Letters, 2007. **48**(35): p. 6084-6087.
12. Green, D.W. and R.H. Perry, *Perry's Chemical Engineers' Handbook.* 8th Edition ed. : McGraw-Hill. .
13. Pinet, É., *Fabry-Pérot Fiber-Optic Sensors for Physical Parameters Measurement in Challenging Conditions.* Journal of Sensors, 2009. **2009**: p. 9.
14. Diagne, C., et al., *Hydrogen production by ethanol reforming over Rh/CeO2-ZrO2 catalysts.* Catalysis Communications, 2002. **3**: p. 565-571.
15. Hoz, A.d.l., et al., *Microwaves in organic synthesis. Thermal and non-thermal microwave effects.* Chemical Society Reviews, 2005. **34**(2): p. 164-178.
16. Kappe, C.O., *Controlled Microwave Heating in Modern Organic Synthesis.* Angewandte Chemie International Edition, 2004. **43**(46): p. 6250-6284.

3

Microwaves and heterogeneous catalysis[*]

The effects and interactions of microwaves irradiation with gas-solid catalytic reaction systems have been presented. The application of microwave heating in heterogeneous catalytic reaction systems has been reviewed. The experimental and numerical approaches have been shown. Temperature measuring methods applicable for the microwave dielectric heating of solid particles has been discussed. The temperature distributions of the solid particles bed have been examined in order to perceive existence of the thermal gradients when the catalytic bed is exposed to microwaves.

3.1 Application of the microwaves to heterogeneous gas-solid catalysis

The concept of using microwave energy as an activation source for heterogeneous catalytic reactions has been studied since early eighties. For many chemical reactions significant improvements of conversion and/or selectivity and a reduction of reaction time have been reported [1-5].

One of the first groups who applied microwave energy for gas–solid chemical reactions was the group of Wan. Ioffe, Pollington and Wan [6] studied the catalytic conversion of methane to acetylene over activated carbon. Higher selectivity to acetylene was observed compared to the conventional heating. It was postulated that non-uniform temperature conditions inside the catalytic bed could be present, especially when the catalyst consisted of randomly oriented particles or pellets. This temperature gradient may have been responsible for the observed high selectivity for acetylene.

The group of Wan also reported on other microwave-assisted catalytic reactions including decomposition of olefins [7], decomposition of organic halides over alumina-supported iron oxide catalyst [8], synthesis of cyanide [9], synthesis of methane from carbon dioxide and water over nickel catalyst [10, 11], methane decomposition to C_2 and C_3 hydrocarbons [6, 12, 13], production of acetylene via the reactions of carbon and water [10, 14] or oxidation of hydrocarbons by water [10, 12]. However, lack of information about applied temperature measurement techniques and the fact that the results in the microwave system were compared with literature data only create difficulties in evaluation of the obtained results.

To investigate the influence of microwave irradiation on gas-solid catalysis Whittaker and Mingos [15] performed simple experiments to synthesize a range of metal chlorides, oxochlorides, bromides and nitrides by direct combination of metals with gases. However, similarly to the studies of Wan and coworkers no experiments with conventional heating were performed.

Zhang *et al.* [16] studied the catalytic reduction of sulfur dioxide with methane to form carbon dioxide and sulfur over MoS_2/Al_2O_3 catalysts. A higher conversion of SO_2 and CH_4 was claimed when microwave heating was applied. The conversion under

electromagnetic field was as high as the one obtained with the conventional heating at temperatures around 200 K higher (Figure 3.1).
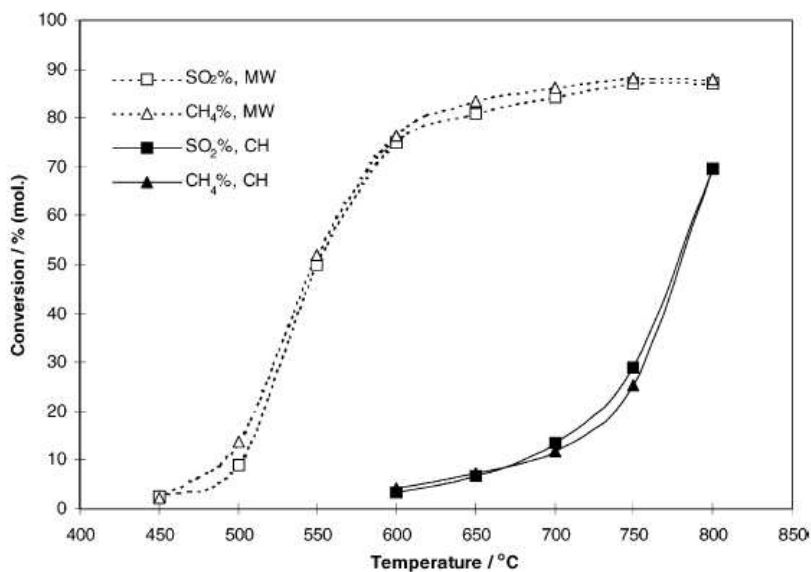

Figure 3.1. SO_2 and CH_4 conversion as a function of temperature over catalyst MC-2 (Reprinted from *Appl. Catal. B: Environ.*, X. Zhang, D. O. Hayward, C. Lee, D. M. P. Mingos,, Microwave assisted catalytic reduction of sulfur dioxide with methane over MoS2 catalysts ,137-148, Copyright (2001), with permission from Elsevier)

Zhang, Hayward and Mingos [17] investigated the decomposition of hydrogen sulphide. When the reaction was carried out with conventional heating the results obtained were in very good agreement with the equilibrium data. When the microwave heating was applied the conversion of H_2S was twice the one obtained in the previous experiment at the same temperature.

Microwave irradiation was also studied in the reduction of SO_2 and NO_x. The first study was published by Tse [12] in 1990. The reaction was performed in a microwave pulsed reactor with a Ni-based catalyst. Significant decrease of the SO_2 concentration and production of O_2 were observed. Another work in this field was published by Cha [18] who investigated the NO_x and SO_2 decomposition in a char-bed reactor. A significant reduction of SO_2 and NO_x concentrations was observed when microwave power was applied.

Another approach to the NO_x reduction was presented by Cha and Kong in their work on microwave–enhanced adsorption and reaction on carbon-based adsorbents [19, 20]. Investigation of the decomposition of NO_x to N_2 over a coal-based adsorbent

showed that by applying microwave energy NO_x can be easily reduced. Moreover, the regeneration of the adsorbent under microwave conditions increases the adsorption capacity and rate of NO_x adsorption in the subsequent adsorption cycle. Chang and Wang [21, 22] used ZSM-5 zeolite based catalysts for the reduction of NO with methane. It was demonstrated that microwave irradiation significantly increased the reduction of NO. Under conventional heating some catalysts showed no conversion of NO and CH_4 even at high temperature, while under the microwave heating conversion around 35% was observed.

Roussy *et al.* [23, 24] who studied the oxidative coupling of methane reported that the C_2 selectivity was much higher under the microwave irradiation than conventional heating especially at low conversions (0-40 %). The C_2 selectivity under microwave irradiation was almost constant (60 %) within the whole reaction temperature range investigated (550-750 ^{o}C) while for the conventional heated process the selectivity was systematically increasing with increasing reaction temperature, to achieve 60 % at 700°C.

Zhang *et al.*[25] who investigated the same reaction as Roussy *et al.*[23, 24] discovered that when methane was converted to higher hydrocarbons in the absence of oxygen, the microwave radiation had significant effect on the achieved conversion and selectivity. The effect was explained by arcing and plasma formation. However, when reaction was carried out in the presence of oxygen no microwave effect was observed.

Marun, Conde and Suib *et al.* [26, 27] investigated oligomerization of methane to higher hydrocarbons over nickel powder, iron powder and activated carbon catalysts in the presence of helium. Selectivity and product distribution of C_2's were investigated as a function of applied power, microwave frequency and used catalyst. However, the results from microwave experiments were compared neither with literature data nor with the results from conventionally heated system.

Perry *et al.* [28, 29] studied CO oxidation over Pt and Pd/γ-Al$_2$O$_3$ catalysts in a dedicated microwave system. A higher rate was observed when microwave heating was applied. However, the authors concluded that the observed effect was related more to inaccurate temperature measurements than to the microwave irradiation. Furthermore, the theoretical analysis on possible hot-spot formation showed that local overheating of

the catalyst active sites is in a range of magnitude 10^{-10}K which is far below detection limit of any temperature measuring technique.

The CO oxidation reaction was investigated also by Silverwood *et al.* [30, 31]. A comparison study between the conventional and the microwave system showed no significant difference in conversion.

Seyfried *et al.* [32], Thiebaut *et al.* [33], Roussy *et al.* [34] studied the isomerization reaction of 2-methylpentane over Pt/Al_2O_3 catalyst under the microwave and conventional heating. Higher conversion of reactants was observed when the reaction was carried out in the presence of electromagnetic field. Also, an increased selectivity of isomers, by factor 2, was reported. However, this effect was only observed when the thermal treatment of catalyst was also carried out under the microwave conditions. It was suggested that the higher selectivity was caused by a different distribution of platinum particles on catalytic support. The size and perhaps also the shape and nature of the active sites can vary when the catalyst is thermally treated under the microwave conditions. Another hypothesis given by Seyfried was that irradiated particles of platinum could be less positively charged, thereby leading to higher isomer selectivity.

A similar approach of using the microwave irradiation for the activation of heterogeneously catalyzed reactions and for the preparation of the catalyst was followed by Liu *et al.* [35] in oxidation of o-xylene over the V_2O_5/SiO catalyst and in oxidation of toluene over the V_2O_5/TiO_2 catalyst [43]. Higher conversions and yields were observed when the reactions were carried out on catalysts prepared under microwave conditions. A more homogeneous dispersion of V_2O_5 particles on the catalytic support and superheating of V_2O_5 molecules were postulated as explanation for the observed results.

Bond *et al.* [36] investigated the effect of microwave heating on the reaction of propan-2-ol over carbon (charcoal and graphite) supported catalysts. A lower temperature of reaction (up to 200 K difference) was needed when the reaction was carried out under microwave conditions. This decrease of required temperature was independent of the catalyst used.

Bond *et al.* [37] and Chen *et al.* [38, 39] studied oxidative coupling of methane under conventional and microwave conditions. Both research groups concluded that the

process under the microwave conditions could be carried out at temperatures about 200-400K lower than with the conventional heating with product selectivity remaining at the same level.

Will *et al.* [40, 41] investigated $LaCoO_2$, $LaMnO_3$ and $La_xSr_{1-x}MnO_3$ catalysts in terms of their activity under microwave and classical heating for oxidation of propane. To minimize temperature differences between the catalyst surface and the catalyst bed, the reactor was thermally isolated. Very small differences in conversion and selectivity were observed between experiments under the microwave and classical conditions.

Contrary to the above, Beckers *et al.* [42] showed that propane oxidation was greatly enhanced by microwave irradiation. On the $La_{0.9}Sr_{0.1}MnO_3$ catalyst the same conversion was reached at temperature circa $200^{\circ}C$ lower when microwave heating was applied.

Cooney and Xi [43] studied also the production of ethylene and propylene from ethane, propane and n-butane on silicon carbide in a fixed-bed reactor . However, all experiments were performed under microwave conditions and no comparison with classical heating was presented.

The hydrogen cyanide (HCN) synthesis via two competitive routes was investigated by Koch *et al.* [44]. The first approach was synthesis of HCN from ammonia over solid carbon. The second investigated reaction was the reaction of ammonia and methane over Pt/Al_2O_3 catalyst. In both cases the selectivity to HCN was close to 95% which was slightly higher than for the conventional process. Observed higher selectivity was explained by existence of a thermal gradient between the surface of the catalyst, at higher temperature, and the gas phase at lower temperature.

One of the recent investigations on microwave application for heterogeneous gas-solid system was performed by Sinev [45]. This comparative study on dehydrogenation of ethane over vanadium-based catalysts under conventional and microwave heating showed that depending on the composition of the catalyst different conclusions regarding influence of microwave irradiation could be drawn. It was shown that for some catalysts the conversion of ethane was not affected by the application of dielectric heating. For other catalysts the conversion of ethane under the microwave heating was higher than for conventional heating. It was also observed that the increased conversion

was affected by the phase transition of catalysts, which occurred only when the microwave heating was applied.

3.1.1 Microwave-assisted catalytic hydrogen production

Another group of research works constitutes investigation of microwave irradiation on heterogeneous catalysis for hydrogen or synthetic gas production. This field of microwave-assisted catalysis is far less documented in a literature and hasn't received much attention so far. However, growing interest in the hydrogen production and the great number of reports describing potential of microwave energy application to chemical reactions attracts more and more attention from research groups.

One of the first groups investigating microwave-assisted hydrogen production was group of Cooney and Xi [46] who in 1996 studied the decomposition of methane and methane steam reforming. Although, methane decomposition reaction was not very successful since obtained conversions were very low and the production of hydrogen sharply decreased with reaction time, these experiments showed great potential of microwaves as an alternative source of heat for the reaction. Contrary to the methane decomposition reaction, in the steam reforming reaction obtained methane conversion was very high and remained stable over the reaction time. Moreover, the results clearly showed that higher conversion of methane was achieved when microwave heating was applied. It was reported that the temperature of the conventional process had to be 30-50K higher than under microwave conditions to produce the same methane conversion. Although in this research work the thermocouples were used to measure the temperature of the catalytic bed authors were aware of the possible interaction of the thermocouple with the electro-magnetic field and certain modifications of the thermocouple were applied to minimize undesired effect. Despite of all effort the researchers could not find explanation of observed effect and admitted that exact mechanism for the microwave effects is not known.

The oxidation of methane to hydrogen under microwave conditions was investigated by Bi and coworkers [47] in 1999. The reaction was examined with Ni and Co catalyst on ZrO_2 and La_2O_3 supports. Results from microwave and conventional heating were compared in terms of methane conversion and selectivity to the reaction

products (H_2, CO, CO_2). For all catalysts higher conversion of methane and higher selectivity to hydrogen were observed when microwave power was applied. It was also observed that at the same conversion the temperature of the catalytic bed under microwave conditions was around 200K lower than for the conventional heating. As a possible explanation of the observed results Bi postulated the existence of the hot-spots inside the catalytic bed. Although the authors were sensitive to correct temperature measurements of the catalytic bed and selected an infrared pyrometer as a more reliable temperature measuring technique, the accuracy was tested in a conventional electric furnace. Secondly, this technique by nature dose not allows for verifying temperature across the catalytic bed and therefore it is rather difficult to evaluate stated hypothesis of hot-spot formation. Moreover, the temperature of the potential hot-spots was not determined.

The formation of hot spot was claimed to be a mechanism responsible for observed improvement in a reaction of a carbon dioxide reforming of methane investigated by Zhang *et al.* [48]. The extensive, parametric study showed that conversion of the feed was significantly higher, exciding the thermodynamic equilibrium conversion, when microwave energy was applied (Figure 3.2). However, it is seen that at temperatures around 800°C the conversions of CO_2 and MeOH eventually cross and they are in good agreement with equilibrium data. This phenomenon indicates that temperature of the catalytic bed could be not adequately measured.

Another research group investigating microwave-assisted hydrogen production is group of Menendez. In their work the methane decomposition over activated carbon under two heating modes – electric and microwave heating - was examined [49]. The experimental results reveal that the methane conversion obtained under microwave heated experiments is significantly higher at the beginning of the process and decreases in time to eventually drop below the methanol conversion obtained for electrically heated process after 100min of experiment. Based on the experimental data and visual observation (small sparks were observed during microwave heating experiment) the authors claimed that microwave heating gives rise to higher conversions than electric heating due to the formation of hot spots inside the catalyst bed, which favors CH_4

decomposition but at the same time decreases activity of the catalyst and favorable carbon deposit formation effecting in reducing a porosity of the catalytic bed.
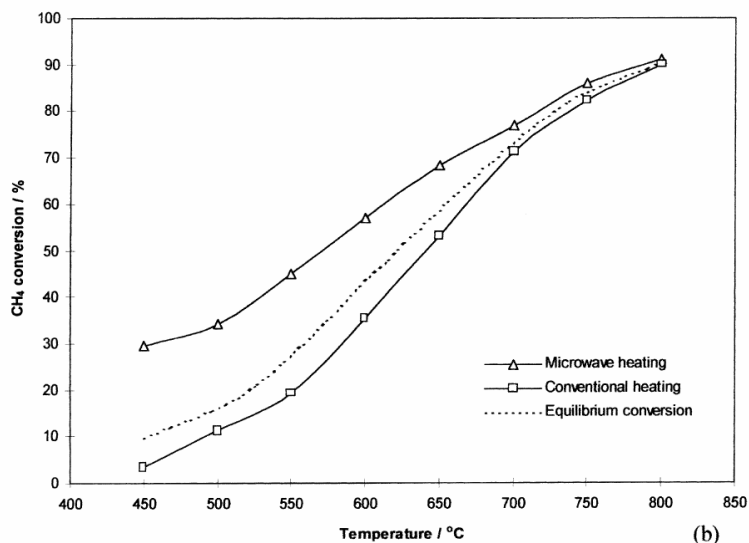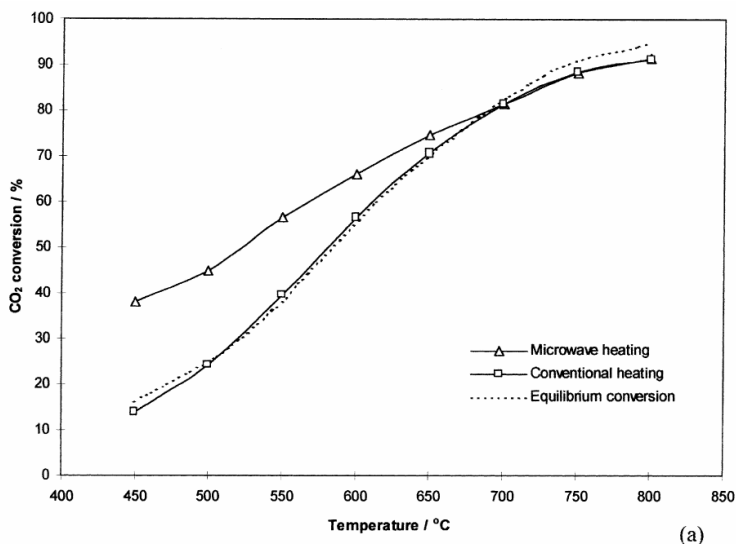

(a)

(b)

Figure 3.2. CO2 (a) and (b) CH4 conversions as a function of temperature over catalyst Ptd(8%)/CeO2(20%)/g-Al2O3. (Reprinted from Xunli Zhang, Carbon Dioxide Reforming of Methane with Pt Catalysts Using Microwave Dielectric Heating. Catal. Lett., 2003. 88(3): p. 129-139. Copyright © 2003, Springer Netherlands, with permission from Springer)

In other work of aforementioned research group the comparative study of conventional and microwave-assisted pyrolysis [50] as well as dry and steam reforming of glycerol over activated carbon was conducted [51]. The conversion of glycerol and gas products distribution was examined not only with respect to heating mode but also taking into account different process parameters, like operation temperature or steam/glycerol ratio. The results proof that regardless of the glycerol converting process, the microwave-assisted reactions promote higher conversions of glycerol to gas products and elevated content of synthesis gas compared to conventional heating processes. Unfortunately the authors of this research did not propose any explanation of observed enhancements.

The group of Menendez and co-workers also conducted research on microwave-assisted dry reforming of methane using an activated carbon as a catalyst and microwave receptor [52]. It was found that conversion of both reagents, CO_2 and CH_4, is up to 40% higher under microwave heating than for reaction carried out at the same conditions but with application of an electric furnace. Similar to their previous work authors propose micro-plasma arcing (hot-spot formation) as a mechanism responsible for observed effect. The parametric study showed that for temperatures below $600^{\circ}C$ and surprisingly above $800^{\circ}C$ conversion of the feed sharply decreases. The phenomenon was explained by graphitic carbon formation originating from methane decomposition which is favourable at temperature above $900^{\circ}C$. The authors suggested that microwave radiation acts on the mixture of gases and contribute to the formation of carbon deposit since the effect was negligible for electrically heated reactor. However, this hypothesis is not well supported taking into account that temperature measurement was conducted by an infrared pyrometer aiming the surface of the reactor wall, what as proposed in other work of the group [53]might rise some doubts.

The hot-spot formation hypothesis was abandoned by Perry [54] in his research on microwave heated methanol steam reforming on Cu/ZnO catalyst. The experimental study on the reaction kinetic showed no significant differences in kinetic expression for two heating modes – electric and microwave. However, it was found that the microwave-enhanced methanol reforming could be carried out at temperature around 20K lower than in the conventional equivalent maintaining similar kinetics for both

processes. The theoretical study revealed that when the catalytic bed is exposed to microwave irradiation the spatial temperature gradients are mitigated resulting in better performance of the reaction and less heat is required to maintain the process.

Different explanation was proposed by Zhang *et al.* [55] in research on microwave-modified $Cu/ZnO/Al_2O_3$ catalyst for methanol steam reforming. It was found that the microwave-irradiated catalyst delivered much higher H_2 and lower CO production rates than the conventionally produced sample despite the higher specific surface area of the latter.

Similar system was investigated by Chen *et al.* who recently investigated a methanol steam reforming reaction on $Cu/ZnO/Al_2O_3$ catalyst [56]. Contrary to the work of Zhang this research was more focus on the reaction performances and influence of the microwave irradiation on MeOH conversion instead of the catalyst morphology. Although the results clearly show that obtaining high MeOH conversion is possible they were compared only with thermodynamic data and therefore it is impossible to evaluate them in terms of microwave effects. However, to rationalize observed results the authors proposed that obtaining of the high MeOH conversion was possible due to the fact that both, the catalyst and the reagents, are good microwave receptors allowing triggering reaction in short time. An examination of the surface characteristics of the catalyst before and after reaction indicated that the microwave irradiation is unable to significantly change property of the catalyst.

Chen and co-workers carried out also a research work on hydrogen generation from a catalytic water gas shift reaction under microwave irradiation [57]. The research demonstrated that the microwave energy can be successfully implemented to WGSR resulting in CO conversions being higher than in conventionally heated reactor.

Moreover, as the results reveal, application of microwave energy effects in constantly decreasing concentration of CO with increase of the reaction temperature what was found to be contrary to thermodynamic analysis and experimental results for electric heating mode (Figure 3.3). The authors suggested, similar to the aforementioned research work, that this microwave promoted effects arises from that microwaves can be efficiently absorbed by catalyst and water, creating better reaction environment.
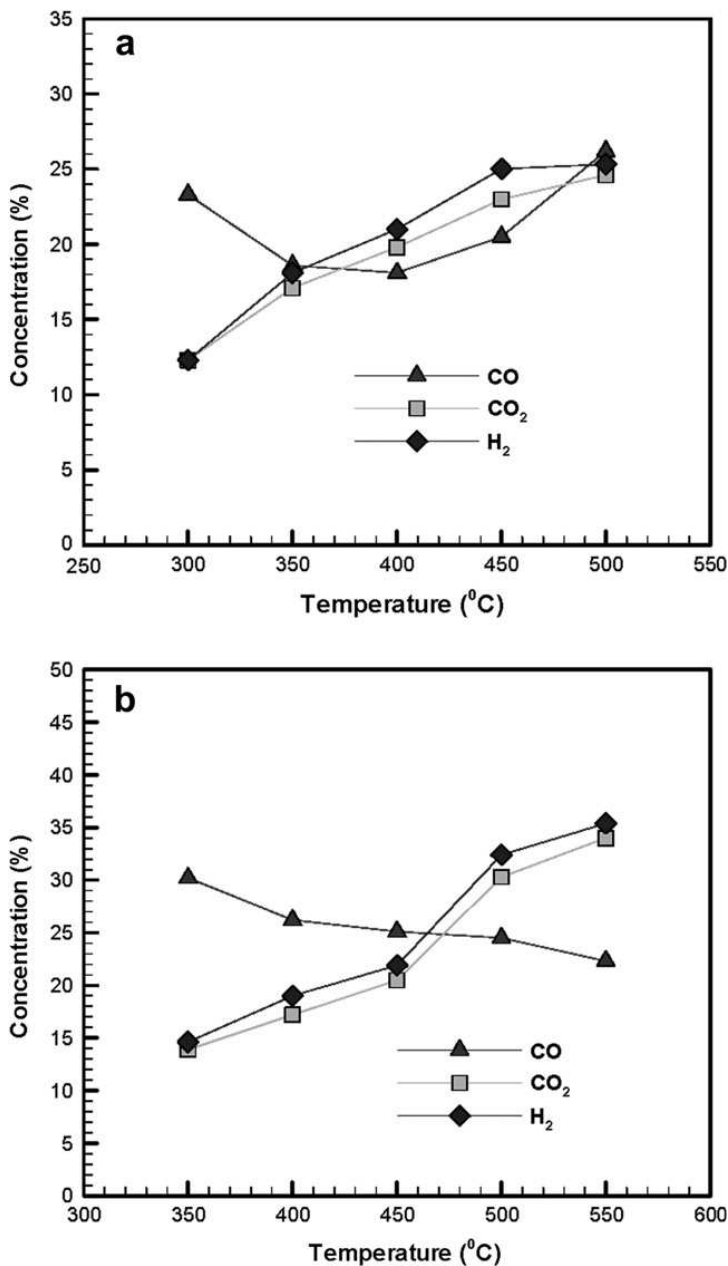
Figure 3.3 Distributions of volumetric concentrations of CO, CO2 and H2 with (a) conventional heating and (b) microwave heating. Reprinted with permission (Wei-Hsin Chen, Jian-Guo Jheng, Hydrogen generation from a catalytic water gas shift reaction under microwave irradiation, International Journal of Hydrogen Energy A.B. Yu Elsevier September 2008)

3.2 Modeling approaches in microwave-assisted heterogeneous catalysis.

Gas-solid catalysis presents a complex system. The system models require simultaneous solving of heat and mass balances. The system becomes even more difficult to describe when the microwave heating is applied. While the mass balances remain the same for conventional and microwave-irradiated systems, the description of thermal energy delivered by the microwave and dissipated inside the system requires solving of Maxwell equations and Fourier's Law. Microwave irradiation has been applied for chemical processes for more than 20 years. However, due to the complicated nature of the interactions of electromagnetic waves with the irradiated material and problems with measuring of the temperature and the electromagnetic field distribution without changing them by the measurement procedure itself, the modeling approaches are often simplified. The distribution of electromagnetic fields in space and time governed by Maxwell's equations is simplified by assuming plane waves that are exponentially dumped when penetrating material (Lambert's Law) [58]. Another approach is via solving the heat generation equation (Eq.1.10 or 1.13) together with heat transfer equations.

The possible hot-spot formation during the microwave heating was investigated by Perry *et al*. [29, 54]. Temperature differences between metal particles – (Pd, Pt) and a catalytic support –(Al_2O_3) were simulated as a function of particle diameter. A steady-state energy balance describing the power absorbed by the porous particle and the heat losses only to the gas-phase were assumed. The calculated temperature differences appeared negligible: 1.6×10^{-10} K for 1 nm particles and 1.1×10^{-10} K for 100 nm particles, respectively. The numerical results were in a good agreement with performed experiments.

Zhang *et al.* [59-61] investigated behaviour of MoS_2/Al_2O_3 catalyst under the microwave conditions. The research work was carried out at two scales; the macro-scale where a temperature of the catalytic bed was investigated as a function of the applied power and the metal content, and in the micro-scale where the temperature difference between the active sites and the support was modelled. In the macro-scale a clear preferential heating of the MoS_2 nanoparticles was documented.

Following the procedure proposed by Perry, Zhang performed calculations of temperature differences between the MoS_2 nanoparticles and the Al_2O_3 support. It appeared that metal particles were only 8×10^{-4} K hotter than the alumina support. The calculations showed therefore that the existence of the hot-spots could be excluded. However, opposite conclusions could be drawn from the performed experiments.

A numerical approach to the microwave-heated fluidized-bed reactor was presented by Roussy *et al.* [62] and Thomas and Faucher [63]. The modelling work performed by Roussy *et al.* showed no significant temperature gradients between the gas and the solid phases despite the direct interaction of the microwave energy with the solid phase. In contrast to Roussy *et al.*, Thomas calculated that the temperature of the solid phase could be 30-40K higher than the temperature of the gas phase. However, Thomas and Faucher assumed the homogeneity of the electromagnetic field, which in fact is not true as pointed out by Roussy *et al*.

Thomas [64] investigated the heating of a catalyst pellet as a function of metal particle size and the frequency of the applied microwave irradiation. The model assumed all metal particles to be spherical, highly conductive and completely separated from each other. Temperature gradients within a particle were assumed negligible. The numerical solution of the energy balance equation showed that for 10 nm particles the temperature difference between the nanoparticle and the support was about 0.1 K. For particles bigger than 30 nm the effect was more pronounced and strongly dependent on the frequency of the electromagnetic field (Fig. 5).

Thomas and Faucher [63] estimated also the temperature differences between the catalyst particles and the gas phase in a packed-bed reactor. The numerical solution showed no significant temperature differences between the pellets and the gas. These results were confirmed by a work of Cecilia *et al.* [65].

As one can see in the above review, the number of modelling studies on microwave-enhanced heterogeneous catalysis is limited. On the other hand, a significant number of the heterogeneous microwave heating models have been developed in food processing. Although the review of food processing is not the aim of this publication, we would like to point out the analogy of some process aspects and applied methodology, as far as the modelling of microwave-assisted gas-solid processes is

concerned. In our opinion, some of the approaches developed for microwave-assisted food processing could be successfully used for describing and solving problems in microwave-assisted gas-solid catalysis. For instance, Souraki, Andres and Mowla focused on drying of the cylindrical carrot samples in a microwave-assisted fluidized-bed drier [66]. A numerical model of drying of a porous material was proposed for predicting the moisture and temperature distributions inside the sample. The obtained numerical solution was in a good agreement with the experimental results.

3.3 Conclusions

The microwave heating has been investigated in catalytic gas-phase reaction applications for many years. Numerous investigators report clear enhancement of the reaction yields/selectivities or the lowering of the bulk operational temperature due to the dielectric heating. On the other hand, the not fully established mechanism of solid (nano)particles heating and imperfect temperature measurement techniques implicate that different effects are often observed and contradictory conclusions are drawn. For further progress here development of accurate and possibly non-invasive techniques for local temperature measurements under the microwave irradiation is needed.

The presented results show clearly that uniform heating of a fixed-bed catalytic reactor, even in macroscopic scale, presents a technical challenge. This, together with the limited penetration depth of microwaves in solid materials brings us to the conclusion that possible applications of the microwave-assisted gas-phase catalysis will require either fluidized-/spouted-bed or specially structured reactors.

Bibliography

1. Loupy, A., *Microwaves in Organic Synthesis*. 2002, Germany: Wiley-VCH: Weinheim.
2. Hayes, B.L., *Microwave Synthesis: Chemistry at the Speed of Light*. 2002, Matthews, NC: CEM Publishing.
3. Hoz, A.d.l., et al., *Microwaves in organic synthesis. Thermal and non-thermal microwave effects.* Chemical Society Reviews, 2005. **34**(2): p. 164-178.
4. Kappe, C.O., *Controlled Microwave Heating in Modern Organic Synthesis.* Angewandte Chemie International Edition, 2004. **43**(46): p. 6250-6284.
5. Lidstrom, P., et al., *Microwave assisted organic synthesis-a review.* Tetrahedron, 2001. **57**(45): p. 9225-9283.
6. Ioffe, M.S., et al., *High-Power Pulsed Radio-frequency and Microwave Catalytic Processes: Selective Production of Acetylene from the Reaction of Methane over Carbon.* Journal of Catalysis, 1995. **151**(2): p. 349-355.
7. Cameron, K.L., et al., *Pulsed Microwave Catalytic Decomposition of Olefins.* Research on Chemical Intermediates, 1991. **16**(1): p. 57-70.
8. Dinesen, T.R.J., et al., *A Mechanistic Study of the Microwave Induced Catalytic Decompositions of Organic Halides.* Research on Chemical Intermediates 1991. **15**(2): p. 113-127.
9. Wan, J.K.S. and T.A. Koch, *Application of Microwave Radiation for the Synthesis of Hydrogen Cyanide.* Research on Chemical Intermediates, 1994. **20**(1): p. 29-37.
10. Wan, J.K.S., *Microwaves and Chemistry: the Catalysis of an Exciting Marriage.* Research on Chemical Intermediates, 1993. **19**(2): p. 147-158.
11. Wan, J.K.S., et al., *Microwave Induced Catalytic Reactions of Carbon Dioxide and Water: Mimicry of Photosynthesis.* Research on Chemical Intermediates, 1991. **16**(3): p. 241-255.
12. Tse, M.Y., et al., *Applications of high power microwave catalysis in chemistry.* Research on Chemical Intermediates, 1990. **13**(3): p. 221-236.
13. Wan, J.K.S., et al., *High-Power Pulsed Microwave Catalytic Processes: Decomposition of Methane.* Journal of Microwave Power and Electromagnetic Energy 1990. **25**(1): p. 32-38.
14. Bamwenda, G., et al., *Production of acetylene by a microwave catalytic reaction of water and carbon.* Research on Chemical Intermediates 1992. **17**(3): p. 243-262.
15. Whittaker, A.G. and D.M.P. Mingos, *Microwave-assisted solid-state reactions involving metal powders and gases.* Journal of the Chemical Society, Dalton Transactions, 1993(16): p. 2541-2543.
16. Zhang, X., et al., *Microwave assisted catalytic reduction of sulfur dioxide with methane over MoS2 catalysts.* Applied Catalysis B: Environmental, 2001. **33**(2): p. 137-148.
17. Zhang, X., et al., *Apparent equilibrium shifts and hot-spot formation for catalytic reactions induced by microwave dielectric heating.* Chemical Communications, 1999(11): p. 975-976.
18. Cha, C.Y., *Microwave Induced Reactions of So2 and Nox Decomposition in the Char-Bed.* Research on Chemical Intermediates, 1994. **20**(1): p. 13-28.
19. Cha, C.Y. and Y. Kong, *Enhancement of NOx adsorption capacity and rate of char by microwaves.* Carbon, 1995. **33**(8): p. 1141-1146.

20. Kong, Y. and C.Y. Cha, *NOx Abatement with Carbon Adsorbents and Microwave Energy.* Energy & Fuels, 1995. **9**(6): p. 971-975.

21. Chang, Y.-f., et al., *Microwave-assisted NO reduction by methane over Co-ZSM-5 zeolites.* Catalysis Letters, 1999. **57**(4): p. 187-191.

22. Wang, X., et al., *Microwave effects on the selective reduction of NO by CH4 over an In–Fe2O3/HZSM-5 catalyst.* Chemical Communications, 2000(4): p. 279 - 280.

23. Roussy, G., et al., *Controlled oxidation of methane doped catalysts irradiated by microwaves.* Catalysis Today, 1994. **21**: p. 349-355.

24. Roussy, G., et al., *C2+ selectivity enhancement in oxidative coupling of methane over microwave-irradiated catalysts* Fuel Processing Technology, 1997. **50**(2-3): p. 261-174.

25. Zhang, X., et al., *Oxidative coupling of methane using microwave dielectric heating.* Applied Catalysis A: General, 2003. **249**(1): p. 151-164.

26. Marun, C., et al., *Catalytic Oligomerization of Methane via Microwave Heating.* The Journal of Physical Chemistry A, 1999. **103**(22): p. 4332-4340.

27. Conde, L.D., et al., *Frequency Effects in the Catalytic Oligomerization of Methane via Microwave Heating.* Journal of Catalysis, 2001. **204**(2): p. 324-332.

28. Perry, W.L., et al., *Kinetics of the Microwave-Heated CO Oxidation Reaction over Alumina-Supported Pd and Pt Catalysts.* Journal of Catalysis, 1997(171): p. 431–438.

29. Perry, W.L., et al., *On the possibility of a significant temperature gradient in supported metal catalysts subjected to microwave heating.* Catalysis Letters, 1997. **47**(1): p. 1-4.

30. Silverwood, I., et al., *Comparison of conventional versus microwave heating of the platinum catalysed oxidation of carbon monoxide over EUROPT-1 in a novel infrared microreactor cell.* Journal of Molecular Catalysis A: Chemical, 2007. **269**(1-2): p. 1-4.

31. Silverwood, I.P., et al., *A microwave-heated infrared reaction cell for the in situ study of heterogeneous catalysts.* Physical Chemistry Chemical Physics, 2006. **8**(46): p. 5412 - 5416.

32. Seyfried, L., et al., *Microwave Electromagnetic-Field Effects on Reforming Catalysts .: 1. Higher Selectivity in 2-Methylpentane Isomerization on Alumina-Supported Pt Catalysts.* Journal of Catalysis, 1994. **148**(1): p. 281-287.

33. Thiebaut, J.M., et al., *Durable changes of the catalytic properties of alumina-supported platinum induced by microwave irradiation.* Catalysis Letters, 1993. **21**(1): p. 133-138.

34. Roussy, G., et al., *Permanent change of catalytic properties induced by microwave activation on 0.3% Pt/Al2O3 (EuroPt-3) and on 0.3% Pt-0.3% Re/Al2O3 (EuroPt-4).* Applied Catalysis A: General, 1997. **156**(2): p. 167-180.

35. Liu, Y., et al., *The effects of microwaves on the catalyst preparation and the oxidation of o-xylene over a V2O5/SiO2 system.* Catalysis Today, 1999. **51**(1): p. 147-151.

36. Bond, G., et al., *The effect of microwave heating on the reaction of propan-2-ol over alkalised carbon catalysts.* Topics in Catalysis, 1994. **1**(1): p. 177-182.

37. Bond, G., et al., *Recent applications of microwave heating in catalysis.* Catalysis Today, 1993. **17**(3): p. 427-437.

38. Chen, C., et al., *Microwave effects on the oxidative coupling of methane over proton conductive catalysts.* Journal of the Chemical Society, Faraday Transactions, 1995. **91**(7): p. 1179-1180.

39. Chen, C.-l., et al., *Microwave effects on the oxidative coupling of methane over Bi2O3-WO3 oxygen ion conductive oxides.* Reaction Kinetics and Catalysis Letters, 1997. **61**(1): p. 175-180.

40. Will, H., et al., *Multimode Microwave Reactor for Heterogeneous Gas-Phase Catalysis.* Chemical Engineering & Technology, 2003. **26**(11): p. 1146-1149.

41. Will, H., et al., *Heterogeneous Gas-Phase Catalysis Under Microwave Irradiation—a New Multi-Mode Microwave Applicator.* Topics in Catalysis, 2004. **29**(3): p. 175-182.

42. Beckers, J., et al., *Clean Diesel Power via Microwave Susceptible Oxidation Catalysts.* ChemPhysChem, 2006. **7**(3): p. 747-755.

43. Cooney, D.O. and Z. Xi, *Production of ethylene and propylene from ethane, propane, and n-butane mixed with steam in a mocrowave-irradiated silicon-carbide loaded reactor.* Petroleum Science and Technology, 1996. **14**(10): p. 1315 - 1336.

44. Koch, T.A., et al., *Improved safety through distributed manufacturing of hazardous chemicals.* Process Safety Progress, 1997. **16**(1): p. 23-24.

45. Sinev, I., et al., *Interaction of vanadium containing catalysts with microwaves and their activation in oxidative dehydrogenation of ethane.* Catalysis Today, 2009. **141**(3-4): p. 300-305.

46. Cooney, D.O. and Z. Xi, *Production of hydrogen from methane and methane/team in a microwave irradiated char-loaded reactor.* Petroleum Science and Technology, 1996. **14**(8): p. 1111 - 1141.

47. Bi, X.-J., et al., *Microwave effect on partial oxidation of methane to syngas.* Reaction Kinetics and Catalysis Letters, 1999. **66**(2): p. 381-386.

48. Zhang, X., et al., *Carbon Dioxide Reforming of Methane with Pt Catalysts Using Microwave Dielectric Heating.* Catal. Lett., 2003. **88**(3): p. 129-139.

49. Domínguez, A., et al., *Microwave-assisted catalytic decomposition of methane over activated carbon for CO2-free hydrogen production.* International Journal of Hydrogen Energy, 2007. **32**(18): p. 4792-4799.

50. Fernández, Y., et al., *Pyrolysis of glycerol over activated carbons for syngas production.* Journal of Analytical and Applied Pyrolysis, 2009. **84**(2): p. 145-150.

51. Fernández, Y., et al., *Comparative study of conventional and microwave-assisted pyrolysis, steam and dry reforming of glycerol for syngas production, using a carbonaceous catalyst.* Journal of Analytical and Applied Pyrolysis, 2010. **88**(2): p. 155-159.

52. Fidalgo, B., et al., *Microwave-assisted dry reforming of methane.* International Journal of Hydrogen Energy, 2008. **33**(16): p. 4337-4344.

53. Menendez, J.A., et al., *Thermal treatment of active carbons: A comparison between microwave and electrical heating.* Journal of Microwave Power and Electromagnetic Energy, 1999. **34**(3): p. 137-143.

54. Perry, W.L., et al., *Microwave heating of endothermic catalytic reactions: Reforming of methanol.* AIChE Journal, 2002. **48**(4): p. 820-831.

55. Zhang, X.-R., et al., *A unique microwave effect on the microstructural modification of Cu/ZnO/Al2O3 catalysts for steam reforming of methanol.* Chemical Communications, 2005(32): p. 4104-4106.

56. Chen, W.-H. and B.-J. Lin, *Effect of microwave double absorption on hydrogen generation from methanol steam reforming.* International Journal of Hydrogen Energy, 2010. **35**(5): p. 1987-1997.

57. Chen, W.-H., et al., *Hydrogen generation from a catalytic water gas shift reaction under microwave irradiation.* International Journal of Hydrogen Energy, 2008. **33**(18): p. 4789-4797.

58. Knoerzer, K., et al., *Microwave Heating: A New Approach of Simulation and Validation.* Chemical Engineering & Technology, 2006. **29**(7): p. 796-801.

59. Zhang, X., et al., *Microwave Dielectric Heating Behavior of Supported MoS2 and Pt Catalysts.* Industrial & Engineering Chemistry Research, 2001. **40**(13): p. 2810-2817.

60. Zhang, X., et al., *Effects of Microwave Dielectric Heating on Heterogeneous Catalysis.* Catalysis Letters, 2003. **88**(1): p. 33-38.

61. Zhang, X. and D.O. Hayward, *Applications of microwave dielectric heating in environment-related heterogeneous gas-phase catalytic systems.* Inorganica Chimica Acta, 2006. **359**(11): p. 3421-3433.

62. Roussy, G., et al., *Modeling of a fluidized bed irradiated by a single or a multimode electric microwave field distribution.* Journal of Microwave Power and Electromagnetic Energy 1995. **30**(3): p. 178-187.

63. Thomas Jr., J.R. and Faucher F., *Thermal modeling of microwave heated packed and fluidized bed catalytic reactors.* Journal of Microwave Power and Electromagnetic Energy 2000. **35**(3): p. 165-174.

64. Thomas, J.R., *Particle size effect in microwave-enhanced catalysis.* Catalysis Letters, 1997. **49**: p. 137-141.

65. Cecilia, R., et al., *Possibilities of process intensification using microwaves applied to catalytic microreactors.* Chemical Engineering and Processing, 2007. **46**(9): p. 870-881.

66. Souraki, B.A., et al., *Mathematical modeling of microwave-assisted inert medium fluidized bed drying of cylindrical carrot samples.* Chemical Engineering and Processing: Process Intensification, 2009. **48**(1): p. 296-305.

4

Microwave-activated methanol steam reforming for hydrogen production[*]

Methanol steam reforming (MSR) was carried out in a catalytic packed bed reactor under electrical and microwave heating using the two most common catalysts for this process - $CuZnO/Al_2O_3$ and $PdZnO/Al_2O_3$. Significant two-dimensional temperature gradients were found, especially in the latter case. Our result show that for the same average bed temperature, methanol conversion is higher under microwave heating (>10%). On the other hand, the product distribution is not affected by the heating mode. We demonstrate that even in cases where the maximum temperature along the entire height of the bed is significantly higher under electrical heating, conversion is either higher in the microwave case or approximately the same between the two heating modes. Finally, our experimental data indicate that a given methanol conversion can be achieved with lower net heat input to the reactor under microwave heating. This does not mean lower total energy consumption in the microwave process due to the limitations in the magnetron efficiency and the reflected power. However, it may be an implicit indication of higher temperature at metal sites than in bulk phase (microscale hot spot formation) due to the selective heating principle.

---

[*] This chapter is published in International Journal of Hydrogen Energy, 36(20), 12843-12852, **2011**

4.1 Introduction

Clean electricity generation from H_2-fuelled proton-exchange-membrane fuel cells (PEMFCs) is one of the possible near to mid-term solutions for distributed power, electronic devices and various auxiliary power units in homes, businesses and transportation. Fuel reforming reactors for hydrogen production are designed to maximize hydrogen yield and minimize carbon formation with proper choice of operating conditions (temperature, pressure, residence time, etc.) and catalysts [1, 2]. Among the reforming processes available, steam reforming (SR) achieves the highest H_2/CO ratio [2, 3]. H_2 can be produced in-situ via catalytic steam reforming of (oxygenated) hydrocarbon fuels in micro-/millireactors [4-9], monolith [10-12], membrane [13-16], foam or packed bed reactors [1]. The choice of the reformed fuel strongly depends on the type of application, the fuel accessibility, the existing infrastructure, the cost and its environmental footprint [17]. Methanol has the advantage of being logistic fuel, biodegradable, sulfur-free, reformed at low temperatures (200-300°C), and producing very small amounts of CO, thus rendering secondary water-gas shift unnecessary [7, 18]. On the other hand, toxicity of methanol vapour is the most important drawback. Steam reforming reactions are endothermic by nature and thus require external heat supply. The heat can be delivered to the reactor by conventional heat sources, i.e. steam, electric heating, oil bath, or by using alternative energy forms like plasma [19-28] or microwaves [29-35]. Application of microwave irradiation, as alternative energy source, to several chemical systems has been identified as one of the process intensification methods. The ability of microwaves to provide fast, selective and volumetric heating can induce benefits in heterogeneous catalytic systems unachievable with classical heating methods, i.e. higher conversion and/or selectivity [36-43], higher production rate [44-49] and reduction in process temperature [50-52]. A comprehensive review in this field has been presented in [53].

In the literature concerned with application of microwave irradiation to heterogeneous reactions, two arguments are usually cited to explain the observed effects: hot-spot formation [38, 40, 41, 50-52, 54] and change in the catalyst morphology due to irradiation effect [36, 37, 39, 43, 55]. The hot spot formation phenomenon is caused by

differences in microwave absorption ability of metal/-oxide crystals distributed on the catalytic support. Higher absorption of microwave energy by metal/-oxide particles results in higher local (microscale) temperatures ($\Delta=100\text{-}200\text{K}$) compared to the average bulk temperature and thus in increased local reaction rates. However, due to the micro-scale nature of the phenomenon (90-1000 μm) experimental proof of this assumption is still lacking.

In this paper, we present the results of an experimental study on microwave-activated methanol steam reforming for hydrogen production with the aim to explore potential benefits compared to conventional thermal activation. The study is focused on comparison of methanol conversion, product distribution and energy efficiency of the catalytic bed over a range of operating conditions under electric heating (EH) and microwaves (MW).

$$CH_3OH + H_2O \rightarrow CO_2 + 3H_2 \qquad (\Delta H_{298\,K} = 49 \text{ kJ/mol}) \tag{4.1}$$

Previous experimental studies on microwave-activated methanol steam reforming using $Cu/ZnO/Al_2O_3$ catalyst were done by Perry et al. [30] and Chen et al [35]. In [30], the authors found that under microwave heating a nominal conversion of 60% could be reached at an exit temperature $>21^{\circ}C$ lower compared to conventional heating for the same inlet temperature. Only inlet and exit temperatures were measured. In [35], the authors put forward a double microwave absorption mechanism by the catalyst and the reactants to explain the higher conversion obtained in their microwave reforming experiments compared to conversions reported in the literature for conventionally-heated experiments. Temperature measurement at a single point inside the catalytic reactor is reported. In our work, microwave-activated methanol steam reforming is investigated not only with $Cu/ZnO/Al_2O_3$ but also with $Pd/ZnO/Al_2O_3$. Temperature is measured at multiple positions inside the catalytic bed in order to obtain a two-dimensional temperature map, which provides insight into the different heat transfer characteristics inside the reactor with the two heating modes. Finally, the reactor energy efficiency with EH and MW is reported over a range of conversion levels.

4.2 Experimental

4.2.1 Reaction system

A schematic drawing of the entire reaction system is presented in Figure 4.1. The key unit is a tubular packed bed reactor with glass wall (O.D. 24 mm) shown in Fig. 4.2. The most common catalysts for methanol steam reforming being $CuZnO/Al_2O_3$ and $PdZnO/Al_2O_3$ are used in this work.
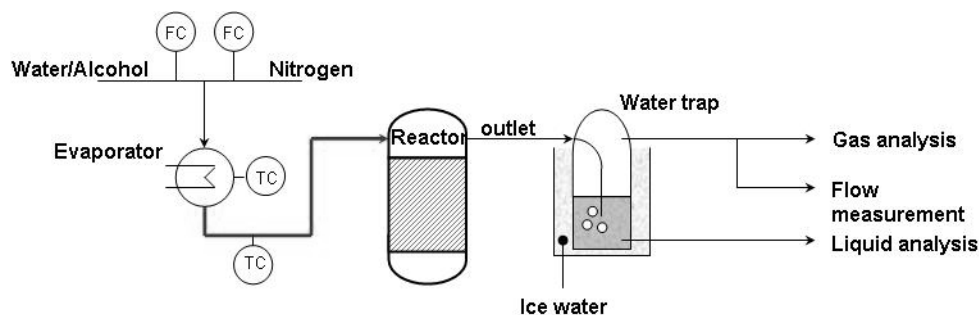

Figure 4.1. Schematic view of the reaction system (adapted from M.Reus, Microwave-assisted low temperature steam reforming of methanol for hydrogen production).

$CuZnO/Al_2O_3$ is a commercial methanol reforming catalyst (Alfa Aesar) in form of ~ 3 mm pellets, containing ~52 wt% Cu and ~30 wt% Zn. The $PdZnO/Al_2O_3$ catalyst was prepared by one-step co-impregnation method [18, 56-58]. A concentrated Palladium nitrate solution (~40 wt% Pd, Stream Chemicals) was mixed with $Zn(NO_3)_2 \cdot 6H_2O$ (99 wt% Aldrich) at 60 ^{o}C. Commercial α-Al_2O_3 (Alfa Aesar) pellets of ~3 mm size with BET surface of 230 m^2/g were used as catalytic support. The support was calcined at 550°C for 8h and then kept at 100°C prior to the impregnation step. The Pd and Zn nitrate solution was prepared with an appropriate amount of nitrate to obtain the final product with ~8.5 wt% of Pd and Pd/Zn molar ratio of 0.38. The total percentage of metal sites in the catalyst is ~23 wt%.

The methanol steam reforming reaction was activated by two heating modes: microwave irradiation and electric heating. For a fair comparison between the two heating modes, the experimental system used in the two cases was the same and only the applied heating device was changed. In the event of electric heating, the lower part of the reactor containing the catalyst bed (see Figure 4.2) was heated by a coil heating

element placed around it. In the microwave-driven experiments, the reactor was introduced into a monomode laboratory microwave applicator (Discover, CEM Corporation) where the lower part of the reactor containing the catalyst bed was exposed to the radiation. In both heating methods, the upper part of the reactor (above the catalyst bed) was heated by means of silicon oil flowing inside a rubber tubing wrapped around the reactor to prevent condensation of the unreacted methanol/water feed and thus unstable reaction conditions.
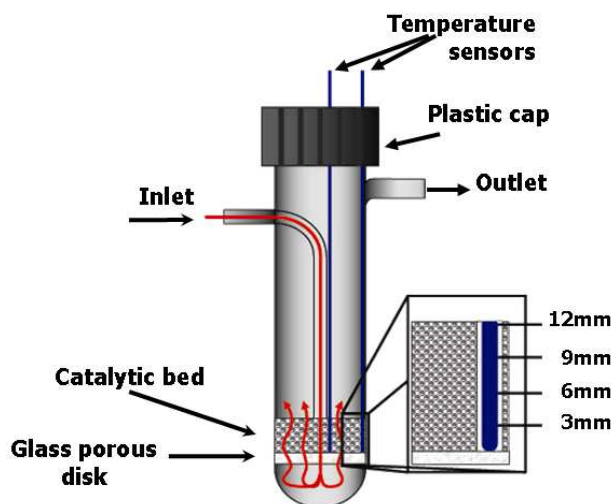

Figure 4.2. Schematic view of the reactor with magnification of the fiber optic sensor position

In both heating modes, temperature in the catalytic bed was monitored by two external fiber optic probes (FISO L-BA) vertically placed in the axis and near the glass wall of the reactor (Figure 4.2). The electric heating element was controlled by an external temperature regulator based on the temperature reading from a thermocouple immersed in the catalytic bed. When microwave heating was applied, the power delivered to the reactor was controlled manually. This choice was made because our previous studies [59] showed that the built-in IR sensor, which monitors the temperature at the outer surface of the glass reactor and provides signal to the power control unit, significantly underestimates the real temperature inside the catalytic bed, rendering automatic power control unreliable.

4.2.2 Experimental procedure

Prior to each experiment, the catalyst used for the reaction was weighed (~4 g $CuZnO/Al_2O_3$ or ~3 g $PdZnO/Al_2O_3$) and placed in the lower part of the reactor on a porous glass disk support, as shown in Figure 4.2. The reactor was shaken in order to compact the randomly packed catalytic bed resulting in a structure of ~10 mm height. The reaction was preceded by in-situ activation of the catalyst in a mixture of H_2 (flow rate: 25 ml/min) and N_2 (250 ml/min) at 220°C for 1-1.5 h. The methanol (MeOH) – water (H_2O) feed mixture in molar composition 1:1.5 (checked with a calibrated density meter (DMA 5000, Anton Paar)) was prepared before each experiment. The feed was supplied from a beaker to an evaporator, where it was mixed with a carrier gas (N_2) at a ratio feed:N_2 = 1:1.4. The flow rates of the feed mixture and the carrier gas were controlled by mass flow controllers (Bronkhorst). Experiments with the $CuZnO/Al_2O_3$ catalyst were performed at three gas hourly space velocities (GHSV) of 37000 h^{-1}, 64000 h^{-1}, and 120000 h^{-1}. Experiments with $PdZnO/Al_2O_3$ were performed only at GHSV=12000 h^{-1}, which corresponds to comparable flow rate as in GHSV=37000 h^{-1} in the event of Cu-based catalyst (but the difference in residence time comes from the different amount of catalyst used). This was done to maintain similar height between the two catalytic beds. It needs to be stressed that the purpose was not to achieve the best performance of the two catalysts for methanol reforming, but rather to compare the effects of two heating modes (EH and MW) on methanol steam reforming with two different catalysts.

The mixture of MeOH/H_2O/N_2 is fed to the reactor from the inlet at the top-left side and flows downward through the glass tube placed axially inside the reactor. The gas mixture is distributed below the catalytic bed at the bottom of the reactor, and then flows upward through the porous glass disk and the catalytic bed, where reaction takes place. The unreacted feed and gas products leave the reactor from the outlet at the top-right side, opposite to the inlet (Figure 4.2). The effluent stream passes through a water trap, where it is cooled down to -20°C to remove the condensable vapours (Figure 4.1). The flow of dry gas products, exiting the water trap, is measured by a bubble flow meter before being directed to online gas chromatograph (Varian CP 4900), where the product distribution (N_2, CO, CO_2, H_2, CH_4, CH_3OH) was analyzed. Measurements were

conducted every hour, while the reactor remained at steady-state for at least 4 hours before the flow of the feed was stopped. The condensate from the water trap was analyzed after the reaction to determine methanol conversion. In all experiments presented here, the error for the total mass balance is less than 2.5%.

Finally, temperature inside the catalytic bed was measured simultaneously by two fiber optic sensors placed in the center and near the wall of the reactor, respectively (Figure 4.2). The sensors were introduced into the system via glass capillaries for three reasons: 1) to ensure well-defined, reproducible positioning, 2) to protect them against mechanical damage and 3) to enable variable positioning of the probe tip along the height of the bed. The last feature allowed performance of multipoint temperature measurements inside the catalytic bed in the course of reaction. In order to obtain the temperature map inside the catalytic bed, temperature was measured at the bottom of the bed, with reference position 0 mm, and at 3, 6, 9 and 12 mm from the bottom of the bed, both in the core and near the wall of the reactor (Figure 4.2). The measurement procedure was repeated at least four times during reaction to assure steady temperature conditions.

4.3 Results

4.3.1 Temperature distribution

Incorrect or incomplete reactor temperature data may relinquish important information about the real reaction conditions and lead to erroneous conclusions with respect to MW effects. In this study, particular attention has been paid to map the temperature distribution inside the catalytic reactor for fair comparison of its performance under MW and EH. As mentioned in the previous section, two fiber optic probes were used to monitor temperature near the center and near the wall of the reactor at different axial positions. Significant temperature gradients were found in case of MW heating. Due to the non-uniform temperature field, an average catalytic bed temperature has been calculated to represent the reaction thermal conditions at various heat inputs. This was done by double averaging the experimental temperature data first in the radial direction assuming parabolic profiles and then in the axial direction along the height of the catalytic bed.

Figure 4.3 presents the axial temperature profiles at the core and near the wall of the reactor at an average temperature of $210^{\circ}C$ under EH and MW using CuZnO/Al$_2$O$_3$ and PdZnO/Al$_2$O$_3$ catalysts. It can be seen that there are two noticeable differences in the heating patterns: 1) MW heating results in significantly higher macroscopic temperature gradients both in axial and radial direction and 2) MW heating results in higher temperatures at the core of the reactor than near the wall; the trend is reversed in the case of EH. Both differences are due to the fact that in EH, the heating element is placed around the catalytic bed and delivers heat to the reactor through its wall surface, whereas MW provides volumetric heating and the applicator delivers microwave irradiation such that the peak of the electric field is at the center of the cavity and at a specific reactor height (close to the bottom); this is a specific design feature of the used microwave applicator. The aforementioned observations hold for both catalysts tested (Figure 4.3a and Figure 4.3b). Figure 4.4a and Figure 4.4b are the counterparts of Figure 4.3b (PdZnO/Al$_2$O$_3$ catalyst) for different average temperatures ($T_{avg.} = 230^{\circ}C$ and $250^{\circ}C$); they show that the temperature development in the bed, does not quantitatively affect the temperature gradients and the shape of the profiles remains similar. Figure 4.5 is the counterpart of Figure 4.3a (CuZnO/Al$_2$O$_3$ catalyst) for different flow rates (GHSV = 64k h^{-1} and 120k h^{-1}), respectively. As can be seen, the temperature trends in the bed heated by microwave irradiation hardly depends on the flow rate of the feed, whereas the electrically heated reactor is more sensitive to the change of this parameter. In general, one would expect higher flow-heat transfer coupling in a conventionally heated reactor, where heat is transferred solely via conduction/convection mechanisms compared to a microwave reactor, where heat is provided volumetrically. Further comparison of the temperature profiles with the two heating modes in Figs 4.3-4.5 shows that the temperature near the wall is always significantly higher in case of EH compared to MW. At the core of the reactor, MW irradiation results in higher temperatures in a zone near the entrance; then, the temperature profiles progressively converge, cross and further downstream temperature is higher under EH. The outlet is always colder under MW heating.
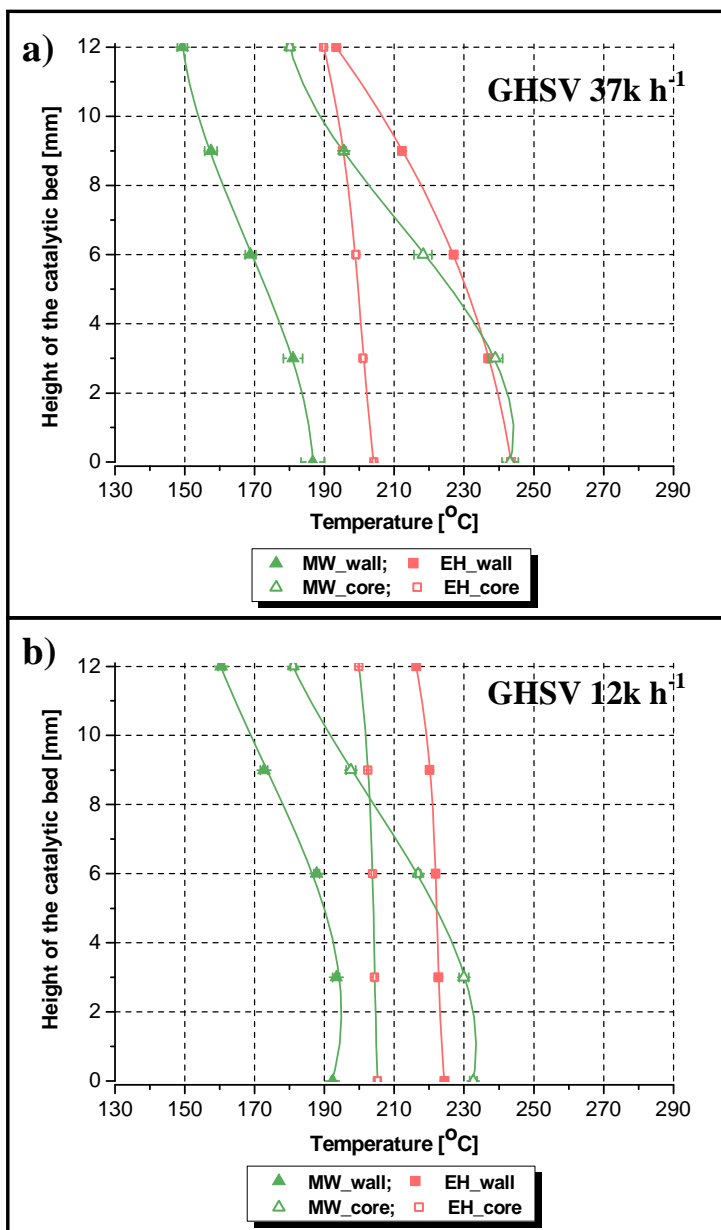
Figure 4.3. Temperature profiles for MSR over (a) CuZnO/Al$_2$O$_3$ and (b) PdZnO/Al$_2$O$_3$ catalyst in the microwave (MW) and electrically heated (EH) reactors at an average temperature of 210°C. The indicated spread of the results is based on measurements of four replicates
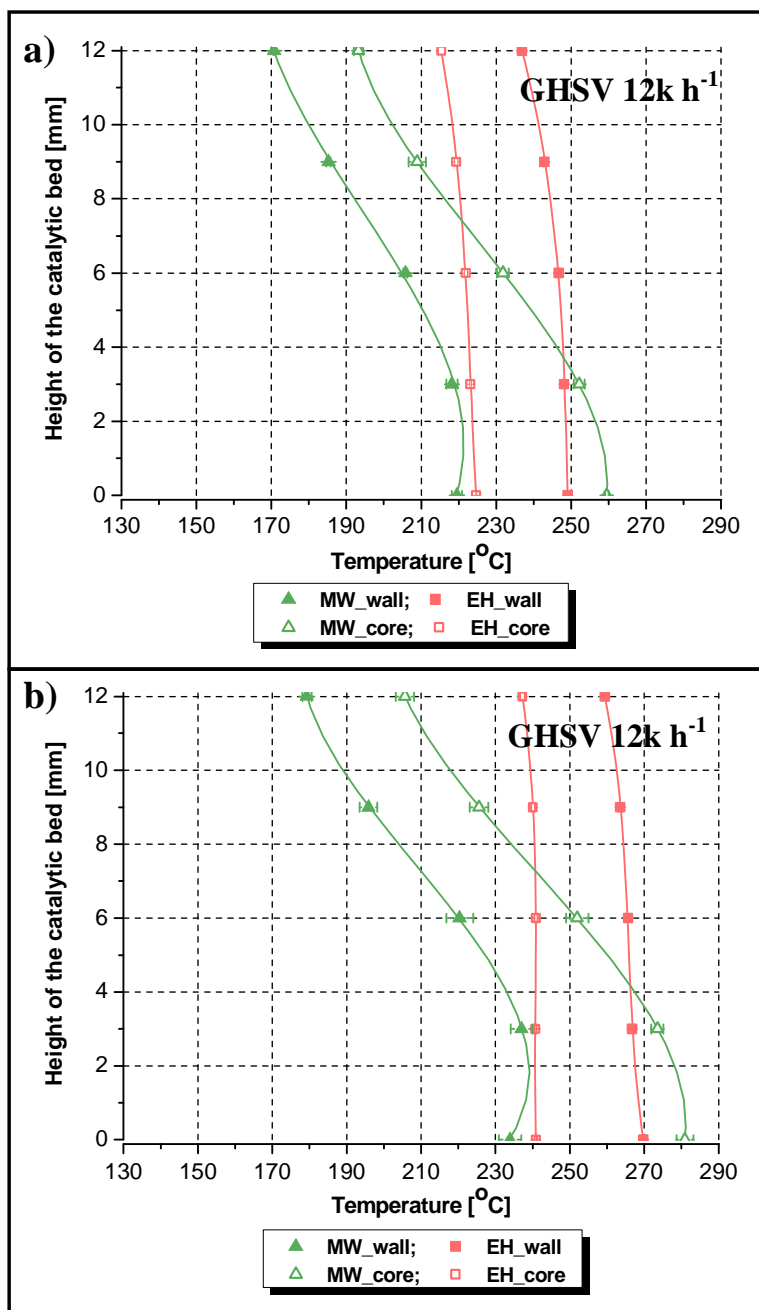
Figure 4.4. Temperature profiles for MSR over PdZnO/Al$_2$O$_3$ catalyst in the microwave (MW) and electrically heated (EH) reactors at an average temperature of (a) 230°C and (b) 250°C. The indicated spread of the results is based on measurements of four replicates
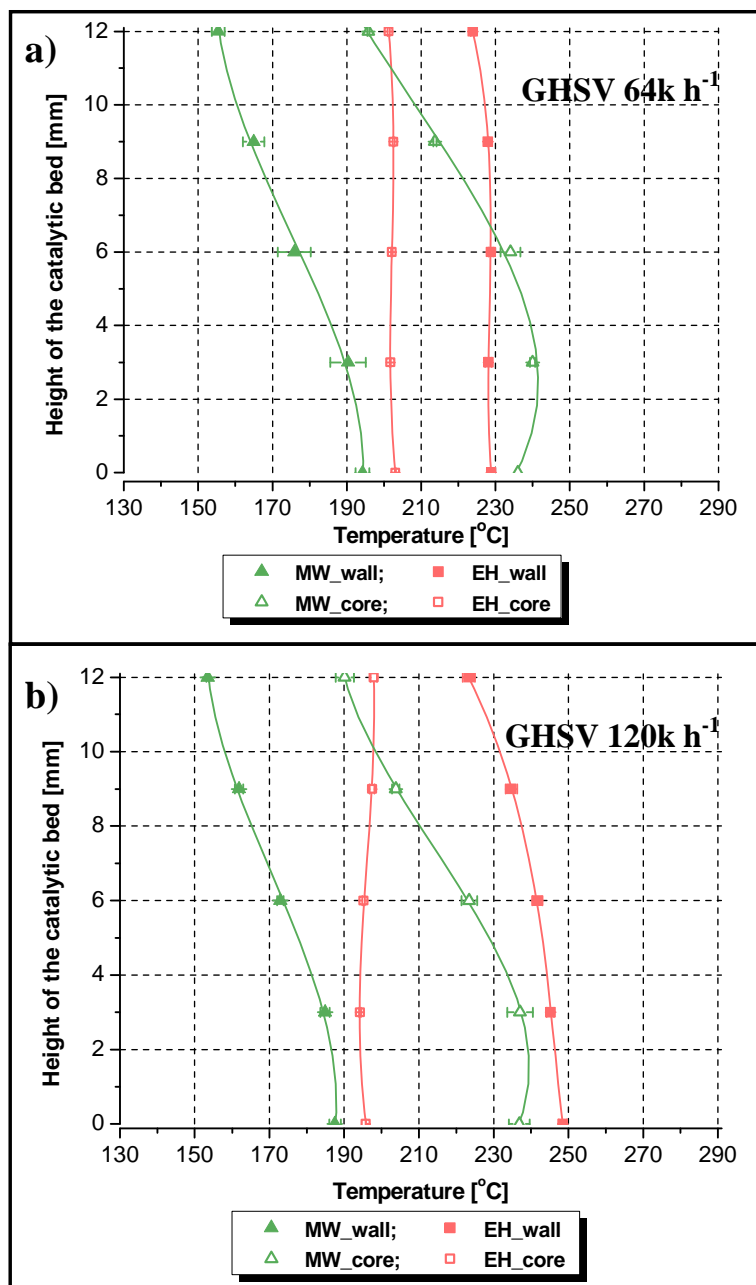
Figure 4.5. Temperature profiles for MSR over CuZnO/Al$_2$O$_3$ catalyst in the microwave (MW) and electrically heated (EH) reactors at an average temperature of 210°C for different gas hourly space velocities; (a) 64k h^{-1} and (b) 120k h^{-1}. The indicated spread of the results is based on measurements of four replicates

4.3.2 Conversion and selectivity

Taking into account the aforementioned differences in the temperature distribution for the two heating modes, direct comparison of the experimental results is not straightforward. Herein, we use the concept of average bed temperature, discussed in the previous section, as independent variable to describe reaction performance at different thermal conditions. In principle, the accuracy of the approach is very high when the variation of bed temperatures around the average value is very small, and decreases with increasing temperature dispersion as the reaction rate is not linearly dependant on the local temperature.

Figure 4.6 presents MeOH conversion as a function of the average temperature in the catalytic bed. Experiments were performed at different heat inputs corresponding to an average temperature range $170^{\circ}C - 230^{\circ}C$ with $CuZnO/Al_2O_3$ and $190^{\circ}C - 250^{\circ}C$ with $PdZnO/Al_2O_3$ catalyst. It should be repeated here, that it was not the aim of the work to optimize reaction conditions for full conversion, but to explore potential microwave effects over a wide conversion range. Furthermore, $250^{\circ}C$ is the temperature limit of the fiber-optic sensors for long-term reliable operation. Exposure to temperatures higher than $250^{\circ}C$ drastically decreases the life time of the probe. The results show that methanol conversion exhibits nearly linear increase with increasing T_{avg} both for EH and MW heating with the latter resulting in clearly higher conversions. The effect is more pronounced for the Cu-based catalyst, most likely due to the ~4 times more metal sites (strong microwave absorbers) available. As mentioned in the previous paragraph, direct comparison of the performance of the catalytic bed at the same uniform temperature is not possible. It can be seen, however, that even in cases where the maximum temperature along the entire height of the bed is clearly higher under EH, conversion is either higher under MW or approximately the same between the two heating modes. Figure 4.6b ($PdZnO/Al_2O_3$ catalyst) shows that methanol conversion with MW at $T_{avg} = 230^{\circ}C$ (solid triangle) is approximately the same as conversion with EH at $T_{avg} = 250^{\circ}C$ (solid square) (72% vs. 74%, respectively), although, comparison, in Figure 4.7, of the MW and EH temperature profiles at $T_{avg} = 230^{\circ}C$ (green lines) and $250^{\circ}C$ (red lines), respectively, shows that the maximum temperature along the height

of the catalytic bed is higher in the latter case: in the range of $10^{o}C$ close to the entrance to $67^{o}C$ at the exit. Furthermore, Fig. 4.3a shows that the maximum temperature in the bed is the same with EH and MW (~$243^{o}C$), while conversion is 12% higher under MW as shown in Fig. 4.6a ($T_{avg} = 210^{o}C$). These results indicate that a MW reactor can be operated at lower maximum temperature, compared to conventional heating, for the same conversion; this is highly desirable in terms of materials and safety.

Figure 4.8 presents the effect of feed flow rate on methanol conversion. The parametric study was done only for Cu catalyst at an average bed temperature of $170^{o}C$. The experiments were performed for three GHSV values:~37k h^{-1}, ~64k h^{-1} and 120k h^{-1} corresponding to residence times in the range ~100-30ms. As expected, conversion increases with decreasing GHSV or increasing residence time. Furthermore, conversion with MW remains higher than with EH by 8%-16% (~60% increase compared to EH) over the entire GHSV range with increasing trend at lower GHSVs and higher conversions. Finally, Figure 4.9 shows the product distribution with MW and EH at different average reactor temperatures for the two catalysts used. H_2 and CO_2 are the main products in all cases and only negligible amounts of CO were detected. The molar ratio of H_2:CO_2 is ~ 3:1, as dictated by the methanol reforming reaction stoichiometry (Eq. 4.1). Clearly, the product yields are not affected by the heating mode, the reaction temperature (over the temperature range examined), or the catalyst used ($CuZnO/Al_2O_3$ and $PdZnO/Al_2O_3$).

Finally, it has been reported in the literature, that MW-activated metal oxide catalysts may induce microstructural modification in their surface resulting in higher activity during reaction [43]. To verify this potential effect, two experiments were performed with MW-activated and MW-pretreated catalyst. In the case of microwave activation, the bed of catalytic oxide precursors ($CuOZnO/Al_2O_3$) was exposed to microwave irradiation for ~1.5 h at 220 ^{o}C in H_2/N_2 flow. After catalyst activation, the reactor remained sealed and under N_2 flow to prevent re-oxidation until it was placed inside the electric heating element to start reaction. In the case of microwave pretreatment, the catalyst was first activated with EH, as described in paragraph 4.2.2, and then exposed to MW irradiation in N_2 flow for 40 min before starting the reaction with EH. In both experiments, $T_{avg} = 190^{o}C$ and GHSV ~64k h^{-1}. Figure 4.10 shows that

the methanol conversions attained, represented by the circle symbols, are very close to the one at the same operating conditions (open square symbol) with conventionally (EH) activated catalyst. This indicates that pretreatment or activation of the catalyst under microwave conditions does not affect the reaction performance, at least for the experimental conditions studied here. Finally, SEM pictures of the catalysts (not shown) showed no visible difference in their morphology when exposed to MW irradiation either before or during reaction.
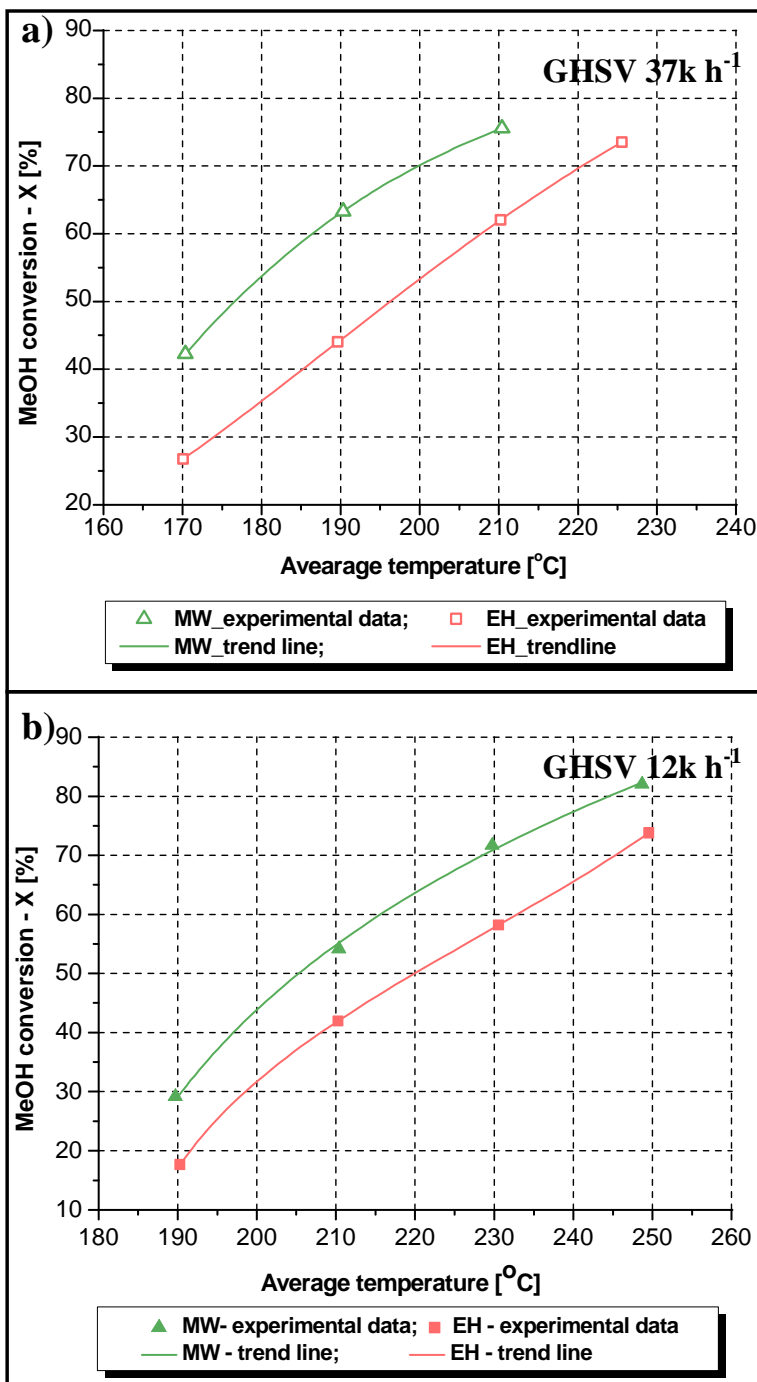
Figure 4.6. Methanol conversion as a function of average temperature in the catalytic bed with (a) CuZnO/Al$_2$O$_3$ and (b) PdZnO/Al$_2$O$_3$ catalyst
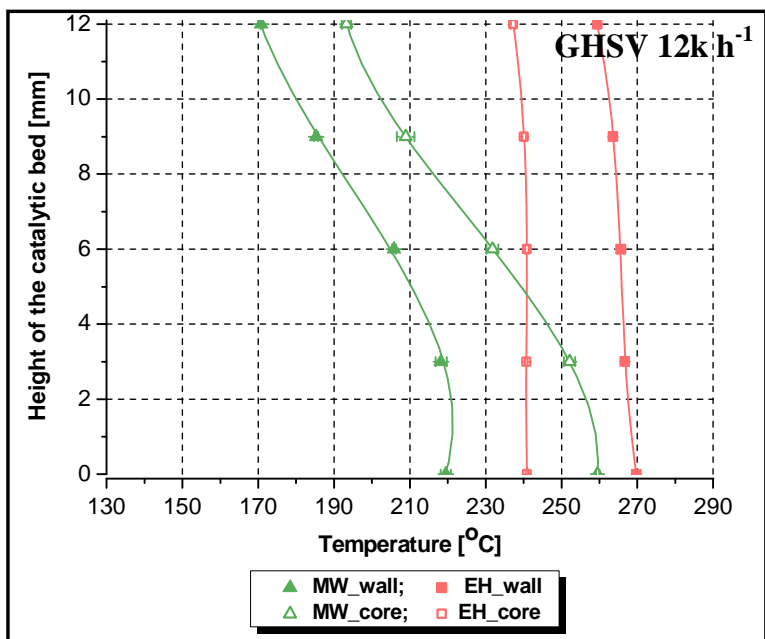
Figure 4.7. Temperature profiles in the MW and EH heated reactor for comparable methanol conversion (71.7% vs. 73.8%, respectively) over PdZnO/Al$_2$O$_3$ catalyst. The indicated spread of the results is based on measurements of four replicates.
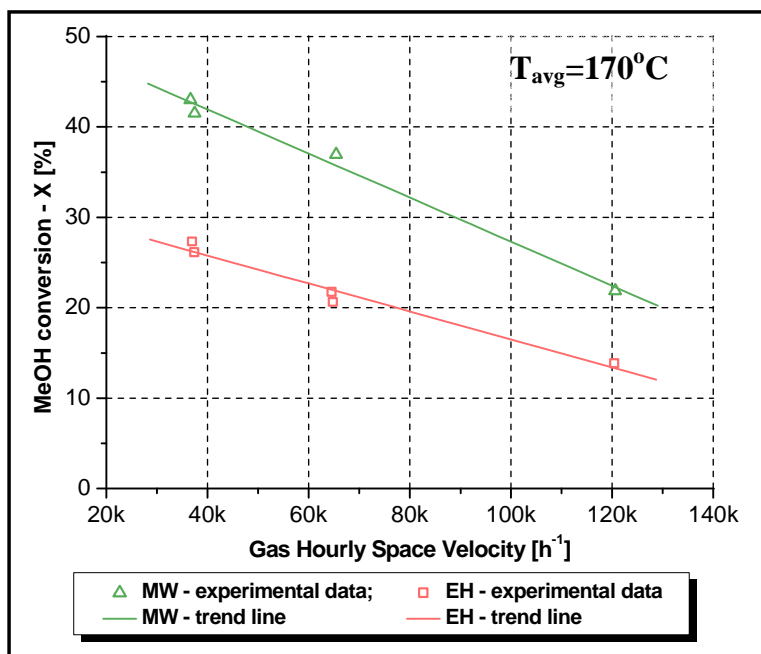

Figure 4.8. Methanol conversion as a function of gas hourly space velocity for the CuZnO/Al$_2$O$_3$ catalyst at an average temperature of 170°C
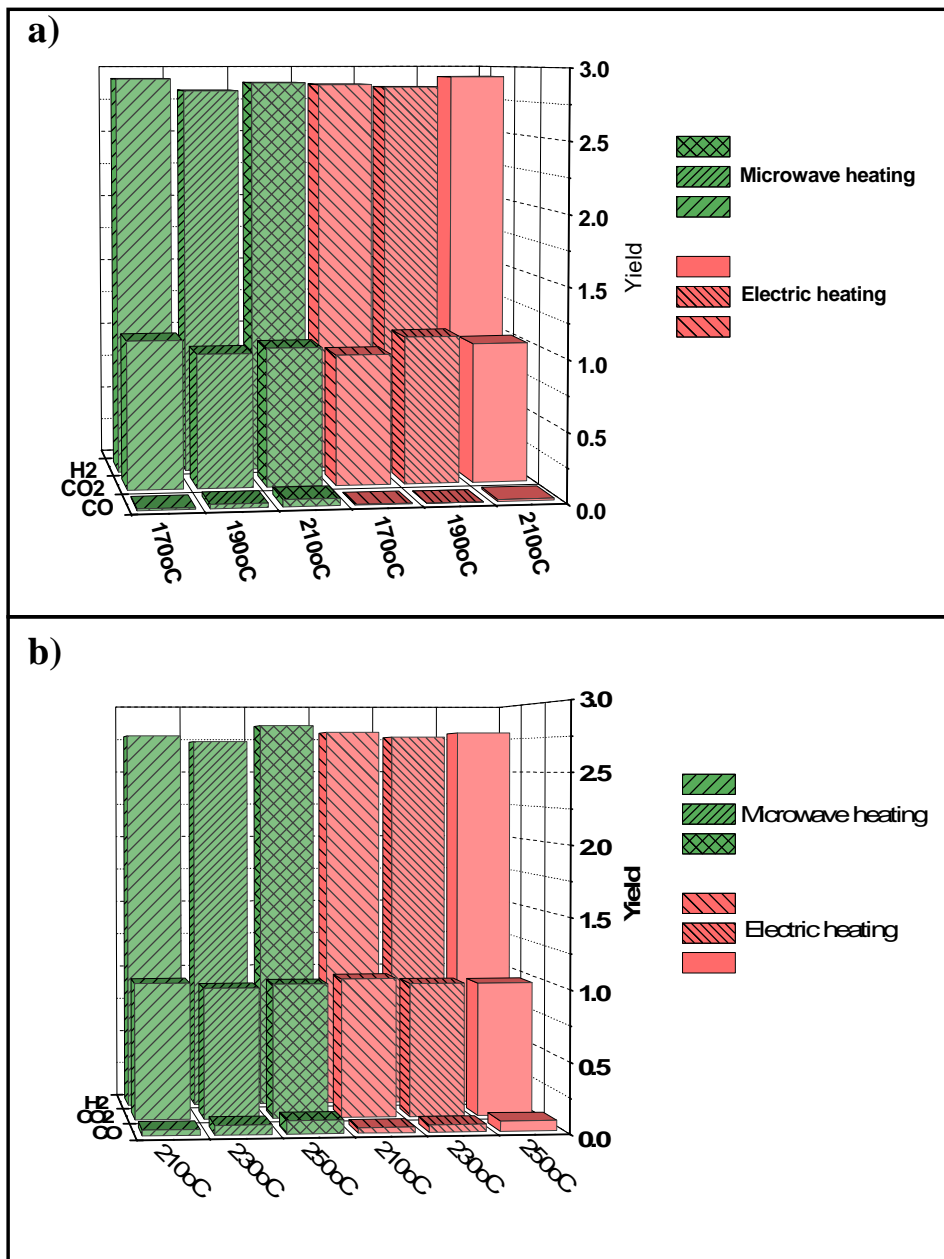
Figure 4.9. Product gas distributions for MSR over (a) CuZnO/Al$_2$O$_3$ and (b) PdZnO/Al$_2$O$_3$ catalyst performed under MW and EH at three average bed temperatures
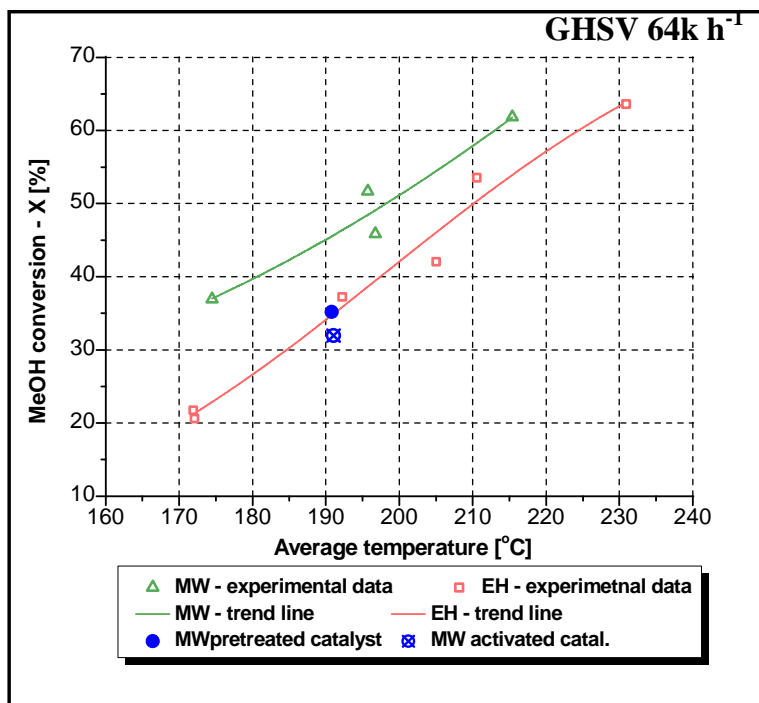
Figure 4.10. Effect of "microwave pretreatment" and "microwave activation" on methanol conversion using a CuZnO/Al₂O₃ catalyst

4.3.3 Reactor energy efficiency

The lower temperatures near the solid and open boundaries, discussed in detail in paragraph 4.3.1, imply potential for reduced thermal losses to the surroundings with direct impact on the energy utilization. The energy efficiency analysis here is based on the macroscopic energy balance over the control volume of the catalytic bed; this reads:

$$\sum_i n_{i_{IN}} \int_{T_0}^{T_p} Cp_i(T)dT - \sum_i n_{i_{OUT}} \int_{T_0}^{T_{OUT}} Cp_i(T)dT - \Delta H_r^{T_0} + Q_{input} - Q_{loss} = 0 \qquad \textbf{(4.2)}$$

In Eq. 4.2, n_i is the number of moles of species i; T_0 is the ambient temperature; T_p is the temperature of preheated reactants entering the catalytic bed; T_{out} is the temperature of the products at the outlet; Q_{input} is the energy delivered to the bed either from the electric heating element or from the magnetron (i.e., electromagnetic energy dissipated in the bed), and Q_{loss} is the heat loss through the solid boundaries. After term rearrangement, Eq. 4.2 can be written as

$$\sum_i n_{i_{IN}} \int_{T_0}^{T_p} Cp_i(T)dT + Q_{input} - Q_{Loss} = \Delta H_r^{T_0} + \sum_i n_{i_{OUT}} \int_{T_0}^{T_{OUT}} Cp_i(T)dT \qquad \textbf{(4.3)}$$

The left-hand side of Eq. 4.3 is the net heat input to the reactor comprising the sensible heat of the preheated reactants stream, which is the same for the two heating modes, and the heat input and heat loss through the side solid boundaries which cannot be directly estimated based on the available data. Eq. 4.3 dictates that the net heat input is partially converted to chemical energy and partially leaves the system as sensible heat of the products (right-hand side of Eq. 4.3). On this basis, we define here energy efficiency as the fraction of net heat input converted to chemical energy according to Eq. 4.4:

$$Efficiency = \frac{\Delta H_r^{T_0}}{\Delta H_r^{T_0} + \sum_i n_{i_{OUT}} \int_{T_0}^{T_{OUT}} Cp_i(T)dT} = \frac{\text{Heat of reaction}}{\text{Net heat input}} \qquad \textbf{(4.4)}$$

Different efficiency values between experiments with the two heating modes at approximately equal conversions, and thus heat of reaction, imply different net heat inputs for the same reactor performance (denominator of Eq. 4.4), which can be due to

uneven temperature distribution between the metal sites and the support and gas phase. Along this line, Figure 4.11 presents energy efficiencies calculated, according to Eq. 4.4, for the two heating modes and the two catalysts. In the event of $CuZnO/Al_2O_3$, the efficiencies are compared at three conversion levels, namely ~41-44%, ~63-64% and ~73-75%, and in the event of $PdZnO/Al_2O_3$ at ~54-58% and ~71-73%. The efficiency values correspond to the experiments, shown in Figure 4.11, which have been grouped in pairs of approximately equal conversions.

Figure 4.11 shows that at the conditions considered, the energy efficiency is 5-7% higher under MW heating. This is intuitively expected given that the reactant streams are preheated to the same temperature ($150^{o}C$), whereas the products in MW heating leave the reactor at significantly lower temperature, compared to EH, at approximately equal conversion. Assuming that MW effects are solely of thermal nature, higher efficiency values with MW than conventional heating suggest that a given conversion can be achieved with lower net heat input to the reactor and may be an implicit indication of higher temperature at metal sites than in bulk phase due to the selective heating principle. It is remarked here, that higher energy efficiency values for the reactor with MW <u>do not</u> mean lower total energy consumption. On the contrary, the total energy consumption is typically higher with general purpose MW applicators, as the one used in this work, due to limitations in 1) magnetron efficiency and 2) converting electromagnetic energy to heat (implying reflected power). Although both can be improved with proper MW engineering, it was not the purpose of this work to optimize total energy consumption (energy values were not registered), but rather to explore the effect of MW heating on the methanol reforming process itself and gain more insight into the application of MW to heterogeneous gas-solid reactions. Further experimental parametric studies with varying parameters the type, amount, composition, shape and size of catalyst as well as microwave frequency are necessary to identify the conditions for maximum reactor energy efficiency.
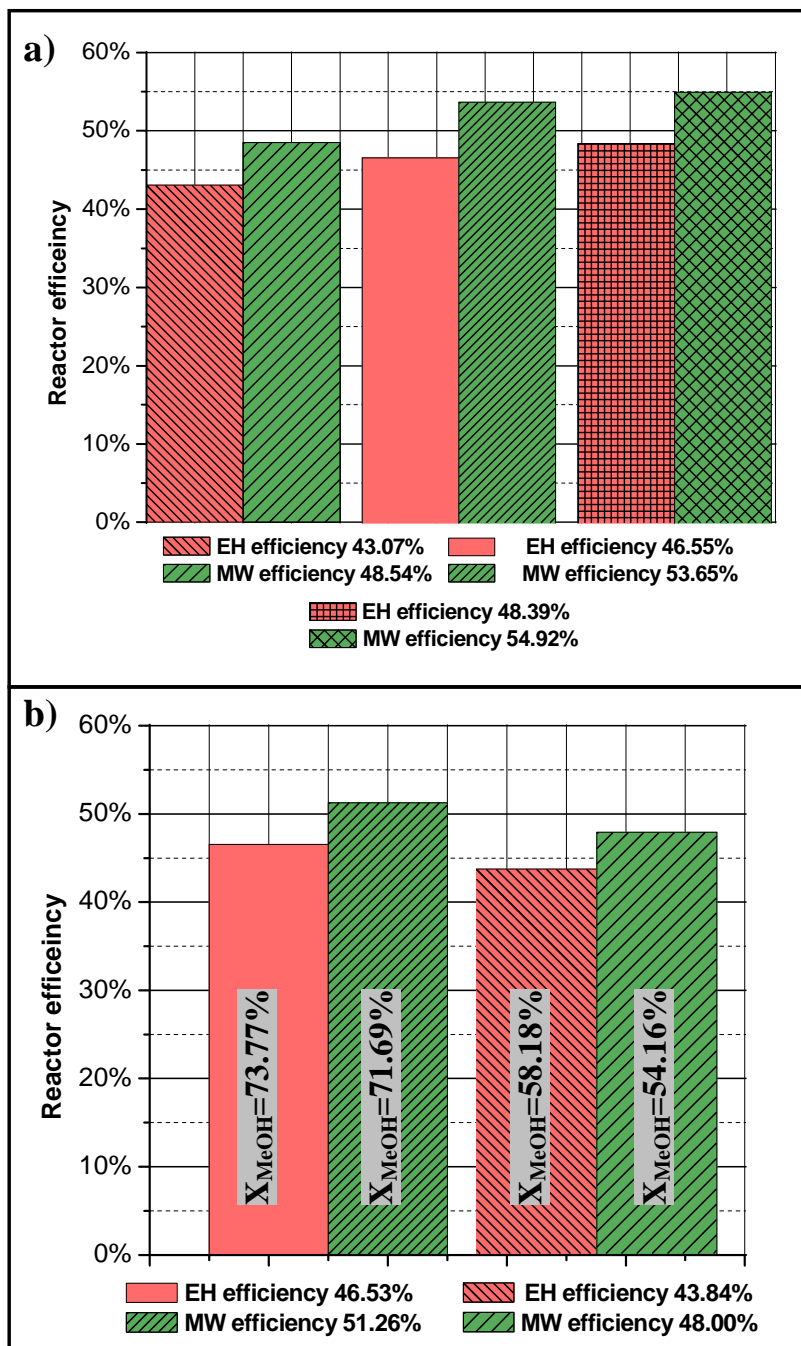
Figure 4.11 Comparison of the reactor energy efficiency for MSR over (a) CuZnO/Al₂O₃ and (b) PdZnO/Al₂O₃ catalyst under MW (green) and EH (red).

4.4 Conclusions

We performed a systematic study of methanol steam reforming on $CuZnO/Al_2O_3$ and $PdZnO/Al_2O_3$ catalysts under electric heating (EH) and microwave heating (MW) with focus on comparison of methanol conversion, product distribution and energy efficiency of the catalytic bed. The results show that higher methanol conversion is obtained under MW for comparable thermal conditions regardless of the catalyst. In other words, the MW reactor can be operated at lower temperature compared to the conventionally heated reactor to achieve the same methanol conversion. Although conversion is strongly influenced by the applied heating mode, there was no effect on the product composition in the range of examined thermal conditions for the two catalysts tested.

Furthermore, application of MW irradiation to packed bed reactors for heterogeneous gas-solid reactions results in significant two-dimensional temperature non-uniformities. This necessitates multi-point temperature measurements in the radial and axial direction in order to rationalize reaction data. Single-point temperature measurements, as often reported or implied in the literature, may lead to erroneous assumptions as to the real thermal conditions inside the reactor and thus incorrect conclusions concerning MW effects. Besides, the lower temperatures observed near the solid and open boundaries imply potential for reduced thermal losses to the surroundings with direct impact on the energy utilization. Indeed, the reactor energy efficiencies of the MW-assisted process are higher than the corresponding ones of the electrically heated process for both catalysts and over the range of reaction temperatures studied. Assuming that MW effects are solely of thermal nature, higher efficiency values with MW than with conventional heating imply that a given conversion can be achieved with lower net heat input to the reactor. This may be an implicit indication of higher temperature at metal sites than in bulk phase (microscale hot spot formation) due to the selective heating principle.

Finally, it is worth noting that the significant temperature gradients in a catalytic bed of only 24 mm O.D. signify a major challenge in process scale-up.

Bibliography

1. Hotz, N., et al., Disk-shaped packed bed micro-reactor for butane-to-syngas processing. Chemical Engineering Science, 2008. **63**(21): p. 5193-5201.
2. Holladay, J.D., et al., An overview of hydrogen production technologies. Catalysis Today, 2009. **139**(4): p. 244-260.
3. Ahmed, S., et al., Decomposition of hydrocarbons to hydrogen and carbon. Applied Catalysis A: General, 2009. **359**(1-2): p. 1-24.
4. Pan, L. and S. Wang, Methanol steam reforming in a compact plate-fin reformer for fuel-cell systems. International Journal of Hydrogen Energy, 2005. **30**(9): p. 973-979.
5. Tonkovich, A.L.Y., et al., From seconds to milliseconds to microseconds through tailored microchannel reactor design of a steam methane reformer. Catalysis Today, 2007. **120**(1): p. 21-29.
6. Kaisare, N.S., et al., Stability and performance of catalytic microreactors: Simulations of propane catalytic combustion on Pt. Chemical Engineering Science, 2008. **63**(4): p. 1098-1116.
7. Arzamendi, G., et al., Integration of methanol steam reforming and combustion in a microchannel reactor for H2 production: A CFD simulation study. Catalysis Today, 2009. **143**(1-2): p. 25-31.
8. Suh, J.-S., et al., Transport phenomena in a steam-methanol reforming microreactor with internal heating. International Journal of Hydrogen Energy, 2009. **34**(1): p. 314-322.
9. Mettler, M.S., et al., Enhancing stability in parallel plate microreactor stacks for syngas production. Chemical Engineering Science, 2010. **66**(6): p. 1051-1059.
10. Lindström, B., et al., Combined methanol reforming for hydrogen generation over monolithic catalysts. Chemical Engineering Journal, 2003. **93**(1): p. 91-101.
11. Giroux, T., et al., Monolithic structures as alternatives to particulate catalysts for the reforming of hydrocarbons for hydrogen generation. Applied Catalysis B: Environmental, 2005. **56**(1-2): p. 95-110.
12. Kolios, G., et al., Heat-integrated reactor concepts for hydrogen production by methane steam reforming. Fuel Cells, 2005. **5**(1): p. 52-65.
13. Lattner, J.R. and M.P. Harold, Comparison of conventional and membrane reactor fuel processors for hydrocarbon-based PEM fuel cell systems. International Journal of Hydrogen Energy, 2004. **29**(4): p. 393-417.
14. Gallucci, F., et al., Methanol and ethanol steam reforming in membrane reactors: An experimental study. International Journal of Hydrogen Energy, 2007. **32**(9): p. 1201-1210.
15. Gallucci, F. and A. Basile, Pd-Ag membrane reactor for steam reforming reactions: A comparison between different fuels. International Journal of Hydrogen Energy, 2008. **33**(6): p. 1671-1687.
16. Iulianelli, A., et al., Methanol steam reforming reaction in a Pd-Ag membrane reactor for CO-free hydrogen production. International Journal of Hydrogen Energy, 2008. **33**(20): p. 5583-5588.
17. Stefanidis, G.D. and D.G. Vlachos, High vs. low temperature reforming for hydrogen production via microtechnology. Chemical Engineering Science, 2009. **64**(23): p. 4856-4865.

18. Conant, T., et al., Stability of bimetallic Pd-Zn catalysts for the steam reforming of methanol. Journal of Catalysis, 2008. **257**(1): p. 64-70.

19. Cormier, J.M. and I. Rusu, Syngas production via methane steam reforming with oxygen: plasma reactors versus chemical reactors. Journal of Physics D: Applied Physics, 2001. **34**(18): p. 2798-2803.

20. Sekiguchi, H. and Y. Mori, Steam plasma reforming using microwave discharge. Thin Solid Films, 2003. **435**(1-2): p. 44-48.

21. Yanguas-Gil, A., et al., Reforming of ethanol in a microwave surface-wave plasma discharge. Applied Physics Letters, 2004. **85**(18): p. 4004-4006.

22. Aubry, O., et al., On the use of a non-thermal plasma reactor for ethanol steam reforming. Chemical Engineering Journal, 2005. **106**(3): p. 241-247.

23. Paulmier, T. and L. Fulcheri, Use of non-thermal plasma for hydrocarbon reforming. Chemical Engineering Journal, 2005. **106**(1): p. 59-71.

24. Jasinski, M., et al., Production of hydrogen via methane reforming using atmospheric pressure microwave plasma. Journal of Power Sources, 2008. **181**(1): p. 41-45.

25. Wang, W., et al., DFT study on pathways of steam reforming of ethanol under cold plasma conditions for hydrogen generation. International Journal of Hydrogen Energy, 2009. **35**(5): p. 1951-1956.

26. Wang, Y.-F., et al., Methane steam reforming for producing hydrogen in an atmospheric-pressure microwave plasma reactor. International Journal of Hydrogen Energy, 2009. **35**(1): p. 135-140.

27. Henriques, J., et al., Microwave plasma torches driven by surface wave applied for hydrogen production. International Journal of Hydrogen Energy, 2010. **36**(1): p. 345-354.

28. Wang, Y.-F., et al., Production of hydrogen by plasma-reforming of methanol. International Journal of Hydrogen Energy, 2010. **35**(18): p. 9637-9640.

29. Cooney, D.O. and Z. Xi, Production of hydrogen from methane and methane/team in a microwave irradiated char-loaded reactor. Petroleum Science and Technology, 1996. **14**(8): p. 1111 - 1141.

30. Perry, W.L., et al., Microwave heating of endothermic catalytic reactions: Reforming of methanol. AIChE Journal, 2002. **48**(4): p. 820-831.

31. Domínguez, A., et al., Microwave-assisted catalytic decomposition of methane over activated carbon for CO2-free hydrogen production. International Journal of Hydrogen Energy, 2007. **32**(18): p. 4792-4799.

32. Chen, W.-H., et al., Hydrogen generation from a catalytic water gas shift reaction under microwave irradiation. International Journal of Hydrogen Energy, 2008. **33**(18): p. 4789-4797.

33. Fidalgo, B., et al., Microwave-assisted dry reforming of methane. International Journal of Hydrogen Energy, 2008. **33**(16): p. 4337-4344.

34. Fernández, Y., et al., Comparative study of conventional and microwave-assisted pyrolysis, steam and dry reforming of glycerol for syngas production, using a carbonaceous catalyst. Journal of Analytical and Applied Pyrolysis, 2010. **88**(2): p. 155-159.

35. Chen, W.-H. and B.-J. Lin, Effect of microwave double absorption on hydrogen generation from methanol steam reforming. International Journal of Hydrogen Energy, 2010. **35**(5): p. 1987-1997.

36. Seyfried, L., et al., Microwave Electromagnetic-Field Effects on Reforming Catalysts .: 1. Higher Selectivity in 2-Methylpentane Isomerization on Alumina-Supported Pt Catalysts. Journal of Catalysis, 1994. **148**(1): p. 281-287.

37. Roussy, G., et al., Permanent change of catalytic properties induced by microwave activation on 0.3% Pt/Al2O3 (EuroPt-3) and on 0.3% Pt-0.3% Re/Al2O3 (EuroPt-4). Applied Catalysis A: General, 1997. **156**(2): p. 167-180.

38. Bi, X.-j., et al., Microwave effect on partial oxidation of methane to syngas. Reaction Kinetics and Catalysis Letters, 1999. 66(2): p. 381-386.

39. Liu, Y., et al., The effects of microwaves on the catalyst preparation and the oxidation of o-xylene over a V2O5/SiO2 system. Catalysis Today, 1999. **51**(1): p. 147-151.

40. Bi, X.-J., Microwave effect on partial oxidation of methane to syngas over Ni/ZrO2. Fuel and Energy Abstracts, 2001. **42**(1): p. 19-19.

41. Zhang, X., et al., Carbon Dioxide Reforming of Methane with Pt Catalysts Using Microwave Dielectric Heating. Catalysis Letters, 2003. **88**(3): p. 129-139.

42. Zhang, X., et al., Oxidative coupling of methane using microwave dielectric heating. Applied Catalysis A: General, 2003. **249**(1): p. 151-164.

43. Zhang, X.-R., et al., A unique microwave effect on the microstructural modification of Cu/ZnO/Al2O3 catalysts for steam reforming of methanol. Chemical Communications, 2005(**32**): p. 4104-4106.

44. Tse, M.Y., et al., Applications of high power microwave catalysis in chemistry. Research on Chemical Intermediates, 1990. **13**(3): p. 221-236.

45. Cha, C.Y., Microwave Induced Reactions of So2 and Nox Decomposition in the Char-Bed. Research on Chemical Intermediates, 1994. **20**(1): p. 13-28.

46. Cha, C.Y. and Y. Kong, Enhancement of NOx adsorption capacity and rate of char by microwaves. Carbon, 1995. **33**(8): p. 1141-1146.

47. Kong, Y. and C.Y. Cha, NOx Abatement with Carbon Adsorbents and Microwave Energy. Energy & Fuels, 1995. **9**(6): p. 971-975.

48. Chang, Y.-f., et al., Microwave-assisted NO reduction by methane over Co-ZSM-5 zeolites. Catalysis Letters, 1999. **57**(4): p. 187-191.

49. Wang, X., et al., Microwave effects on the selective reduction of NO by CH4 over an In–Fe2O3/HZSM-5 catalyst. Chemical Communications, **2000**(4): p. 279 - 280.

50. Bond, G., et al., Recent applications of microwave heating in catalysis. Catalysis Today, 1993. **17**(3): p. 427-437.

51. Chen, C., et al., Microwave effects on the oxidative coupling of methane over proton conductive catalysts. Journal of the Chemical Society, Faraday Transactions, 1995. **91**(7): p. 1179-1180.

52. Chen, C.-l., et al., Microwave effects on the oxidative coupling of methane over Bi2O3-WO3 oxygen ion conductive oxides. Reaction Kinetics and Catalysis Letters, 1997. **61**(1): p. 175-180.

53. Will, H., et al., Microwave-Assisted Heterogeneous Gas-Phase Catalysis. Chemical Engineering & Technology, 2004. **27**(2): p. 113-122.

54. Zhang, X., et al., Microwave Dielectric Heating Behavior of Supported MoS2 and Pt Catalysts. Industrial & Engineering Chemistry Research, 2001. **40**(13): p. 2810-2817.

55. Thiebaut, J.M., et al., Durable changes of the catalytic properties of alumina-supported platinum induced by microwave irradiation. Catalysis Letters, 1993. **21**(1): p. 133-138.
56. Xia, G., et al., Development of Highly Active Pd-ZnO/Al2O3 Catalysts for Microscale Fuel Processor Applications. Chemical Engineering & Technology, 2005. **28**(4): p. 515-519.
57. Karim, A., et al., The role of PdZn alloy formation and particle size on the selectivity for steam reforming of methanol. Journal of Catalysis, 2006. **243**(2): p. 420-427.
58. Dagle, R.A., et al., PdZnAl catalysts for the reactions of water-gas-shift, methanol steam reforming, and reverse-water-gas-shift. Applied Catalysis A: General, 2008. **342**(1-2): p. 63-68.
59. Durka, T., et al., On the accuracy and reproducibility of fiber optic (FO) and infrared (IR) temperature measurements of solid materials in microwave applications. Measurement Science and Technology, 2010. **21**(4): p. 045108.

5

Application of microwave energy to exothermic reactions: the case of Water-Gas Shift Reaction

5.1 Introduction

The water-gas shift reaction (WGSR) is an important step in many hydrocarbon and oxygenated fuel reforming processes, which shifts carbon monoxide, by use of steam, to carbon dioxide and hydrogen thus maximizing the production of the latter (Eq.(5.1).

$$CO + H_2O \rightarrow H_2 + CO_2 \qquad (\Delta H_{298K} = -41 \text{kJ/mol}) \qquad \textbf{(5.1)}$$
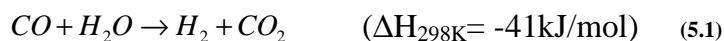
This well-known heterogeneous catalytic reaction becomes very important when processing of fossil fuels for fuel cell applications is considered. Proton exchange membrane fuel cells (PEMFCs) do not tolerate CO content above 20ppm[1]; thus, efficient removal of CO is essential for proper working of fuel cell stacks. To this end, WGSR is very often employed in the process.

WGSR is moderately exothermic and, therefore, is thermodynamically limited at higher temperatures, whereas it favours CO conversion at lower temperatures. The common practice is to divide the process into two steps; high temperature shift (HTS) in the temperature range 350°C-450°C, where most of CO is converted, and low temperature shift (LTS) in the temperature range 190°C-250°C to complete the reaction [2].

WGSR has been often investigated to develop catalysts with special focus on their sulphur tolerance. In the last few decades, due to increased interest in electricity production from fuel cells and employment of WGSR in this process, the scope of research has been shifted to discovery of catalysts, which are highly active[3]. However, not much research work has been done so far on application of the microwave energy to the water gas shift reaction. The main reason for this is probably that WGSR is not considered as a separate, single stage, process for hydrogen production, but rather, part of the global steam reforming reaction.

Pioneering research work on the application of microwaves to WGSR was done by Chen and co-workers in 2008 [2, 4]. The investigation was focused on the so-called "double-absorption effect of microwaves by water and the catalyst". In particular, the authors postulated that the presence of a catalyst doped with a good microwave absorber (iron oxide) in combination with water, being both a reaction component and a good

microwave absorber, create very favourable conditions for effective triggering of the reaction with microwave energy. Their results show that microwave energy can be successfully applied to WGSR allowing a maximum CO conversion of ~96% at steam to carbon ratio (S/C)=8 and T~550°C. Further, the observed CO conversion increased with increasing reaction temperature, contrary to chemical equilibrium predictions and the results from the electrically heated reactor.

During an electro-microscopic inspection of the spend catalyst, it was discovered that a low S/C ratio results in appearance of various size cracks on the catalyst surface. The effect was not observed for higher S/C ratios. It was proposed that iron oxide contained in the catalyst may cause a high thermal gradient, due to effective absorption of microwave energy, which cannot be released with low content of steam. Therefore, high S/C ratios are favourable both from the reaction equilibrium point of view and the catalyst stability.

From a careful analysis of the aforementioned research work of *Chen* and taking into account our own experience and the obtained results from the microwave driven steam reforming of methanol, the question aroused whether application of microwave energy, and therefore the generation of hot-spots in the catalytic bed, can create some benefits over the application of conductive heating in case of exothermic reactions.

In this chapter, the results of an experimental study on microwave-activated and electrically-heated WGSR for hydrogen production are presented. The reaction performance was evaluated in terms of CO conversion as function of gas hourly space velocity (GHSV), S/C and (average) reaction temperature (T).

5.2 Experimental

The experimental reaction system employed for the investigation is very similar to the reaction system used for the steam reforming of methanol (Chapter 4). Therefore, the description of the employed system is limited only to the list of main differences. The schematic representation of the system is presented in Figure 5.1.

The main difference between the presented configuration in Fig. 5.1 and the one used for the steam reforming reaction is that for the water gas shift reaction no carrier gas was used.
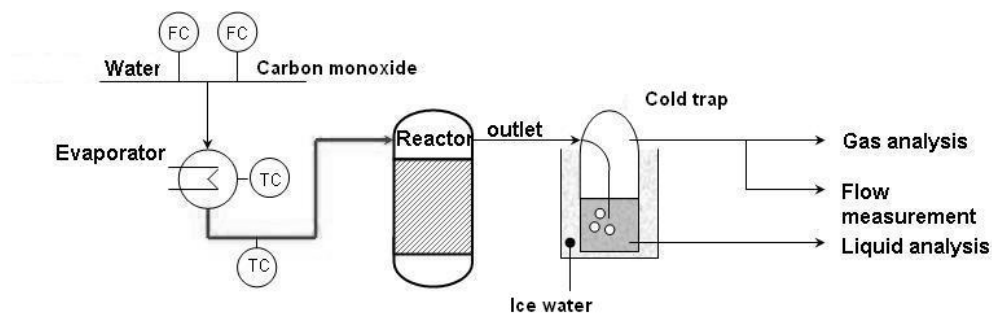
Figure 5.1. Schematic representation of the reaction system (adapted from M.Reus, Microwave-assisted low temperature steam reforming of methanol for hydrogen production).

The role of carrier gas, which is necessary for the proper operation of the evaporator, is taken on by carbon monoxide which at the same time is a reaction compound. It has to be mentioned that both flow controllers, for water and carbon monoxide respectively, were re-calibrated before the experimental campaign began.

The catalyst employed in this stage of investigation was the same commercial copper-based, low temperature, water gas shift catalyst ($CuZnO/Al_2O_3$), delivered by Alfa Aesar, as was previously used in the steam methanol reforming process. Besides, the experimental procedure employed in this phase of investigation corresponds to the methodology employed in the previously mentioned experiments on microwave-assisted steam reforming of methanol.

5.3 Results

5.3.1 Spatial temperature distribution

As discussed in the previous chapter, application of microwave energy to the packed bed reactor results in significant two-dimensional temperature non-uniformities, which correspond to non-uniform energy dissipation inside the bed. Moreover, non-uniform temperature conditions imply difficulties in meaningful comparison between different experimental runs. Therefore, mapping of temperature in the catalytic bed is necessary to obtain good insight into the actual reaction conditions and thus to reliably evaluate the reaction performance.

To account for the temperature gradients while maintaining the comparison method relatively simple, an average temperature of the bed was calculated. This was done by double averaging the experimental temperature data first in the radial direction, assuming parabolic profiles, and then in the axial direction along the height of the catalytic bed. The detailed description of the method was discussed in the previous chapter.

Figure 5.2 shows axial temperature profiles near the wall and in the core of the reactor for microwave (MW) and electrically heated (EH) reactions performed at 210°C and 230°C. The initial concentration and feed composition as well as the residence time in all events were maintained identical. It can be seen that the temperature patterns in the events of microwave heating and electric heating differ remarkably. In particular, microwave heating results in more pronounced temperature gradients in both, radial and axial direction compared to electric heating. This observation is consistent with that made in the case of microwave-activated steam reforming of methanol and is expected based on the specific design of the microwave applicator used.

However, Figure 5.2 shows that, in contrast to the endothermic steam reforming reaction, the direction of thermal gradients does not depend on the employed heating mode. In both cases, the temperature in the core of the reactor is higher than the temperature near the wall of the reactor.

Figure 5.3 illustrates temperature development in the bed for increased flow rate of the feed (GHSV=35000h^{-1}) and for two different steam to carbon ratios, S/C=1 and S/C=1.5, respectively. It can be seen that the temperature profiles in case of the microwave-activated reaction remain practically unaffected with varying S/C. In contrast, increased amount of steam affects the temperature profile inside the catalytic bed when the electric heating element is used as a means of energy source. More specifically, the observed temperature difference near the wall of the reactor is in the range 5-15°C, whereas the core temperatures are hardly affected. One may ask here how the average temperature remains the same in both compared experiments if the temperature gradient in case of S/C=1 is smaller than for S/C=1.5. This is due to the methodology of the average temperature calculation, which assumes a parabolic
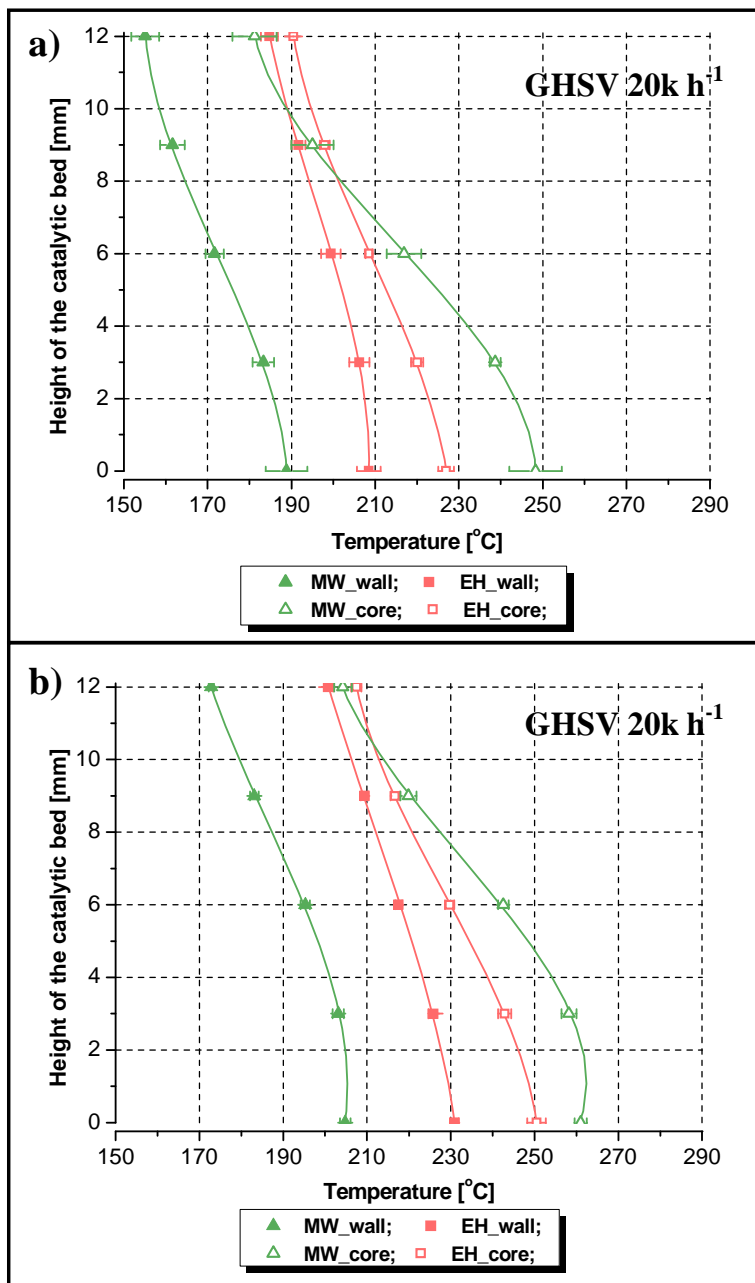
Figure 5.2 Temperature profiles in the microwave (MW) and electrically heated (EH) reactors at an average temperature of a) 210°C and b) 230°C. The indicated spread of the results is based on measurements of four replicates. The steam to carbon ratio is S/C=1.5 and GHSV=20000h[-1]

temperature profile in the radial direction, thus rendering the average temperature more dependent on the higher temperatures at the core of the reactor and less dependent on the lower temperatures near the wall of the reactor.

The effect of flow rate on the temperature distribution inside the catalytic bed can be evaluated based on Fig.5.2b and Fig.5.3b together. The figures show that increasing flow rate mostly affects the temperature gradients at the entrance of the reactor (at the bottom). Furthermore, the microwave heated reactor is more sensitive to flow rate change since both temperatures (in the core and at the wall) are affected, whereas in the case of the electric spiral element, only the core temperature is influenced.

Overall, comparison of the temperature profiles under the two heating modes in Figures 5.2-5.3 shows that at the core of the reactor, microwave irradiation results in higher temperatures in the zone near the entrance compared to the electric heating mode. In contrast, the temperature near the wall is always significantly lower under microwave irradiation. Finally, regardless of the shape of the profiles, the outlet temperatures are always somewhat lower under microwave heating.

5.3.2 Conversion and selectivity

As already mentioned, the comparison of conversion and selectivity of the reactor for the two different heating modes, microwave and electric, is the main focus in this research work as an indirect method for the examination of the so called hot-spot formation in the microwave heated catalytic bed.

Figure 5.4 shows conversion of carbon monoxide as function of the reactor average temperature for the two investigated heating modes. It is shown that contrary to the results on microwave activated methanol steam reforming, conversion of the feed in the water gas shift reaction hardly depends on the applied energy source; i.e., the green triangles representing CO conversion under microwave heating in Figure 5.4 virtually coincide with the red square symbols (direct electric heating). Besides, it can be noticed that the conversion profile for the microwave assisted process covers only the temperature range between 195°C and 250°C, whereas for electric heating, the investigated temperature range extends from 150°C to 250°C. While the upper temperature limit is dictated by the limitation of the temperature sensors used, the lower
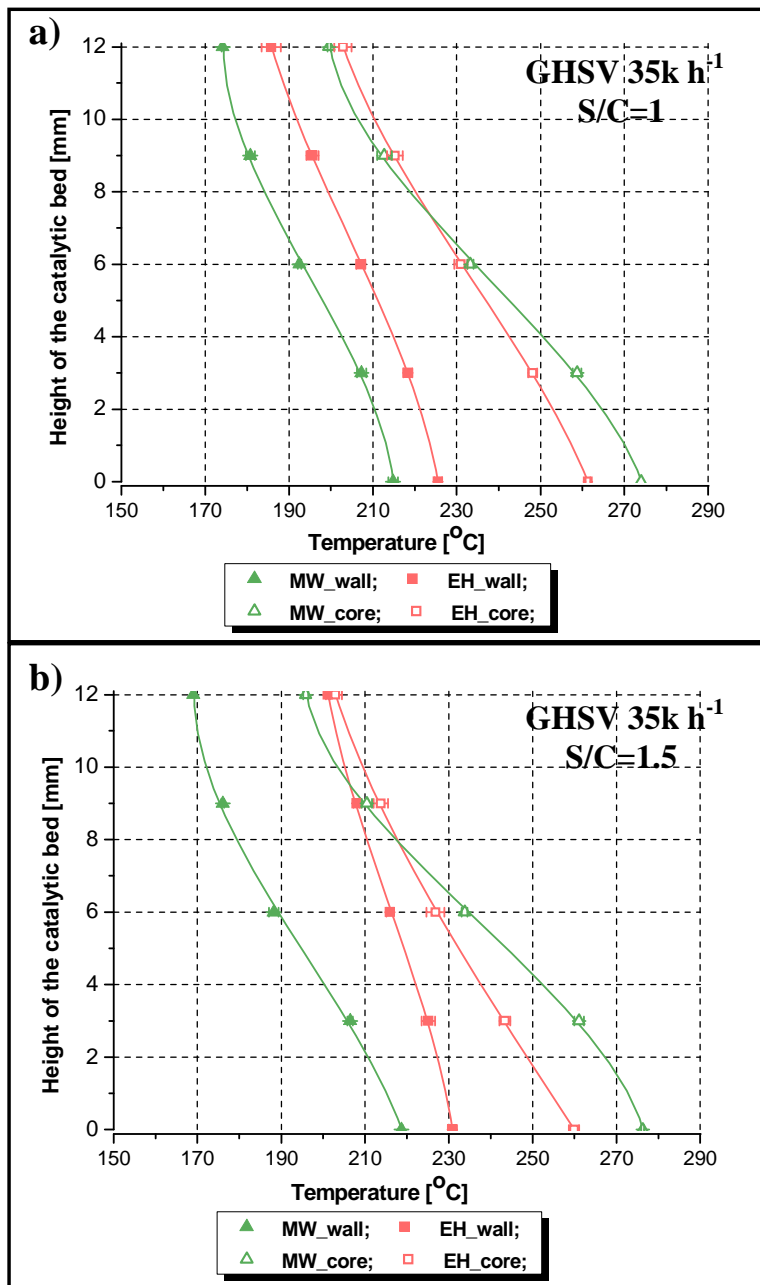
Figure 5.3 Temperature profiles in the microwave (MW) and electrically heated (EH) reactors at an average temperature of 230°C for two steam to carbon ratios (S/C=1 and 1.5). The indicated spread of the results is based on measurements of four replicates.

temperature limit is (surprisingly) related to the minimum of the power delivered by the microwave device. More specifically, in the case of the microwave experiment, application of the minimum available continuous power (1W) results in the already high average reactor temperature of ~195°C.Further, conversion of carbon monoxide increases with reaction temperature contrary to the Le Chatelier's principle of chemical equilibrium (Figure 5.5). In general, it depends on the catalyst and applied temperature range whether the process is at equilibrium. Consideration of Figure 5.4 and Figure 5.5 together shows that the conversions achieved in the reactor are lower than the equilibrium conversions at the corresponding reactor conditions and, therefore, hydrogen production increases with reaction temperature.

Figure 5.6 presents the effect of S/C on carbon monoxide conversion. The parametric study was done at an average bed temperature of 230 °C for GHSV~35k h^{-1}. Increasing the steam content in the reactor feed results in increase in the carbon monoxide conversion (under both heating modes) in agreement with the reaction kinetics from the literature indicating first order dependence of the reaction rate on CO and steam concentration [5]. Furthermore, although CO conversion in the case of microwave heated reactor is slightly higher than for the electric heating mode (in the entire S/C range investigated) the observed difference (up to 2%) is rather related with the uncertainty of measurements and shall not be granted as an argument confirming the positive effect of microwave energy on the water gas shift reaction.

Finally, figure 5.7 shows the distribution of the main reaction products, H_2 and CO_2, for the microwave activated and electrically activated process at different average reactor temperatures at S/C =1.5 and GHSV~20k h-1. Due to unavoidable leaks of hydrogen from the system, the amount of hydrogen is slightly lower than the amount of carbon dioxide; however the molar ratio of H_2:CO_2 is very close to 1:1, as dictated by the reaction stoichiometry. It can be safely concluded that the product distribution is not affected by the heating mode and the reaction temperature.
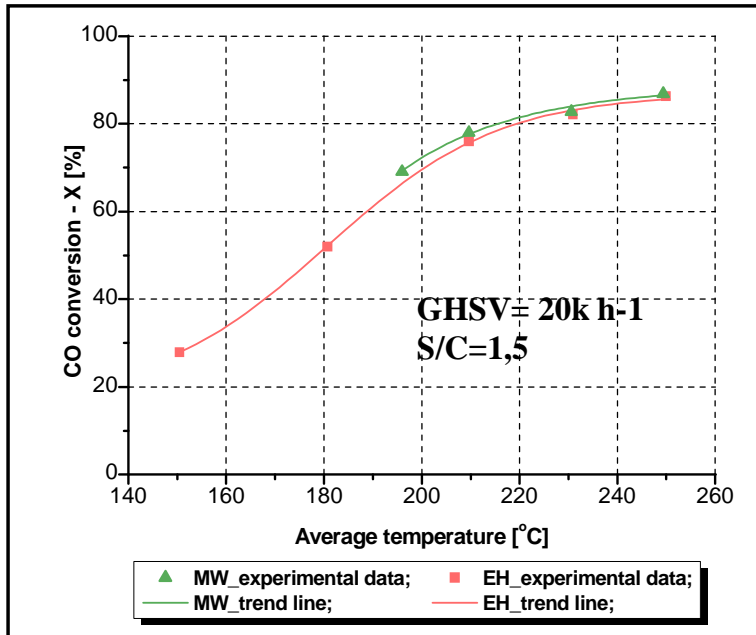
Figure 5.4. Conversion of CO as function of the average reactor temperature under microwave (MW) and electric heating (EH). S/C=1.5 and GHSV= 20000h⁻¹.
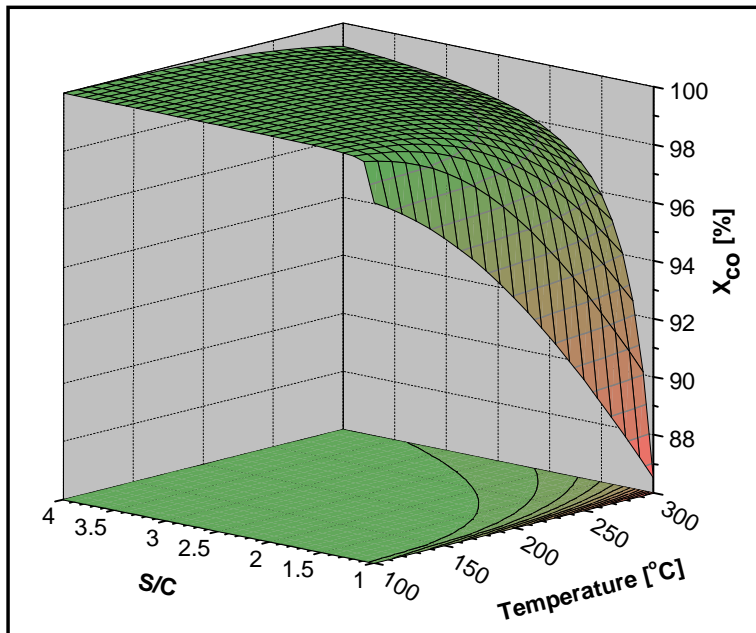

Figure 5.5. CO equilibrium conversion as function of the reaction temperature and S/C ratio.
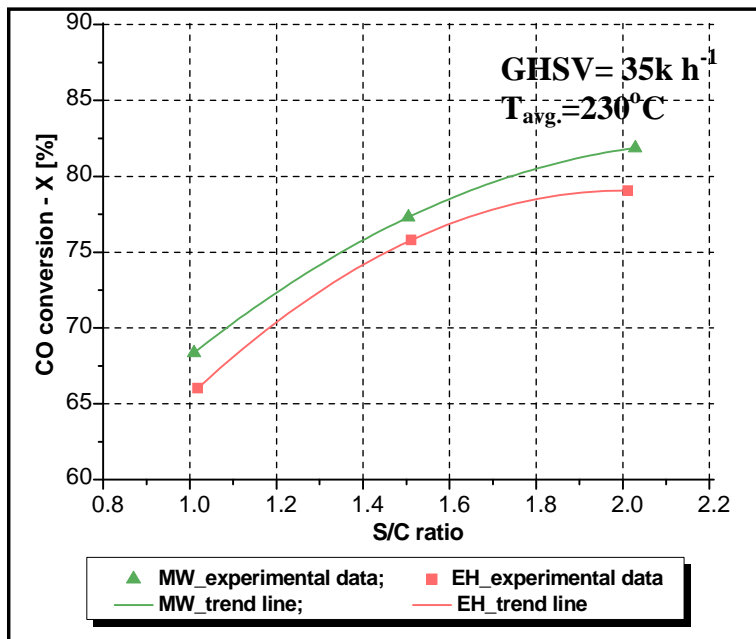
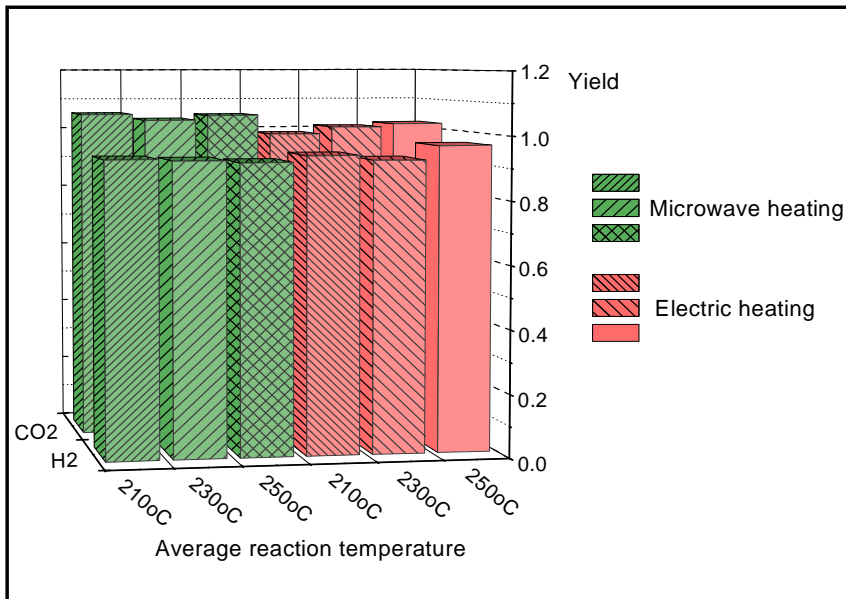**Figure 5.6. Effect of S/C ratio on CO conversion under microwave (MW) and electric heating (EH).**

Figure 5.7. Product gas distribution for WSGR under MW and EH at three average bed temperatures.

5.3.3 Reactor efficiency

The reactor energy efficiency metric used in the previous chapter was defined as the fraction of the net heat input, through solid and open boundaries of the reactor, which is converted to chemical energy through the *endothermic* steam reforming reaction. However, in the case of *exothermic* WGSR, the temperature of catalytic active sites is determined not only by the net heat input, but also by the heat release in the reactor itself. Therefore, it is more meaningful for WGSR to directly compare the net heat inputs to the reactor under the two heating modes. As explained in the previous chapter, it follows from the energy balance that the net heat input is the sum of heat of reaction and the sensible heat of the product gases at the exit of the reactor; both terms can be experimentally calculated. Then the relative heat input between the two processes can be described as follows:

$$\text{Relative Heat Input} = \frac{\left[\Delta H_r^{T_0} + \sum_i n_{i_{OUT}} \int_{T_0}^{T_{OUT}} Cp_i(T)dT \right]_{MW}}{\left[\Delta H_r^{T_0} + \sum_i n_{i_{OUT}} \int_{T_0}^{T_{OUT}} Cp_i(T)dT \right]_{EH}} \qquad \textbf{(5.2)}$$

As presented in Figure 5.4, conversion of carbon monoxide is approximately the same for both heating modes over a range of temperatures. Besides, Figure 5.2 and Figure 5.3 show that the reactor outlet temperature in case of the microwave activated reaction is somewhat lower compared to the electric heating case; from 8.5°C at an average reactor temperature of 250°C to 15°C at T_{avg}=210°C. Further, it has been calculated that the contribution of products sensible heat to the numerator and denominator of Equation 5.2 is ~50-60% depending on the reactor temperature. Overall, Figure 5.8 and Figure 5.9 show that the net heat input under the two heating modes is comparable over the temperature range 210°C - 250°C. Most likely, the combined contribution of reactants preheating and WGSR heat release to reactor heating suppresses selective catalyst heating by microwaves unlike the case of endothermic methanol steam reforming presented in Chapter 4.
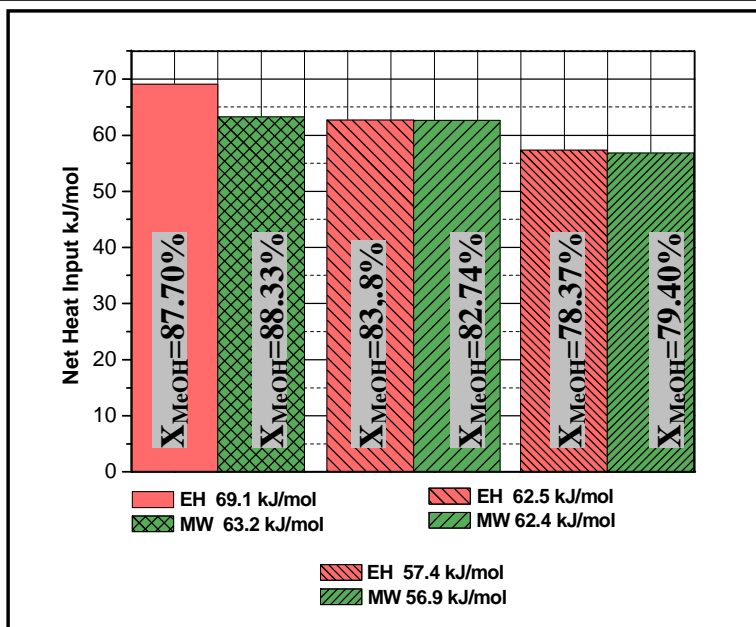
Figure 5.8. Comparison of net heat input of microwave driven and electrically heated reactor for different average reactor temperatures; T=250°C (left set of bars), T=230°C (middle set of bars) and T=210°C (right set of bars). GHSV=20k h^{-1}, S/C=1.5.

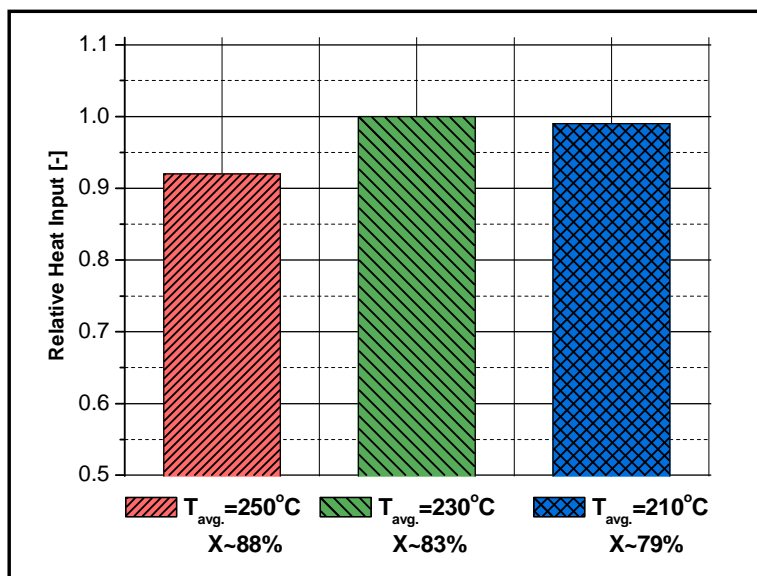**Figure 5.9 Comparison of relative heat input (Equation 5.2) for different average reactor temperatures; T=250°C, 230°C and 210°C. GHSV= 20k h^{-1}, S/C=1.5.**

5.4 Conclusions

Contrary to the results obtained on the endothermic steam reforming reaction, application of microwave energy to the exothermic WGSR process does not bring about significant benefits in terms of higher conversion or better selectivity. It was found that application of microwave energy to WGSR does not have any positive impact on the reactor energy efficiency; the net energy input to the reactor is approximately the same between microwave and conventional heating for the same conversion level. A possible explanation is that due to WGSR being exothermic, a significant part of the net heat input to the reactor comes from the heat of reaction instead of the heat input from microwaves. Since the microwave power delivered to the reactor is controlled by temperature measurement inside reaction zone thus increase of the reaction temperature is compensated by lowering the heat input from microwave radiation. As result the associated local overheating of active sites diminishes. Finally, the experiments confirmed that regardless of the endo-/exothermic nature of the process, application of microwave irradiation to heterogeneous gas-solid reactions results in more pronounced temperature non-uniformities.

Bibliography

1. Galvita, V., et al., *Production of hydrogen with low COx-content for PEM fuel cells by cyclic water gas shift reactor.* International Journal of Hydrogen Energy, 2008. **33**(4): p. 1354-1360.
2. Chen, W.-H., et al., *Modeling and simulation of hydrogen generation from high-temperature and low-temperature water gas shift reactions.* International Journal of Hydrogen Energy, 2008. **33**(22): p. 6644-6656.
3. Ratnasamy, C. and J.P. Wagner, *Water Gas Shift Catalysis.* Catalysis Reviews, 2009. **51**(3): p. 325-440.
4. Chen, W.-H., et al., *Hydrogen generation from a catalytic water gas shift reaction under microwave irradiation.* International Journal of Hydrogen Energy, 2008. **33**(18): p. 4789-4797.
5. Choi, Y. and H.G. Stenger, *Water gas shift reaction kinetics and reactor modeling for fuel cell grade hydrogen.* Journal of Power Sources, 2003. **124**(2): p. 432-439.

6

Microwave assisted heterogeneous catalysis – challenges and opportunities

6.1 Introduction: Limitations of Technology

Despite the fact that microwave technology has been implemented in industry for such as applications like food sterilization, defrosting and drying, ceramic sintering, composite materials curing or rubber vulcanization, the majority of its applications concern chemical analysis (e.g. using digestion, extraction, etc.) or laboratory-scale synthesis of specialized chemicals and pharmaceuticals. Even though small scale microwave reactors have been successfully employed in the latter cases, the shortcomings of the technology have been recognized over the years. The early research works with use of microwaves, as an alternative to conductive energy transfer, were performed in ordinary household microwaves ovens. It was quickly realized though that domestic ovens are not suitable for use in chemistry mainly due to safety issues and limited flexibility. Technical modifications followed in order to meet new, more rigorous requirements of chemical synthesis. Direct temperature measurement units, stirring units, additional openings in the housing for reflux columns and continuous flow operation and pressurized vessels have been implemented to increase flexibility and reduce discrepancy between conventional and microwave reactors. Furthermore, while household microwave ovens exclusively operate with pulsed electromagnetic fields, it was found out that operation with continuously delivered power brings advantages over the pulsed operation mode (no overheating, better controllability in distillation processes). This, however, imposes a higher degree of complexity to the microwave system.

The increased demand by researchers for more sophisticated units became the driver for companies to develop safe, flexible, well equipped and, most importantly, dedicated microwave ovens for research purposes. The first laboratory instrument was introduced by CEM Corporation in 1978 for analysis of moisture in solid materials. Many years later, in 1990, another big player on the microwave oven market, Milestone Inc, introduced the first high pressure laboratory microwave oven for digestion of difficult to digest materials[1]. Since then, fast development of the laboratory microwave applicators for chemical synthesis was observed. Together with the most common, at those times, multimode cavities, a new type of equipment, the so-called mono-mode cavity (oven), was developed.

A multimode cavity can be simply described as a metal box - a Faraday cage - with the targeted material for heating inside (Figure 6.1)

Microwave irradiation is generated by a magnetron and it is directed to the cavity through a waveguide. Inside the cavity, microwaves propagate in all directions and undergo multiple reflections before they finally reach the heated material. The reflections occurring in the cavity have a stochastic nature and therefore interference between waves is unavoidable. Consequently, some of the waves are being amplified and other ones are destructed, thus creating non-uniform electromagnetic field patterns inside the cavity, the so-called oscillation modes.
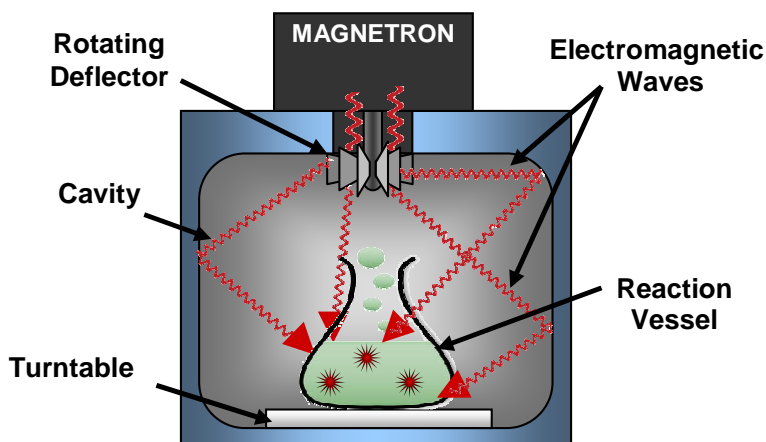

Figure 6.1 Schematic representation of a multimode cavity.

Moreover, a magnetron can never deliver electromagnetic waves at the exact selected frequency (e.g. 2.45GHz); rather, it covers a (very narrow) frequency band (i.e. 2.45GHz ± 50MHz), which also contributes to the random character of the electromagnetic field. One may consider experimental determination of the electromagnetic field distribution inside the cavity; however, the obtained results would be valid only for the material used for the tests and cannot be easily interpreted for other systems. Once the target sample is interchanged, the field distribution changes as well since microwaves interact with the accommodated sample changing the reflection patterns. This particular feature can be considered as a big disadvantage of this microwave system in terms of controllable heating; however, creating a chaotic pattern of the electromagnetic field allows for utilization of bigger sample volumes inside the

cavity. Therefore, multimode cavities are rather applicable to either multi-sample experiments, where a number of samples can be accommodated simultaneously decreasing the time required for experiments, or to relatively large sample volumes (more than 50% of cavity volume). To maximize the probability that multiple samples experience the same microwave irradiation, and thus to maximize uniform heating, a multimode cavity is usually equipped with a turntable platform where the samples must be placed.

In contrast, in a mono-mode (or single-mode) cavity, only one mode of microwave propagation is allowed and thus the electromagnetic field pattern inside the resonant cavity is better defined. In mono-mode applicators, microwaves travel along the wave guide and enter the resonant cavity at a specific phase, creating a standing wave inside the resonant cavity. The sample of irradiated material is always placed at one of the maxima of the electromagnetic field (Figure 6.2). This particular feature of mono-mode applicators entails that both the cavity and reaction vessel size are rather limited to the half length of the wave (about 6 cm for 2,45 GHz). Therefore, mono-mode applicators are usually employed to process volumes up to 200cm^3, which may be considered as their main limitation. However, another advantage of the mono-mode cavities is the high density of the electromagnetic field inside the small cavity itself, implying higher heating rates. Although the electromagnetic field pattern is well defined inside an empty mono-mode cavity, it must be highlighted that as soon as the heated material is placed inside it, the field pattern is affected, resulting in unpredictable heating patterns in the liquid phase [2] and in not-stirred solid systems, where the effect is even more pronounced, as discussed in Chapters 2, 4 and 5.
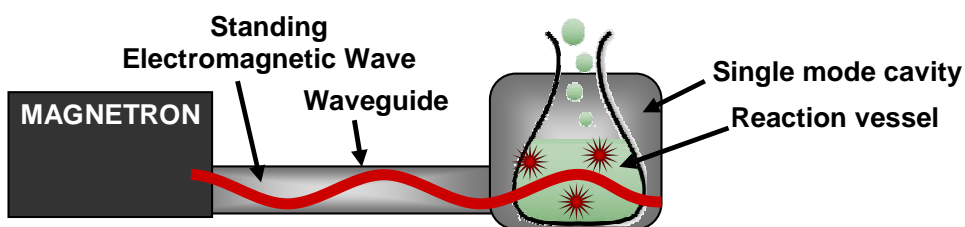

Figure 6.2 Schematic view of a mono-mode microwave applicator.

Uniform heating is indeed one of the biggest challenges in all types of microwave applicators. While in large volume reactors, placed in multimode cavities, the phenomenon is well-known and is usually explained in terms of insufficient penetration depth of the electromagnetic waves into the sample, in mono-mode applicators, it is not widely recognized.

Furthermore, if the temperature measurement technique used is not capable of detecting occurring temperature non-uniformities, as presented in Chapter 2, the overall picture of the microwave-assisted process performance can be misleading and hard to interpret. In this chapter, alternative concepts of microwave applicators to conduct heterogeneous gas-solid catalytic reactions are proposed. Several criteria, determining applicability of the concepts, are taken into account. These are

- avoidance of non-uniform heating patterns inside the reactor
- measurement and control of the real thermal field inside the reactor
- scalability

Finally, the design of the most promising concept is discussed in more detail in the last section.

6.2 Alternative concepts of microwave reactors

As presented in Chapters 2, 4 and 5, application of microwave energy to solid catalytic samples results in significant spatial thermal gradients. Despite the facts that the reactor used in this study has a 12 mm diameter only, the catalytic bed occupied approximately $3.5 cm^3$ and a mono-mode microwave applicator was used, a non-uniform thermal field was unavoidable. As observed, the limiting factor was not the penetration depth of the microwave field since the temperature at the center of the reactor was significantly higher than near the wall, contrary to what was observed for the electrically heated reactor.

How, in such a system, uniform heating can be achieved? Would "stirring" homogenize the temperature field? Does the stochastic nature of the reagents flow affect the heat distribution? Based on our observations and experience, a number of possible solutions can be proposed to address these questions.

6.2.1 Multi Internal Transmission Line Microwave Reactor

Microwaves are essentially a subpart of radio frequency waves; it follows that they do not necessarily have to be applied by cavity-type of applicators and that the difficulties linked with resonant field patterns may be avoidable [6].

The Internal Transmission Line applicator (INTLI) concept, discussed in this section, was originally developed by SAIREM, a French microwave and radio heating system provider that hold a patent for this invention [7]. INTLI, contrary to multimode and single mode applicators, allow for delivering electromagnetic waves directly to the reaction medium by means of lossy transmission lines and thus it is applicable to reactors made of stainless steel or other common construction materials. The great advantage of the equipment lies in its high degree of flexibility (applicable to batch and continuous reactors, wide range of flow rates or batch sizes as well as temperatures and pressures) and easy scalability. Moreover, forward and reflected power can be precisely controlled allowing for improved controllability of the overall process and enhanced safety [8].

In Figure 6.3, a schematic representation of the concept of a packed bed reactor equipped with Internal Transmission Lines is shown. Considering a heterogeneous gas-solid reaction, the internal transmission line applicator offers many advantages over the classical mono-mode applicator. First, as the microwaves are delivered simultaneously along the length of the transmission line (and the reactor height), with controlled intensity (variable cross section of the waveguide), the temperature of the catalytic bed at different reactor positions can be adjusted according to the process requirements. However, it must be emphasized that although such a design allows for control of the power delivered to the system, decrease in the power output from the generator results in uniform decrease in the power input at all cross sections of the applicator. In other words, it is not possible to control temperature at one spot of the bed without affecting temperature at different locations. In order to homogenize the temperature field across the catalytic bed, the coaxial waveguides can be placed at multiple locations, forming a triangle or even star like pattern depending on the process requirements (Figure 6.3).
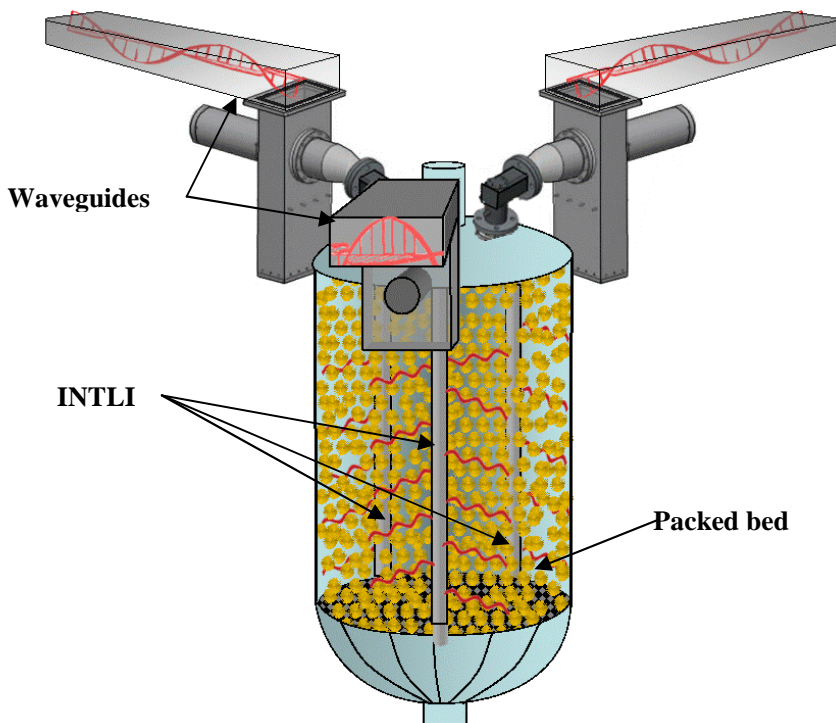
Figure 6.3 Schematic concept of a packed bed reactor with Internal Transmission Lines (coaxial waveguides) in a triangular configuration inside the catalytic bed.

In conjunction with few microwave generators operating independently, such a configuration generates a well-defined system. One can think of a reactor with two or more subsequent heating zones along the height of the reactor, where low and high temperature reactions (e.g. WGS reaction), can be run effectively in one unit. The ultimate advantage of the concept is that the tubular packed bed reactor is a mature technology with known design and scale-up principles, while the INTLI technology offers great flexibility and controllability of the power input.

6.2.2 Fluidized Bed Microwave Reactor

In order to ensure uniform temperature distribution in the catalytic reactor, each of the catalyst particles should experience equal energy absorption from the microwave source. This principle is difficult to fulfill when the catalytic bed is stationary. However, one would think that if the catalyst is in constant movement, forming a circulating fluidized bed, then the particles have a higher probability to become irradiated

uniformly. Although the number of journal papers referring to application of microwaves to fluidized bed catalytic reactors is very limited, the concept was already examined by Thomas and Faucher [3]. The numerical study revealed two important features of the process: *I) the temperature of the catalytic pellet was 20-30°C higher than the gas phase and II) the temperature distribution along the fluidized bed is not uniform.* Although the first outcome is encouraging, as the selectiveness of the investigated catalytic process can be enhanced, the second observation has a negative influence on the process. This is not surprising when the propagation of microwave energy is taken into account. To overcome this obstacle, originating from the non-uniform electromagnetic field distribution, employment of few magnetrons along the fluidized bed reactor should minimize this unfavorable effect. Such a concept was already investigated in food processing for drying of rice [4, 5]. Stacking two sections where each of them was equipped with two microwave generators resulted in homogenized temperature field inside the dryer.

The schematic drawing of a fluidized bed microwave reformer based on a similar concept is shown in Figure 6.4. The main difficulty in practice is that the diameter of the column, although increased, still remains a limiting factor. Furthermore, the combination of high gas velocities, required to sustain fluidization, and the minimum residence time to complete the reaction render the length of the reactor a crucial design parameter.

In principle, the higher the length of the reactor, the more microwave irradiated segments are needed; this increases the difficulty in maintaining a homogeneous temperature field inside the reactor and compromises the controllability of the reactor. Moreover, power consumption will increase significantly. Other possible drawbacks are the abrasion of catalyst particles during their movement and the non-uniform residence time distribution. These features compromise certain process intensification principles and therefore, the fluidized bed microwave reactor concept is not discussed further.
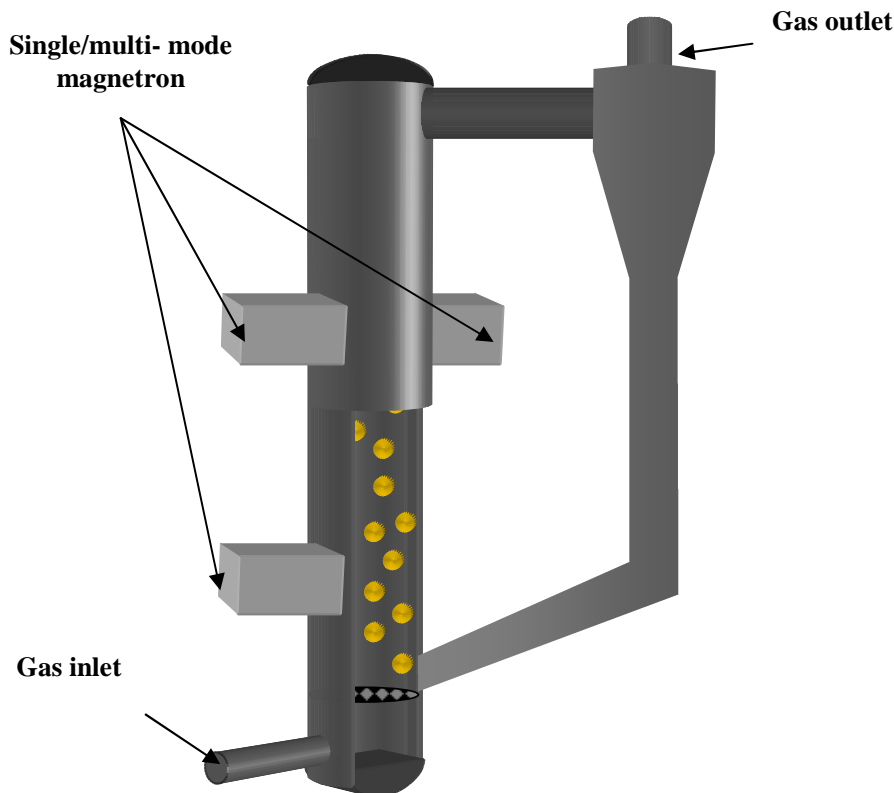
Figure 6.4 The concept of fluidized bed microwave reformer

6.2.3 Traveling Wave Microwave Reactor (TWMR)

Another type of microwave applicator, which is not based on the resonant cavity principle where standing wave patterns are formed, is the coaxial transmission line microwave reactor, which is a type of *traveling* wave reactor. It consists of an inner conductor, a dielectric material, an outer conductor and an insulator similar to the structure of a coaxial cable (Figure 6.5).

The concept of coaxial cable as a method of bringing microwave energy directly into the reaction mixture has been studied in the last few years [9, 10]. However, implemented solutions are based on the so-called open-end technology, which in practice means that the microwave energy is dissipated only at the tip of the coaxial probe, making the technology rather suitable for liquid phase reactions where effective, mechanical stirring can be successfully applied. Therefore, application of the open-end coaxial cables as a tool for delivering microwave energy in a controlled and defined

way into heterogeneous catalytic systems is limited. Nevertheless, a small modification of the concept can satisfactorily solve the problem. Instead of allowing microwaves being transmitted to the end of the applicator without dissipation, the energy can be effectively utilized along the length of the cable.
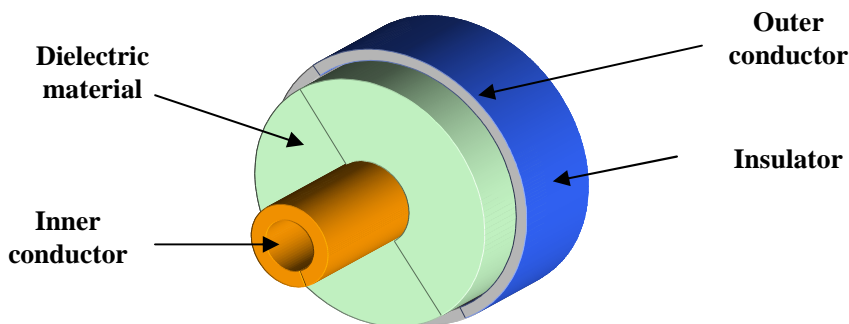

Figure 6.5 Schematic view of a coaxial travelling wave applicator

A variant of the TWMR concept envisioned for gas phase catalytic processes was very recently put forward by Sturm et al. [6] and is shown in Figure 6.6. According to the concept, the space between the inner and outer conductor is filled with a dielectric material and a monolithic layer. The monolith consists of a number of channels, engraved on its surface, which are coated with catalyst. The microwave energy delivered at the inlet is focused and selectively absorbed by the catalytic metal particles deposited on the monolithic structure resulting in high heating rate and efficient energy utilization. The reaction mixture flows through the channels in the same direction as the microwaves (Figure 6.6). Numerical simulations show that uniformly distributed heating rate of the catalytically coated walls can be achieved by varying the diameter of the inner conductor along the length of the reactor applicator (Figure 6.7).

In contrast to the other alternative concepts proposed earlier, TWMR appears to be the one that at most addresses the general principles of process intensification. A TWMR, being a well-defined structure with controlled dimensions of channels, may ensure the same processing experience for all molecules and allows for maximization of the driving forces and specific surface area needed for a heterogeneous reaction to occur. Well-defined and controlled energy utilization supports the principle of maximizing the effectiveness of intermolecular events and limit unfavorable reaction pathways.

Therefore, TWMR is further discussed in the next section in terms of scalability and applicability to microwave-driven catalytic reforming for hydrogen production.
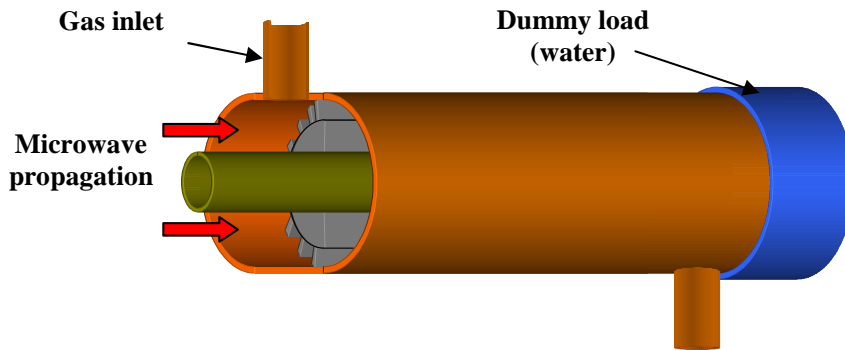

Figure 6.6 The Travelling Wave Microwave Reactor concept tailored for gas phase catalytic reactions (Sturm et al. [6])
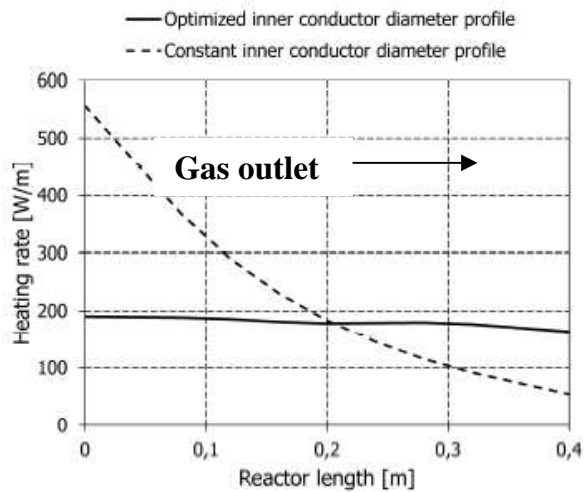

Figure 6.7 Axial heating rate distribution in the case of constant inner conductor diameter (dashed line) and optimized inner conductor diameter (solid line). Taken from Sturm et al. [6].

6.3 Feasibility of the Traveling Wave Microwave Reactor technology for Methanol Steam Reforming reaction – TWMSR reactor

Common practice in designing chemical reactors is first to specify the required production rate and then to calculate reactor dimensions taking the chemical reaction constrains into account. A similar approach has also been adopted in this case; however, since the concept of TWMSR reactor is to a large extend based on microreactor or monolithic reactor technology, the approach is considerably simplified and many assumptions employed in this feasibility study (e.g. channel dimensions or coating layer thickness) are taken from the literature. The design routine used to calculate reactor dimensions and H_2 production rate is presented in Figure 6.8.

In a first step, the production rate of hydrogen is assumed. The operating conditions of the TWMSR reactor have been selected based on literature findings to maximize conversion of the feed and hydrogen concentration (on wet basis) and to minimize the risk of carbon formation [11-18]. The selected conditions are listed in Table 6.1.

Similar to the experimental study on microwave assisted methanol steam reforming described earlier in this book (Chapter 4), a $Cu/ZnO/Al_2O_3$ catalyst, often employed in studies on methanol steam reforming [15, 19, 20], is assumed to be coated on the dielectric filler of the TWMSR reactor.

In the next step, the reactor dimensions are selected based on restrictions concerning electromagnetic wave propagation and typical microchannel dimensions. Typical cross sections of microchannels are of rectangular or square shape with side dimensions between 200μm and 500μm, while the wall thickness ranges from 200μm to 1000μm. Therefore, it is assumed that the TWMSR reactor contains rectangular channels being 300μm wide and 3mm deep with a wall thickness of 350μm at the upper part of the channel and 200μm at the bottom of the channel in contact with the dielectric filler (Figure 6.9).
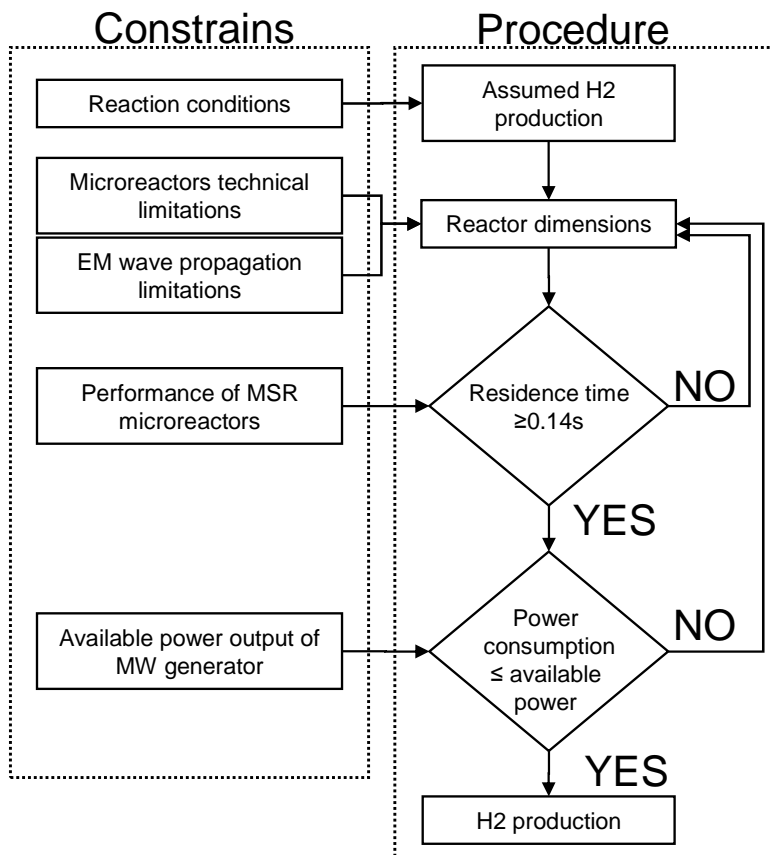
Figure 6.8. Calculation procedure in CMSR reactor design routine.

Temperature (^{o}C)	300
Pressure (atm)	1
S/C	1,1
Equilibrium conversion MeOH (%)	>99,9
Theoretical H$_2$ yield (%)	>97
H$_2$ concentration (% on wet basis)	~72
CO concentration (% on dry basis)	<3
Catalyst load (mg/cm^2)	5

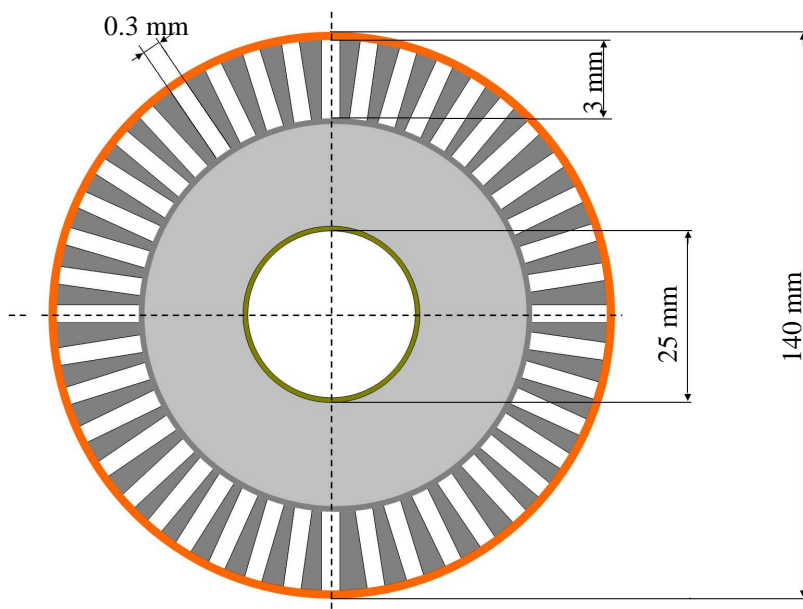**Table 6.1 TWMSR reactor operating conditions**

Figure 6.9 Schematic cross section of the TWMSR reactor.

The TWMSR reactor has a tubular shape and its diameter is a function of the number of channels and their geometry. Theoretically, a bigger reactor diameter, and thus more channels, implies higher production rate for a given reactor length. In practice however, the reactor diameter is limited by the propagation of the electromagnetic waves and cannot exceed half of the length of the electromagnetic waves. Thus, for the frequency of 2,45GHz, the diameter upper limit is ~6,1cm.

Once the initial reactor dimensions have been determined, the information about the methanol steam reforming reaction performed in a microreactor is introduced. In a typical design procedure, the reaction rate expression must be known to determine the residence time needed to achieve a certain conversion. Nevertheless, for the sake of this simplified assessment, the reaction performance and required residence time were assumed based on the previously mentioned literature. For example, in the work of Mei [12], it is suggested that when the MSR reaction is performed in a micro channel reactor at 320°C with S/C=1.2, 0,12s is required to achieve 99% conversion. Other research works [15, 21] suggest that a $Cu/ZnO/Al_2O_3$ coated microreactor can produce up to $870 \text{mmolH}_2 \cdot \text{kg}_{cat}^{-1} \cdot \text{s}^{-1}$ at 300°C and residence time ~0.29s. Based on the collected

information, it was estimated that a residence time of ~0.14s is sufficient to reach the desired methanol conversion (97%) at the selected operating conditions.

Finally, in the last step, the required power consumption by the magnetron is calculated. The available on the market microwave generators, operating at 2,45GHz, can continuously deliver power up to 30kW. Moreover, as indicated by Sturm et al. [6], in order to reach the reaction temperature in short time after the reactor start-up, the heat generation must be in the range of 250MW/m^3. This constraint together with the aforementioned limitations must be satisfied when solving the problem.

Following the procedure, it was found that to fulfill all restrictions; the reactor should contain 130 microchannels. The length of TWMSR reactor has been found to be 40cm and its diameter 1.4cm. The monolith offers a catalyst deposition area of 0.26m^2 and accommodates only 13g of catalyst. The TWMSR reactor is able to produce up to 36mol/h (0.81Nm^3/h) of hydrogen with a power content of ~2.4kW.

It must be noted that the TWMSR reactor performance presented in this chapter is indicative and the optimization of the geometry would probably allow for even higher production rate of H$_2$ gas. This however, would require more in-depth investigation on microstructured reactors and detailed study on the reaction kinetics and fluid flow to optimize channel dimensions, which are out of the scope of this thesis. Nevertheless, further optimization of the channels geometry may lead to miniaturization of the reactor without compromising its performance.

6.4 Conclusions

The applicability of typical mono-mode and multimode microwave applicators to the detailed investigation of heterogeneous gas-solid catalysis is rather limited since both designs suffer from non-uniform heating and difficult to control energy input to the reactor. Combination of a microwave applicator with a fluidized bed reactor although would improve the heat distribution in the catalytic bed, may not be suitable due to residence time limitations and catalyst abrasion. The combination of the recently developed INTLI technology with packed bed reactors brings advantages over the existing technology in terms of better temperature control inside the bed and flexibility in operation; however, the randomness of the packed bed structure is still a major

limitation. Finally, the Traveling Wave Methanol Steam Reforming (TWSR) reactor is seen as the most promising concept since it addresses most of the PI principles. The clear advantage over the other designs lies in the ability to 1) "focus" the electric field where it is needed (i.e. in the catalytic reactor walls) favouring energy utilization efficiency and 2) fully control heating rate distribution over the length of the reactor. A simplified design approach reveals that a multichannel TWMSR reactor having a diameter of 1.4 cm and a length of 40 cm would be capable of producing up to 0.81Nm^3 of hydrogen per hour.

Bibliography

1. Mike Taylor, et al., *Developments in Microwave Chemistry*, in *Chemistry World*. 2005.
2. Sturm, G.S.J., et al., *On the effect of resonant microwave fields on temperature distribution in time and space.* International Journal of Heat and Mass Transfer, 2012. **55**(13-14): p. 3800-3811.
3. Thomas Jr., J.R. and Faucher F., *Thermal modeling of microwave heated packed and fluidized bed catalytic reactors.* Journal of Microwave Power and Electromagnetic Energy 2000. **35**(3): p. 165-174.
4. Sangdao, C., A. Roeksabutr, and M. Krairiksh, *An applicator for uniform heating using perpendicular slots on a concentric cylindrical cavity excited by perpendicular waveguides.* International Journal of Electronics, 2006. **93**(5): p. 313-334.
5. Sangdao, C., S. Songsermpong, and M. Krairiksh, *A Continuous Fluidized Bed Microwave Paddy Drying System Using Applicators with Perpendicular Slots on a Concentric Cylindrical Cavity.* Drying Technology, 2010. **29**(1): p. 35-46.
6. Sturm, G.S.J., A. Stankiewicz, and G.D. Stefanidis, *Microwave Reactor Concepts: From Resonant Cavities to Traveling Fields*, in *Novel Reactor Concepts*, M. van Sint Annaland and F. Gallucci, Editors. 2012, Imperial College Press: London U.K.
7. Grange, A., J.-M. Jacomino, and A. Grandemenge, *Device for applying electromahnetic energy to a reactive medium* 2011.
8. Radoiu, M., *The scale-up of microwave-assisted processes*, in *AMPERE NEWSLETTER*. 2010.
9. Gentili, G.B., et al., *A Coaxial Microwave Applicator for Direct Heating of Liquids Filling Chemical Reactors.* Microwave Theory and Techniques, IEEE Transactions on, 2009. **57**(9): p. 2268-2275.
10. Mehdizadeh, M., *Chapter 6 - Applicators and Probes Based on the Open End of Microwave Transmission Lines*, in *Microwave/RF Applicators and Probes for Material Heating, Sensing, and Plasma Generation*. 2009, William Andrew Publishing: Boston. p. 183-218.
11. Faungnawakij, K., R. Kikuchi, and K. Eguchi, *Thermodynamic evaluation of methanol steam reforming for hydrogen production.* Journal of Power Sources, 2006. **161**(1): p. 87-94.
12. Mei, D., et al., *A micro-reactor with micro-pin-fin arrays for hydrogen production via methanol steam reforming.* Journal of Power Sources, 2012. **205**(0): p. 367-376.
13. Ang, S.M.C., et al., *Fuel cell systems optimisation - Methods and strategies.* International Journal of Hydrogen Energy, 2011. **36**(22): p. 14678-14703.
14. Kundu, A., et al., *Process intensification by micro-channel reactor for steam reforming of methanol.* Chemical Engineering Journal, 2008. **135**(1â€"2): p. 113-119.
15. Leu, C.-H., et al., *Influence of CuO/ZnO/Al2O3 wash-coating slurries on the steam reforming reaction of methanol.* International Journal of Hydrogen Energy, 2011. **36**(19): p. 12231-12237.
16. Lim, M.S., et al., *A plate-type reactor coated with zirconia-sol and catalyst mixture for methanol steam-reforming.* Journal of Power Sources, 2005. **140**(1): p. 66-71.

17. Park, G.-G., et al., *Hydrogen production with integrated microchannel fuel processor using methanol for portable fuel cell systems.* Catalysis Today, 2005. **110**(1â€"2): p. 108-113.

18. Su¨slu¨, O.S. and I.p. Becerik, *On-Board Fuel Processing for a Fuel Cellâ'Heat Engine Hybrid Systemâ€* Energy & Fuels, 2009. **23**(4): p. 1858-1873.

19. Agarwal, V., S. Patel, and K.K. Pant, *H2 production by steam reforming of methanol over Cu/ZnO/Al2O3 catalysts: transient deactivation kinetics modeling.* Applied Catalysis A: General, 2005. **279**(1-2): p. 155-164.

20. Agrell, J., H. Birgersson, and M. Boutonnet, *Steam reforming of methanol over a Cu/ZnO/Al2O3 catalyst: a kinetic analysis and strategies for suppression of CO formation.* Journal of Power Sources, 2002. **106**(1-2): p. 249-257.

21. Park, G.-G., et al., *Hydrogen production with integrated microchannel fuel processor for portable fuel cell systems.* Journal of Power Sources, 2005. **145**(2): p. 702-706.

7

Overall conclusions, recommendations and outlook

7.1 Conclusions

This thesis focuses on application of microwave irradiation, as an alternative energy source, to heterogeneous gas-solid catalytic reactions. Within this framework, two reaction systems, steam reforming of methanol and water-gas shift, were investigated in order to reveal potential benefits as well as challenges stemming from the combination of microwave technology with gas-solid catalytic reactors.

Although the application of microwave energy has been broadly investigated, most of the research efforts have been focused on the comparison with the conventional processes in terms of conversion and/or selectivity; however, not much information has been published on the interaction of microwaves with solid catalyst particles. In this context, a systematic investigation of the microwave interaction with different catalysts, particle sizes and supports was performed in this work. The experimental results showed that for different metal/support combinations, different heating patterns are developed (i.e. from slow rising with low maximum temperature to very fast heating rates end extreme temperatures). Moreover, it was found that higher metal loading increases susceptibility of the catalyst to microwave irradiation. These observations prove that metal nanoparticles might experience different temperature than a catalytic support and thus contribute to achieving higher conversion under microwave heating than when heated by a conventional source of heat. However, above certain metal loading, the opposite effect was observed due to formation of a microwave reflecting metallic shell around the catalytic support.

The catalyst particle size also plays an important role in the process of microwave heating of the catalytic bed. The temperature differences between smaller ($<125\mu m$) and bigger ($300\text{-}425\mu m$) particles of the same catalyst can reach as high as $40^{\circ}C$, which can have a significant effect on a chemical reaction.

Already in the early phase of investigation of microwave heating of catalytic samples, enormous temperature gradients in the reactor in both, horizontal and vertical direction were discovered. Despite the facts that for this study 1) a mono-mode microwave cavity was used, 2) the used sample contained no more than 3 grams of catalyst and 3) the diameter of the sample container was only 12mm, the temperature gradients obtained reached up to $50^{\circ}C$. This finding sheds new light on other research

works published before this work, where the reactor temperature was measured only in one spot and often not with an appropriate method. It was found that the commonly used in microwave chemistry infrared (IR) sensors significantly underestimate the real temperature in the reactor. Therefore, fibre optic (FO) sensors are recommended for use; however, FO sensors, contrary to IR sensors, suffer from a short life time due to their delicateness. Although this shortcoming can be easily improved on lab scale by implementing glass probe guides, it remains a challenge for industrial scale applications. Moreover, the importance of temperature measurement in multiple spots inside the microwave activated gas-solid catalytic reactor was highlighted, in order to obtain the accurate temperature map inside the reactor. This is of high importance in terms of valid interpretation of the reactor performance (conversion and product distribution).

As a model gas-solid catalytic reaction, methanol steam reforming was selected to compare microwave activation and conventional thermal activation using an electric heating element. The study was focused on comparison of methanol conversion, product distribution and hydrogen selectivity over a range of operating conditions with the focus laid on the correct three-dimensional temperature mapping in the catalytic bed. The experiments showed that methanol conversion under microwave heating is significantly higher than that achieved with conventional electric heating under similar bulk temperature conditions. Equivalently, similar methanol conversion was achieved between the two heating modes while the bulk temperature was lower under microwave irradiation. This entails that the reactor can have the same performance with lower net heat input to the reactor. Lower bulk temperature also implies potentially safer operation and lower capital cost.

Further, the experiments showed that the higher conversion under microwaves is not related to the catalyst pretreatment, i.e. activation or conditioning of the catalyst prior to the reaction. Moreover, the examination of catalyst surface before and after the microwave activated reaction showed no change in the catalyst morphology. Those findings indicate that the effect of higher conversion has a rather thermal nature indirectly supporting the speculation of hot spot formation on or, in the vicinity of, metal nanoparticles. Contrary to conversion, the product gas distribution and selectivity remained unaffected when microwave energy was applied.

On the side of water-gas shift reaction, which contrary to methanol steam reforming is an exothermic reaction, it was found that microwaves bring no significant benefits over the electrically heated reaction neither in terms of conversion nor product distribution. A possible explanation is that due to water-gas shift being exothermic, a significant part of the net heat input to the reactor comes from the heat of reaction thus lowering the heat input from microwave radiation and the associated local overheating of active sites.

Finally, based on the knowledge gained about advantages and shortcomings of microwave-assisted gas-solid catalysis and the experimental results from this research, a new relevant microwave reactor concept based on the "coaxial cable" principle is discussed. Although generic for liquid and gas-solid reactions, the concept is detailed here for methanol steam reforming and is thus termed Traweling Wave Methanol Steam Reforming (TWMSR) reactor. The TWMSR reactor has the potential to overcome limitations of traditional cavity-based microwave applicators (mono-mode and multi-mode ones). Implementation of monolithic catalyst instead of a randomly packed bed together with optimized variable reactor diameter may ensure well-defined and well-controlled axial and radial heating rates and temperature. Although the concept is still in the modeling phase only, and certain assumptions on the methanol reforming reaction in microreactors (taken from literature) have been made, TWMSR reactor appears to have great potential to form the next generation of microwave applicators.

7.2 Recommendations

Although this research work had fundamental character and aimed to provide insight in the nature of solid catalyst - microwave energy interactions, some of the ideas and aspects came too late in the picture to investigate them thoroughly. Therefore, the following recommendations for further research can be made based on the results and experience gained:

- A major challenge in this work was the accurate temperature measurement inside the reactor. Although this problem can be addressed by temperature mapping of the catalytic bed, such solution is practical only in a laboratory practice. Furthermore, the available temperature measurement techniques

which are suitable for use under electromagnetic field conditions suffer from a relatively low temperature application range (max $300^{o}C$). Therefore, development of new, or improvement of existing temperature measurement techniques is a necessity.

- Precise measurement of dielectric properties of catalyst samples as function of their composition, moisture content and particle size is recommended. This may help develop catalysts, which are optimal for microwave-assisted heterogeneous reactions.

- Experience with mono-mode microwave cavities shows that this type of applicator is far from being optimal for gas-solid reactions. Therefore, a new type of applicator must be designed; it should allow for more uniform energy dissipation inside the reactor. In this context, a hybrid microwave applicator-micro/millireactor system based on the "coaxial cable" principle should be further investigated.

7.3 Outlook

Microwave-assisted chemistry has been investigated for more than 30 years and big steps have been made both in understanding the principles of microwave-matter interactions and in development of advanced lab scale microwave applicators. Nevertheless, commercial scale microwave-assisted chemical processes are not widely implemented. The major obstacle is the complexity of microwave propagation in large scale units causing difficulties in stable operation. Moreover, microwave-assisted processes do not provide the operational flexibility of conventionally heated processes since the former are more sensitive to feed composition/properties and flow rates. In order to popularize microwave technology in industry, robust reactors providing well defined and controllable microwave fields must be developed. This is not a long-term goal anymore, since more sophisticated techniques are employed in experimental investigations of microwave activated chemical processes and more powerful simulation tools have become available.

Nevertheless, it needs to be stressed that microwave reactors are not going to be implemented in every industrial sector; they do not form the ultimate answer to all

industrial needs and each implementation must be studied independently. Finally, increased investment and operational costs must be compensated by increased reactors efficiency and improved product selectivity and yields.

Curriculum Vitae
Publications and Oral presentations
Acknowledgments

Tomasz Durka was born in Warsaw on December 10th 1981. From early age he was fascinated by computers and electronic systems and he decided to pursue his interest joining the Electro-Mechanical Technical High School. After graduation in 2001 he decided to study Chemical and Processing Engineering at the Warsaw University of Technology. Fascinated by the new field he continued his adventure with chemical engineering and in autumn 2006 he obtained his MSc. degree. Three months later he was appointed as PhD student in the Separation Technology group (later Intensified Reaction and Separation Systems) under supervision of Prof. dr. ir Andrzej Stankiewicz at Process & Energy Department of Delft University of Technology.

His PhD research objective was focused on application of microwave irradiation to heterogeneous catalysis for hydrogen production processes. During this period, he coached both, BSc and MSc students. Parts of the research presented in this thesis have been published in international journals and presented at various domestic and world conferences in the field of microwave application to chemical processes and on general chemical engineering conferences.

In 2010 Tomasz married his true love, Magdalena. After four and half years of doing research at university, in 2012 he started working in the Research, Development & Technology group at Thermphos International B.V.; meanwhile finishing his PhD thesis. Currently he works in the Technology Center at Yara Sluiskil B.V.

Publications

1. <u>Durka T.</u>, Van Gerven T., Stankiewicz A., Microwaves in heterogeneous gas-phase catalysis: experimental and numerical approaches, *Chemical Engineering & Technology*, 32(9), 1301-1312, **2009**

2. <u>Durka T.</u>, Stefanidis G., Van Gerven T., Stankiewicz A., On the accuracy and reproducibility of fiber optic (FO) and infrared (IR) temperature measurements of solid materials in microwave applications, *Meas. Sci. Technol.,* 21, **2010**

3. <u>Durka T.</u>, Stefanidis G., Van Gerven T., Stankiewicz A., Microwave-activated methanol steam reforming for hydrogen production, *Int. J. Hydrogen Energy*, 36(20), 12843-12852, **2011**

Oral Presentations

1. <u>Durka T.</u>, Stefanidis G.D., Van Gerven T., Stankiewicz A. I., "Influence of microwave irradiation on heterogeneous gas-solid reaction systems-dielectric heating of solid catalyst particles", *12th International Conference on Microwave and High Frequency Heating (AMPERE 2009)*, Karlsruhe, Germany, 7-10 September, **2009**.

2. <u>Durka T.</u>, Van Gerven T., Stankiewicz A. I., "Dielectric heating of solid catalyst particles", *8th World Congress of Chemical Engineering (WCCE8)*, Montreal, Canada, 23-27 August, **2009**.

3. <u>Durka T.</u>, Van Gerven T., Stankiewicz A. I., "Novel concept of microwave-enhanced catalytic membrane reactor for in-situ hydrogen production in automotive applications - dielectric heating of solid catalyst particles", *2nd European Process Intensification Conference (EPIC)*, Venice, Italy, 14-17 June, **2009**.

Acknowledgments

Looking back on those years I notice that all research work would not be so enjoyable without my friends, colleagues, co-workers and family who, sometimes unconsciously, support me and encourage finalizing this work. Now, I would like to express my gratefulness to all of the people who contributed directly or indirectly to this thesis.

The completion of this work would be not possible without the excellent guidance of my promoters and supervisors. First, I would like to express my sincere gratitude to Prof. dr. ir. Andrzej Stankiewicz who gave me opportunity to conduct this very interesting research and who guided me throughout the project. Thank you for trust and freedom in doing the research but also for keeping me on track with the project in order to fulfill the targets and fill the pages of this thesis. You always took care about me and Magdalena, not only on professional but also personal level and thanks to your attitude I always felt at work as being at home. *Panie Profesorze, serdecznie dziękuję.*

I'm also very grateful to Dr.ir. Thomas Van Gerven, who was my daily supervisor at early stage of the project, for teaching me how to prepare and give a good presentation and for help with writing my first scientific paper. *Tom, Dank je wel.*

I would like to thank my co-promotor Dr. ir. Georgios Stefanidis for giving critical but very constructive comments. I still remember our first face-to-face meeting in your office. It was a very "stormy" meeting but afterwards our collaboration was like a well-oiled machine. Many thanks for your feedback while preparing presentations, for help with interpretation of the results and your general input to this thesis. Without you it would not be written yet. Finally, thank you for all formal and informal discussions; they were always fruitful and encouraging me for further work. *Γεωργίου,σας ευχαριστώ πολύ.*

As one of my colleagues wrote "brain is nothing without hands" now I would like to express my gratitude to all people from mechanical workshop, especially Andre, Jan, Jasper, Daniel and Martijn for their help in construction of the experimental set-up,

continuous improving it and reparation of all those small things which always break down in the last appropriate moment. *Bedankt jongens!!*

My special thanks go to a team of analytical experts who supported me with variety of analysis – Micheal van der Brink, thank you for help with GC and SEM; Kees Kwakernaak from Material Science Engineering, many thanks for XRD analysis; Harrie Jansma from Catalyst Engineering for allowing me to use TPR apparatus. *Thank you very much.*

I would also like to thank Leslie, Ilona and Helma for taking care of all administrative issues and solving all bureaucratic problems. *Hartelijk bedankt.*

In particular, I would like to thank Prof. Ulrich Nieken and Ir. Vannessa Gepert for hosting me at University of Stuttgart, fruitful discussions and teaching me basics of steam reforming reaction.

My stay at P&E would not be so cheerful without my office mates and colleagues. Aylin, Ernesto, Guido, Stephanie, Xiaohua thank you very much for creating nice working atmosphere - sometimes deadly scientific and sometimes inefficiently relaxed. We have complained together, we have supported each other and we have had fun together. The endless discussions about cultural differences, working habits and PhD life were very inspiring and educative. Special thanks go to Guido, our microwave engineering expert and only native Dutch in the office, for help with translating the summary into Dutch and stimulating discussions. I would love to see one of your microwave reactors being operated.

Marcin, my dear fiend, you have been of great help during my stay at P&E. Thank you for sharing your widespread knowledge and help in solving daily life issues. Your great scientific spirit mixed with practical approach and hands-on attitude are exemplary. I hope that one day we will be able to set up our "small business". *Marcin, dzięki za wszystko!*

Ana, Christian, Cristian, Jelan, Norbert, Richard, Somnath, Widya and also many more – thank you for a very nice time during a number of social and scientific (like NPS) events.

Marloes, Susan – at least I convinced one of you to pursuit your university carrier. We spend a lot of time together in the laboratory during experiments. Despite the fact that I was your supervisor and I suppose to teach you, I learned a lot from you.

Last but not least, I thank my wife Magdalena. Thank you for supporting me in all good and bad times, for you criticism and encourage. You are always there when I need you – *dziękuję Kochanie*.

Tomasz